

Analysis of a Two-Branch Maximal Ratio and Selection Diversity System with Unequal Branch Powers and Correlated Inputs for a Rayleigh Fading Channel

Kai Dietze

Thesis submitted to the Faculty of the Virginia Polytechnic Institute and State University in partial fulfillment of the requirements for the degree of

Masters of Science
in
Electrical Engineering

Dr. Warren L. Stutzman, Chair
Dr. Jeffrey Reed
Dr. Brian Woerner

March 30, 2001
Blacksburg, Virginia

Keywords: Antenna Diversity, Rayleigh Channel, Maximal Ratio, Selection Diversity, QPSK, BPSK, Diversity Gain, Correlated Channels

Copyright 2001, Kai Dietze

Analysis of a Two-Branch Maximal Ratio and Selection Diversity System with Unequal Branch Powers and Correlated Inputs for a Rayleigh Fading Channel

Kai Dietze

(Abstract)

This report, presents an analytical framework for analyzing two-branch diversity systems for a Rayleigh fading channel. In many cases the fading received at both branches (i.e. a two-antenna element system) is correlated because of the proximity of the antenna elements to each other. It is also not uncommon for a diversity system to use antennas with different patterns or polarizations, this usually results in differences in average signal-to-noise ratios at both branches depending on which element is better matched to the signal environment. As will be shown, the performance of a diversity system depends greatly on the envelope correlation, average power imbalance and the combining scheme used on both branches.

An analytical expression for the probability density function of the signal-to-noise ratio at the output of a two-branch maximal ratio and selection diversity system is developed in this report. The two branches are assumed to be Rayleigh fading, correlated, as well as of unequal signal-to-noise ratios. Measurements were made in Rayleigh fading channels and compared to the analytical results. The analytical cumulative distribution functions (derived using probability distributions) were found to be within 1 dB of the measured results (statistics obtained from time combining) for both maximal ratio and selection diversity attesting to the validity of the analytic results. Also developed in this report are the exact analytical average probabilities of symbol error for coherent BPSK and coherent QPSK before and after maximal ratio combining for this environment. The diversity gain for selection, maximal ratio, and equal gain combining for the 10% probability level is presented as a function of power imbalance and correlation between branches for a two-branch Rayleigh diversity system

Acknowledgements

First of all, I would like to thank my thesis advisor Dr. Warren Stutzman for his invaluable support and guidance during the duration of this research. I would also like to thank my committee members, Dr. Brian Woerner and Dr. Jeffrey Reed for reviewing my thesis and for their instruction in the numerous classes I took with them. I am also grateful to Dr. Carl Dietrich for his advise throughout this thesis and for helping me perform the measurements found in Chapter 8.

I would like to thank all the students and staff of the Virginia Tech Antenna Group (VTAG) with whom I interacted every day and established a strong friendship. I would also like to thank the students and staff of MPRG with whom I worked with on various occasions on joint projects.

Most of all, I am grateful to my parents and brother who have been a source of inspiration and support throughout my life.

Contents

1 Introduction	1
1.1 Introduction	1
1.2 Motivation for Research	2
1.3 Thesis Outline	4
1.4 Previous Work and Contributions	5
2 The Wireless Channel and Diversity Basics	8
2.1 Overview of the Wireless Communications Channel	8
2.1.1 Frequency Selective and Flat Fading Channels	10
2.1.2 Slow and Fast Fading Channels	11
2.2 Flat and Slow Fading Channels	12
2.3 Diversity Systems	13
2.3.1 Establishing Diversity Branches	13
2.3.2 Factors Affecting Diversity Performance: Power Imbalance	15
2.3.3 Factors Affecting Diversity Performance: Envelope Correlation	16

2.3.3.1 Behavior of Envelope Correlation in Spatial Diversity Systems	17
2.3.4 Diversity Combining Techniques	21
2.3.5 Diversity Gain	21
2.3.6 Interpretation of Diversity Measurements and Extraction of Statistics	22
2.3.7 Additional Factors Affecting Diversity Systems	25
3 Combining Schemes and the Rayleigh Channel	27
3.1 Diversity Combining Schemes	28
3.1.1 Selection Diversity	28
3.1.2 Maximal Ratio Combining	33
3.1.3 Equal Gain Combining	39
3.2 Analysis of Rayleigh Fading Channels	42
4 Evaluation of the Joint Probability Density Function of Two Correlated and Unbalanced Rayleigh Signals	52
4.1 Separating Two Rayleigh Signals Into Gaussian Components	53
4.1.1 Correlation Between the Gaussian Components of Two Rayleigh Signals	55
4.1.2 Joint Probability Density Function of Four Gaussian Variables	59
4.2 Transforming a Four Dimensional Gaussian pdf into the Joint Probability Density of Two Rayleigh Signals	61
4.2.1 Joint Probability Density Function of Two Rayleigh Signals	61
4.2.2 Relating the Gaussian Correlations to the Rayleigh Envelope Correlation and Branch Power	66
4.2.2.1 Branch Power	66
4.2.2.2 Envelope Correlation (\mathbf{r})	68

4.2.2.3 Power Envelope Correlation (r_p)	73
4.3 Summary of Results and Examples	75
5 Two-Branch Selection Diversity In a Rayleigh Channel	80
5.1 Introduction	81
5.2 Probability Density Function of the SNR_{V_S}	82
5.3 Probability Density Function of the SNR_{P_S}	88
5.4 Selection Diversity Example	90
6 Two-Branch Maximal Ratio Combining In a Rayleigh Channel	93
6.1 Introduction	94
6.2 Distribution of the SNR_{V_M}	94
6.2.1 Probability Density Function of the SNR_{V_M}	94
6.2.2 Cumulative Distribution Function of the SNR_{V_M}	102
6.3 Probability Density Function of the SNR_{P_M}	103
6.4 Maximal Ratio Combining Example	106
7 Performance of Coherent BPSK and QPSK in a Rayleigh Channel with a Two Branch Diversity Maximal Ratio Combiner	109
7.1 Introduction	109
7.2 Channel Model	110
7.3 Symbol Error Rate of Coherent QPSK and BPSK in the Rayleigh Channel	111
7.4 Performance of Coherent QPSK and BPSK after Maximal Ratio Combining for the Rayleigh Channel	117
7.4.1 Average E_s/N_0 After Two-Branch Maximal Ratio Combining	117
7.4.2 Average Probability of Bit Error using Coherent BPSK	118

7.4.3 Average Probability of Symbol Error using Coherent QPSK	121
7.5 Example of the Performance of QPSK and BPSK after Two-Branch Maximal Ratio Combining	124
8 Comparison of Theory to Measurements	129
8.1 Experiment Setup	130
8.2 Comparisons of Experiments to Theory	132
8.3 Comparisons of Theory to Measured Data Found in Literature	140
9 Conclusions	150

Chapter 1

Introduction and Motivation

1.1 Introduction

The purpose of any communication system is to reliably transfer information between the source and destination. The wireless communications channel is dynamic and random and, at times, the received signal is not strong enough for a dependable link to exist between transmitter and receiver. The average signal strength received by an antenna element over a local area in the propagation environment can be quite large, but during some instances it is not uncommon for the instantaneous signal level in a multipath environment to fall 30 dB or more below its mean level. It is during these abrupt drops in local signal level that the message is most likely to be received incorrectly. In order to compensate for the fading brought upon by the channel and to ensure that the data is not erroneously decoded, the transmit power can be increased during the times a low signal strength is received by the antenna. Most wireless communications systems, however,

are low power and do not have the dynamic range available to counter the effects introduced by the propagation environment. An increase in reliability in a multipath fading environment without increasing transmit power can be efficiently achieved using a receive antenna diversity system.

Multiple antennas at the receiver have been used successfully in operational systems to diminish the variance of local signal strength fluctuations by using the signals on all antenna elements to reduce the incidences of severe signal degradation that occur during a fade. Using several antennas increases the probability that one or more of the elements will receive signals with adequate signal strength. Reducing the occurrences of fades improves the overall reliability of the received information and therefore allows for greater coverage distances.

In present cellular mobile radio communications (824-894 MHz), the use of multiple antennas was almost exclusively limited to base stations where a sufficiently large area was available to place several bulky antennas. It is well known that the size of the antenna is directly proportional to its operating wavelength [1]. The increase in communication frequencies, as a consequence, was accompanied by a reduction in size of the antenna elements. In addition, at PCS frequencies (1850-1990 MHz) or higher, it has become feasible to have multiple antennas not only at the base station but also on the handset.

1.2 Motivation for Research

Diversity is an effective method for increasing the received signal-to-noise ratio in a flat fading environment (i.e. nearly constant fading over the bandwidth of interest). The mobile radio channel varies with time and at times a receiver might receive a signal that is indistinguishable from the noise. Diversity is meant to provide the receiver with alternate paths to the transmitted signal to ensure the signal is reliably received. This

this thesis will examine a two-branch diversity system with focus on receive antenna diversity.

The signal envelope received by an antenna in a multiple reflective non-dispersive medium can, in theory, be modeled as Rayleigh fading in an environment where multipath components have equally distributed amplitudes. Measurements performed by the author with colleagues, as well as others in literature have established that it is not uncommon to find Rayleigh channels in blocked line of sight indoor and outdoor propagation. This thesis presents a theoretical approach to predict the performance of a two-branch diversity system in these types of channels. The motivation for this analysis is to evaluate the performance of a two-antenna element handheld receiver. Due to size constraints, antenna elements on a handset are closely spaced (less than λ). When identical elements are closely spaced, the signal envelopes received by both elements can exhibit a large degree of correlation, or similarity. A large correlation implies that when one antenna receives a low signal level, the second element most likely also attains a similar degraded signal level. It is also not uncommon for an antenna diversity system to use different antennas at each diversity branch. Using non-identical elements at the receiver (e.g. antennas with different polarizations or patterns) could lead to average power imbalances between branches of a diversity system. Antennas that are different usually receive unequal average signal levels depending on which antenna is better matched to the received signal environment.

The performance of any diversity system also depends on the combining technique used to merge the signals received by the antenna elements. Among the most popular combining schemes are selection, equal gain, and maximal ratio. Some combining techniques outperform others under certain conditions and implementation issues usually determine which method is preferred. As mentioned earlier, often the signals received by a diversity system may have antennas that are close together so signals are correlated, or may use different antennas so average power imbalances between branches becomes an issue. It could also happen that branches are both correlated and unbalanced. The results presented in this thesis are meant to quantify the achievable gain of a two-branch

diversity system which combines a pair of correlated and unbalanced channels. The theory developed in this paper assumes that both received signals undergo Rayleigh fading.

1.3 Thesis Outline

This thesis begins with an overview (Chapter 2) of various channel-induced distortions that affect received signal quality in wireless data communications. Discussions on how these channel impairments can be mitigated as well as the conditions under which diversity is effective are examined. Chapter 2 also introduces some definitions and concepts of diversity systems that are used in latter chapters of this report. Chapter 3 examines three of the most popular combining techniques used for processing the signals received by the branches of a diversity system. A mathematical analysis of the output signal-to-noise ratios (SNR) for each of these combiners is derived. This chapter also includes a detailed theoretical examination of channels that exhibit Rayleigh fading. Analyzing the makeup of Rayleigh signals gives insight into which physical channels exhibit this type of behavior.

Subsequent chapters are primarily concerned with two-branch diversity systems in Rayleigh fading channels. Chapter 4 discusses a mathematical technique used to create the joint probability density function (pdf) of two signals that are Rayleigh distributed and are correlated with unbalanced average SNR's. The joint pdf is expressed as a function of correlation between the branches of the diversity system. Chapter 5 applies the combining schemes to the joint probability density function of both branches to develop an expression for the pdf of the SNR after selection combining. The SNR distribution after maximal ratio combining is derived in Chapter 6. The distribution of the SNR at the output of the maximal ratio combiner is used in Chapter 7 to evaluate the performance of digital modulations such as coherent BPSK and QPSK in a diversity environment.

Diversity measurements made in an indoor channel were used to validate the theoretical derivations of the probability density functions of the selection and maximal ratio combiner; the results of this comparison are presented in Chapter 8. Additionally, the diversity gain of the three combining techniques were match up to measured data presented by Turkmani et. al [2]. Finally, Chapter 9 summarizes the results presented in this thesis and states some concluding remarks and discussions.

1.4 Previous work and Contributions

There has been significant theoretical research reported in the area of diversity systems and combining techniques for Rayleigh fading channels [3,4-11]. Some analysis was performed for Nakagami channels of which Rayleigh is a special case [7-11]. Most papers consider diversity systems with uncorrelated branch signals [4-11]. Few have addressed the problems of correlated and unbalanced branches and their effects on diversity performance [8-11]; and among these only maximal ratio combining was considered. References [8-11] present equations for the performance of a correlated diversity system that use maximal ratio combining with differential phase shift keying and non-coherent frequency shift keying as modulation schemes. Non-coherent and differential modulation schemes have exponential bit error rate performances in additive white Gaussian noise (AWGN) and are therefore more readily integrable over Nakagami or Rayleigh fading channels. In [11] an expression for the bit error rate of coherent BPSK is presented for a maximal ratio combining diversity system for correlated Nakagami channels but requires to be numerically integrated. All results in [8-11] are expressed as a function of power correlation coefficient (or envelope squared correlation) because the joint probability density function of the signals in the diversity system can be directly expressed in terms of this variable. The envelope correlation coefficient (or \mathbf{r}), on the other hand, is the parameter that is commonly extracted from measurements and consequently the theory developed in this paper is based on this variable. An equation that relates the power correlation (\mathbf{r}_p) to the envelope correlation (\mathbf{r}) is given in Chapter 4. References [12] and [13] have presented expressions for the pdf after maximal ratio

combining for the Rayleigh channel once the eigen values are extracted from the correlations matrix. The probability density function of dual selection diversity for correlated branches in a Rayleigh channel is presented in [14] and [15] but in both cases the result is left in integral form.

This report presents the exact expressions for the distributions of the signal-to-noise ratios for a two-branch selection and maximal ratio combining diversity system in a Rayleigh fading channel. Both branches can be correlated and have unequal average SNR's. In addition, the exact analytical average probabilities of symbol error for coherent BPSK and QPSK before and after maximal ratio combining are presented for this environment. All steps in the derivations of these results are also included for analysis in this thesis.

References:

- [1] Warren L. Stutzman, Gary A. Thiele, *Antenna Theory and Design*, John Wiley & Sons, New York, NY, 1998.
- [2] A.M.D. Turkmani, A.A. Arowogolu, P.A. Jefford, and C.J. Kellent, "An Experimental Evaluation of Performance of Two-Branch Space and Polarization Diversity Schemes at 1800 MHz," *IEEE Trans. Veh. Tech.*, vol. 44, no.2, pp. 318-326, May 1995.
- [3] John G. Proakis, *Digital Communications*, McGraw-Hill, New York, NY, 1995
- [4] Thomas Eng, Ning Kong, and Laurence B. Milstein, "Comparison of Diversity Combining Techniques for Rayleigh-Fading Channels," *IEEE Trans. Commun.*, vol. COM-44, pp. 1117-1129, Sept. 1996.
- [5] Ning Kong and Laurence B. Milstein, "Combined Average SNR of A Generalized Diversity Selection Combining Scheme," *IEEE ICC98*, Atlanta, pp. 1556-1560, June 1998.
- [6] J. Lu, T. T. Tjhung, and C. C. Chai, "Error Probability of L-Branch Diversity Reception of MQAM in Rayleigh Fading," *IEEE Trans. Commu.*, vol. 46, no.2, pp. 179-181, Feb. 1998.

- [7] V. Aalo and S. Pattaramalai, "Average Error Rate for coherent MPSK Signals in Nakagami Fading Channels," *IEE Electronics Letters*, vol. 32, pp. 1538-1539, Aug. 1996.
- [8] Emad K. Al-Hussaini and Abdel Aziz M. Al-Bassiouni, "Performance of MRC Diversity Systems for the Detection of Signals with Nakagami Fading," *IEEE Trans. Commun.*, vol. COM-33, no. 12, pp. 1315-1319, Dec. 1985.
- [9] Francois Patenaude, John H. Lodge, and Jean-Yves Chouinard, "Noncoherent Diversity Reception Over Nakagami-Fading Channels," *IEEE Trans. Commun.*, vol. 46, no. 8, pp. 985-991, Aug. 1998.
- [10] Q. T. Zhang, "Exact Analysis of Postdetection Combining for DPSK and NFSK System Over Arbitrarily Correlated Nakagami Channels," *IEEE Trans. Commun.*, vol. 46, no. 11, pp. 1459-1467, Nov. 1998.
- [11] Pierfrancesco Lombardo, Gennaro Fedele, and Murli Mohan Rao, "MRC Performance for Binary Signals in Nakagami Fading with General Branch Correlation," *IEEE Trans. Commun.*, vol. 47, no. 1, pp. 44-52, Jan. 1999.
- [12] O. Norklit and R.G. Vaughan, "Method to Determine Effective Number of Diversity branches," *Global Communications Conference 1998*, vol. 1, pp. 138-141, 1998.
- [13] M. Z. Win, J. H. Winters, "On Maximal Ratio Combining in Correlated Nakagami channels with unequal fading parameters and SNR's among branches: an Analytic Framework," *Wireless Communications and Networking Conference*, vol. 3, pp. 1058-1064, 1999.
- [14] F. Adachi, K. Ohno, and M. Ikura, "Postdetection Selection Diversity Reception with Correlated, Unequal Average Power Rayleigh Fading Signals for $\pi/4$ -shift QDPSK Mobile Radio," *IEEE Trans. Vehic. Tech.*, vol. 41, pp. 199-210, May 1992.
- [15] M. K. Simon, M.-S. Alouini, "A Unified Performance Analysis of Digital Communications with Dual Selective Combining Diversity over Correlated Rayleigh and Nakagami-m Fading Channels," *IEEE Trans. on Commun.*, vol. 47, no. 1, pp. 33-43, Jan. 1999.

Chapter 2

The Wireless Channel and Diversity Basics

This chapter summarizes some of the problems encountered during wireless data reception. An overview of channels encountered during mobile radio propagation and their effects on signal quality are discussed. The latter part of the chapter will focus on diversity systems which is the main topic of this thesis. The purpose of diversity systems, the implementation issues, as well as some of the factors affecting performance are put into context. Subsequent chapters will examine in more detail much of the material discussed here.

2.1 Overview of the Wireless Communication Channel

As with any communication link, the channel places fundamental limitations on the performance of wireless communication systems. The propagation channel varies with the operating environment. Electromagnetic waves in a realistic environment undergo

diffraction, reflection, and scattering. A typical received signal contains multiple components reflected off buildings or other large objects that arrive with different time delays and phases. Waves scattered off irregular surfaces or are diffracted around objects add to a cluttered received signal. Vegetation and other semi-transparent electrical objects contribute to shadowing (attenuating) the signal that finds these objects in its path. The final received signal consists of a superposition of multiple variations of the transmitted signal and the goal of the receiver is to adequately decipher the transmitted signal.

Ideally, the propagation path should be free of any objects, as in a free space region. However, there is a large demand for communications in dense urban areas where the propagation path is cluttered. Receiver and/or transmitter motion or changes in the propagation environment further complicate the communication link, resulting in a time-varying radio channel. For non-static channels, the receiver has to constantly track changes in the propagation environment to ensure optimal extraction of the signal of interest. As the receiver moves, the surrounding environment changes, which in turn affects the received signal's amplitude, phase, and structure. At some locations along the receiver path, the signals scattered from the surrounding obstructions from the surroundings interfere at the antenna. The signal components are summed inside the antenna and its RF circuitry, and can combine constructively or destructively. During destructive combining the received signal may not be strong enough to produce reliable communications because of a significant degradation in the *signal-to-noise ratio (SNR)*. The sometimes drastic amplitude (or *envelope*) variations over small distances are referred to as *fading* and when the signal experiences destructive cancellation it is said to be in a *null*. In blocked line-of-sight cases, it is not uncommon for the amplitude of the received signal to drop by 30 dB or more within a distance of a fraction of a wavelength (at 2 GHz, a wavelength is only 15 cm).

2.1.1 Frequency Selective and Flat Fading Channels

A wireless channel can distort or transform the signal in several different ways. A propagation channel is distinguished by how much *inter-symbol-interference (ISI)* it introduces and by how fast the channel changes with time. When the channel introduces *ISI*, the individual multipath components arrive at the receiver with different time delays (because of shorter or longer propagation paths between arriving echos of the transmitted signal), causing a previous symbol (or symbols) to interfere with the current symbol. Upon demodulation, the receiver has the task to decipher the desired symbol from a superposition of present and past symbols. Depending on the strength of the interfering symbols, the receiver may or may not make the correct symbol detection decision. Channels with significant ISI have strong multipath components that arrive at the receiver delayed by about a tenth of a symbol duration or greater after the primary component [6]. Channels with severe inter-symbol-interference, when examined in the frequency domain, have the property of distorting the frequency spectral shape of the transmitted message over the bandwidth of the signal and therefore are labeled as *frequency selective* channels. Equalizers have been successfully used to reconstruct the signal back to its original shape by compensating for the distortions introduced by the channel [6].

Some channels do not introduce, or add negligible, amounts of inter-symbol-interference. Under these circumstances, the multipath delay spread is small relative to the symbol duration or the components of the signal that arrive with a delay larger than about a tenth of a symbol duration are severely attenuated by the channel. Signals transmitted into channels that introduce negligible amounts of ISI have multipath components that arrive at the receiver at approximately the same time. Unlike the frequency selective channels, these channels do not distort the signal over its bandwidth and hence the channel is said to experience *flat fading*. The antenna element receives a signal that is the superposition of several versions of the current symbol interfering with each other at the antenna port. The received signal in flat fading channels looks exactly like the transmitted signal except that it is time delayed and modified by the complex valued gain of the channel. At times, all reflected signals could add destructively at the receiving antenna leaving the

receiver with a signal that might not be recognizable in the presence of noise. When the signal-to-noise ratio is unacceptably low, the receiver needs an alternate path for the signal of interest to ensure reliable reception. Antenna diversity systems provide alternate path outputs using two or more antennas at the receiver to increase the probability that at least one antenna receives an acceptably high signal-to-noise ratio. Section 2.3.1 has a description of different types of antenna diversity configurations. Diversity can also be achieved in time or frequency as will be explained later.

2.1.2 Slow and Fast Fading Channels

In addition to potentially introducing inter-symbol-interference, a channel can be time varying. Dynamic channels are characterized as having *slow or fast fading*. The latter term applies to channels that change significantly during the duration of a symbol. A dynamic channel is often experienced in systems that communicate with mobile terminals. When the channel varies rapidly, the modulation of the symbol is lost as a result of the channel distorting the symbol's amplitude and phase erratically over its interval. Fast fading is difficult to overcome and under these types of circumstances it is better to use a form of non-coherent robust modulation scheme such as *on/off keying (OOK)*. With OOK the receiver decides whether the signal is present or absent and no information is carried in the phase or amplitude of the symbol.

Slow fading, on the other hand, occurs when the channel changes much slower than a symbol duration preserving its modulation. This does not imply that the effects of the channel can be neglected but it is possible to track the changes in the channel to appropriately compensate for channel dynamics. More elaborate modulation schemes can be used since amplitude and/or phase information is now preserved over the channel.

The mobile radio propagation environment is constantly changing. At some point in time the signal might undergo flat fading while at some later instance it might be frequency selective. A swift moving receiver might introduce fast fading when in motion and when at rest experience slow fading. Ideally, a receiver should be able to reconstruct the

desired signal consistently regardless of the environment. The following chapters and sections will primarily be concerned with evaluating the performance of two branch diversity systems to overcome channels that are flat and slow fading.

2.2 Flat and Slow Fading Channels

It is virtually impossible to find a general deterministic model that describes all channels encountered by a wireless system. The radio channel is therefore usually modeled in a statistical fashion. Channel statistics can be obtained from analytical models, simulation, or from measured data collected from various types of environments. In flat and slow fading channels, a tone is typically used to measure the behavior of the channel. Measuring at one frequency directly extends to signals of wider bandwidths as long as the signal bandwidth and operating frequencies fall in the range over which the channel is considered flat. The amplitude (or envelope) of the received signal for the environment under test is used as the criterion for how a particular system will perform in such a scenario. As mentioned earlier, flat fading channels are SNR limited and it is the amplitude of the received signal that contains the information on the received signal strength. The strength of the received signal determines if the communication link is reliable; as for the phase, the receiver is assumed to track the phase correctly.

Measurements made by the author and colleagues, as well as others found in literature have established that the distribution of the envelope of the received signal in a flat and slow fading channel with blocked line of sight and significant multipath can usually be described by a Rayleigh *probability density function (pdf)*; Chapter 8. This result can also be predicted through theory as will be discussed in Chapter 3. When a dominant line-of-sight or multipath component is present together with multiple secondary reflections, the envelope of the received signal behaves more like a Ricean distribution.

2.3 Diversity Systems

A substantial decrease in SNR occurs in a flat fading channel when all arriving multipath components add destructively at the receiver antenna. The receiver is essentially located in a deep fade or null. During these times the receiver requires an alternate signal path to the transmitted signal with a sufficiently large signal-to-noise ratio in order to reliably decipher the desired signal. That is, a secondary *branch* (referred to as a diversity branch) or channel is introduced in order to increase the probability that an adequate signal level is received. The concept is simply that uncorrelated or slightly correlated diversity branches have a low probability of simultaneously experiencing a deep fade. Depending on the desired reliability, it may be necessary to add more than one additional branch (it could happen that both branches are in a null). *Diversity* is achieved by using the information on the different branches available to the receiver in order to increase the signal-to-noise ratio at the decoding stage. Having additional branches increases the probability that at least one branch, or the combined branch outputs, produces a sufficiently high SNR to permit reliable decoding of the message at the receiver.

2.3.1 Establishing Diversity Branches

There are several ways to produce additional diversity branches; the main ones are *antenna*, *time*, and *frequency* [1]. *Time diversity* takes advantage of the dynamics of the channel; at some point in time the received signal might be in a deep fade while at a later time the channel has changed significantly such that the received signal-to-noise ratio is at an acceptable value. Time diversity requires the transmitter to re-transmit the information again at a later time giving the receiver two chances to acquire the signal and properly decode it. If a higher dependability is desired, the message can be repeated several times. As mentioned earlier, nulls occur when all arriving components add destructively at the receiver. This is a property that is frequency dependent; that is, at one frequency the signal can cancel while at other frequencies the signal level might peak in the same location. *Frequency diversity* systems transmit the message simultaneously at

two or more different frequencies to take advantage of frequency diversity at the receiver. The copies of the message received at different frequencies are combined at the receiver using a predetermined algorithm. The main disadvantages of time and frequency diversity are that they require valuable resources that reduce communication system capacity. A common way of achieving diversity without additional system resources is through antenna diversity. *Antenna diversity* requires multiple antennas at the receiver and is therefore usually bulkier. However, operating at high frequency bands allows for the size reduction of antennas elements and it is feasible to have multiple antennas not only at the base stations but also on the mobile handset.

Antenna diversity can be achieved through *spatial*, *polarization*, or *pattern* configurations. Spatial diversity is the most common of the three and requires two or more antennas to be separated in space at the terminal. Two antennas that are physically separated in space experience different propagation environments and multipath components sum differently at each antenna. Ideally for a spatial diversity system, the antennas are spaced far enough in distance such that the branch signals have a higher probability of fading independently. The polarization of the transmitted signal is often altered (i.e. depolarized) as it travels along the channel and the signal arrives at the terminal with a polarization that can greatly differ from the transmitted one. Additionally, the mobile transmitter or receiver rarely transmits or receives with a fixed polarization as a result of random antenna movement by the user. Antennas with orthogonal polarizations are used as part of polarization diversity systems to benefit from the times when there might be a larger signal received on one polarization than at another. It is not uncommon for one polarization to fade while the orthogonal one has adequate signal strength. One of the advantages of *polarization diversity* is that it permits the antennas to be co-located. *Pattern diversity*, on the other hand, uses antennas with different patterns on each branch. The multipath components are weighed differently at each antenna creating unlike interference patterns of the signal at each branch. As a result each channel receives the transmitted signal with different strengths depending on the branch pattern and the propagation characteristics at that moment in time. As with polarization diversity, pattern diversity may allow for the co-location of the antenna

elements. The signal-to-noise ratio can be successfully increased in a flat fading channel by using one or a combination of the above mentioned diversity systems. Subsequent chapters and sections will focus on antenna diversity but the results apply equally well to other diversity mechanism such as the ones achieved through time or frequency.

2.3.2 Factors Affecting Diversity Performance: Power Imbalance

Regardless of what diversity mechanisms are used to improve signal reliability the two factors affecting the performance of a diversity system are *correlation* and *power imbalance* between the branches. Average envelope power imbalance (or just power imbalance) is a term commonly used in literature but it actually refers to the difference in the average distribution of the signal-to-noise ratio (in dB) between two diversity branches. Both terms are equivalent and can be used interchangeably as long as all diversity branches are affected with equal noise powers. In this report, these two terms will also be used to address the differences in average received SNR between channels. The average envelope power received at each branch (P_1 and P_2) can be computed from the distribution of the envelope at the individual branches (in this case branch 1 and 2) as follows [1]:

$$\begin{aligned}
 P_1 &= E[e_1^2] = \int_0^{\infty} e_1^2 f_{E_1}(e_1) de_1 \\
 P_2 &= E[e_2^2] = \int_0^{\infty} e_2^2 f_{E_2}(e_2) de_2
 \end{aligned}
 \tag{2.1}$$

the subscripts 1 and 2 denote the channel number and $f_{E_{1,2}}(e_{1,2})$ is the distribution of the envelope for that particular branch. $E[\cdot]$ is the expected value of the term in the brackets. As long as the noise powers in each branch are equal, power imbalance in a two-channel diversity system is defined as

$$P_{imb}(dB) = 10 \log_{10}(\max[P_1, P_2]) - 10 \log_{10}(\min[P_1, P_2])
 \tag{2.2}$$

As mentioned earlier, power imbalance is a measure of the difference in the average signal-to-noise ratio between the branches of a diversity system. Intuitively, if one branch has a much larger mean SNR than the other, it is likely the weaker branch will not contribute much to the final signal-to-noise ratio. Under these conditions there is not much gain achieved by having a second branch. Results that quantify the gain achieved by a two-branch diversity system with unbalanced branches in a Rayleigh fading channel are presented in Chapters 5-8. The differences in mean signal-to-noise ratio between two branches affect the performance of diversity systems and so does correlation.

2.3.3 Factors Affecting Diversity Performance: Envelope Correlation

Envelope correlation (\mathbf{r}) is a measure of how much a signal in one branch behaves like another. When two branches are completely correlated, or \mathbf{r} is unity, the signals in the branches fade, peak, increase, and decrease at the same time. If two branches are completely uncorrelated, the received envelope in one branch behaves independently of the other and \mathbf{r} is zero. Mathematically, envelope correlation is given by [1]

$$\mathbf{r} = \frac{E[(e_1 - \overline{e_1})(e_2 - \overline{e_2})]}{\sqrt{E[(e_1 - \overline{e_1})^2]E[(e_2 - \overline{e_2})^2]}} \quad (2.3)$$

where

$$\overline{e_{1,2}} = E[e_{1,2}] = \int_0^{\infty} e_{1,2} f_{E_{1,2}}(e_{1,2}) de_{1,2} \quad (2.4)$$

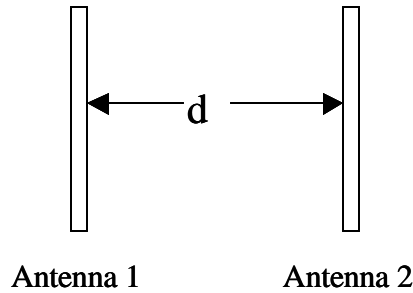
As in (2.1), $f_{E_{1,2}}(e_{1,2})$ are the distributions of the envelope e_1 and e_2 while $E[\cdot]$ is the expected value operator. The lower the envelope correlation in a diversity system, the larger the achievable diversity gain as will be shown in Chapter 8. When \mathbf{r} is small, the envelopes of the two diversity branches do not exhibit the same fading behavior, which

translates into a lower probability of having both branches in a null at the same time. Figure 2.1 shows an example of a two-branch spatial antenna diversity system. Both antennas are identical and are separated by a distance d . The magnitude of the received signal is included vs. distance and as a function of antenna location. As d approaches zero, antenna 2 approaches the location of antenna 1. As this occurs the envelope received by the second antenna approaches that of the first and hence the correlation approaches unity. When both antennas are co-located, both antennas will receive the same signal and consequently have an envelope that will peak and fade at the same time. This means that both antennas receive low signal-to-noise ratios at the same time so the receiver is confronted with two possibly indiscernible signals during these instances. Ideally, the diversity branches should fade independently and when one branch is receiving a signal that is not distinguishable over the noise the system depends on the other to provide the receiver with a reliable link to the transmitted signal. In a spatial diversity system, the antennas have to be spaced far enough apart to ensure a low envelope correlation between the branches.

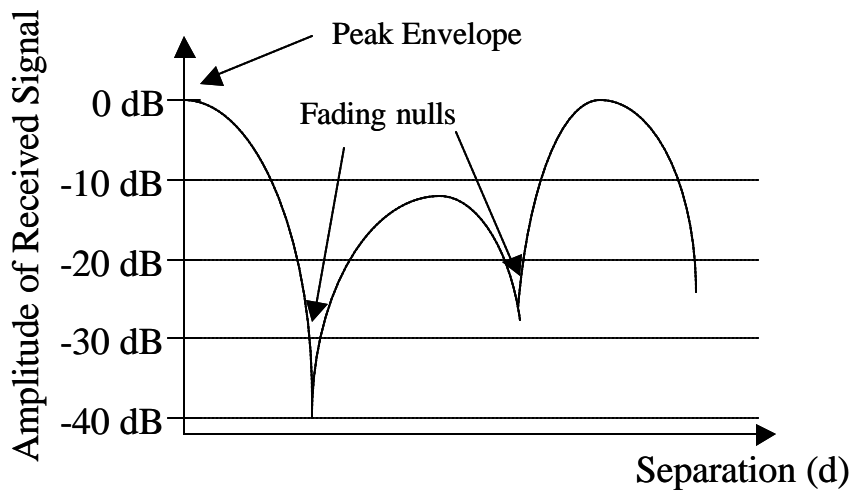
A value $r=0.7$ or less has been used as the guideline for successful diversity operation [4]. In time diversity systems a low correlation between the fading envelopes at the times the signal is transmitted and repeated is desired. Equivalently, independent fading between the envelopes of a message received at two different frequencies through a frequency diversity system results in a higher reliability. The retransmission period, the frequency separation, or the antenna spacing necessary to obtain uncorrelated fading between the branches of a diversity system strongly depends on the propagation characteristics of the environment.

2.3.3.1 Behavior of Envelope Correlation in Spatial Diversity Systems

Independent fading is achieved using spatial diversity by separating the antennas far apart. The numbers of scatterers as well as their locations around the transmitter or receiver have a strong influence on r as a function of this separation. Figure 2.2 shows two typical scenarios that are encountered mobile communications.



(a) Two branch spatial diversity system.



(b) Received envelope as a function of antenna separation d .

Figure 2.1 Typical variations of the received envelope at antenna 1 and 2 in a spatial diversity system as a function of antenna separation.

Macro-cell environments are characterized by having a base station elevated over the coverage area located on hilltops or tall buildings while buildings or other obstructions surround the mobile user. Figure 2.2a illustrates this example where the scatterers are predominantly around the mobile. The signal transmitted from the mobile and its multipath components arrive at the base station spread over a very small angle in the

direction of the mobile location. In micro-cells (Fig. 2.2b) the base station and the mobile are inside the clutter of buildings and other obstacles. The distance between mobile and base is usually much smaller in these environments than the ones encountered in macro-cell channels. A transmitted signal and its multipath components arrive from the mobile at the base station from any angle in the micro-cellular environment. The reflected components reach the base station with a distribution usually covering the full 360° . The extent of the angle spread has a direct effect on the envelope fading rate as a function of antenna displacement. For illustration purposes, the influence of wide and narrow angle spread on the received envelope are presented in Figure 2.2. When the signals arrive at the receiver from a small angle spread (Fig. 2.2a), the multipath components arrive from approximately the same direction. Antenna displacement in this environment affects all received components with nearly the same phase progression. Even large movements of the receiver (when compared to λ) cause very little change in the envelope of the received signal because the multipath components add up in the same fashion except for the introduction of a constant phase shift experienced by all components due to the translation of the receiver. When components arrive from all directions, on the other hand, some reflections exhibit larger phase shifts than others and small antenna displacements (when compared to λ) are enough to create a new interference pattern at the receiving antenna. The rate of change of the fading envelope vs. distance directly influences the behavior of the correlation as a function of antenna separation. For channels that have slowly fading envelopes (Fig. 2.2a) with respect to displacement, the antennas need to be separated by several λ to achieve independent fading of the branches. In a fading channel where the envelope changes significantly with slight displacements of the antenna, the antennas as part of a spatial diversity system achieve lower correlation at closer spacings. The mobile station in macro or micro-cell environments is usually surrounded by scatterers with reflections arriving at the antenna from a wide angle spread. From the previous discussion of angle spread, close antenna separations on the order of fractions of a wavelength produce a low \mathbf{r} between diversity branches at the mobile. Base stations in a macro-cellular environment, experience narrow angle spread and usually require antennas separated by 10 to 20 λ to ensure low envelope correlations between the branches [2]. As a side note, having two uncorrelated

branches does not eliminate the possibility that both channels might be in a null at the same time but the probability of such an event occurring is lower when the fading is independent. In frequency diversity systems, the frequency separation between branches depends on the time delays with which the multipath components arrive at the receiver. The larger the time delay spread, the closer the diversity channels can be placed in frequency.

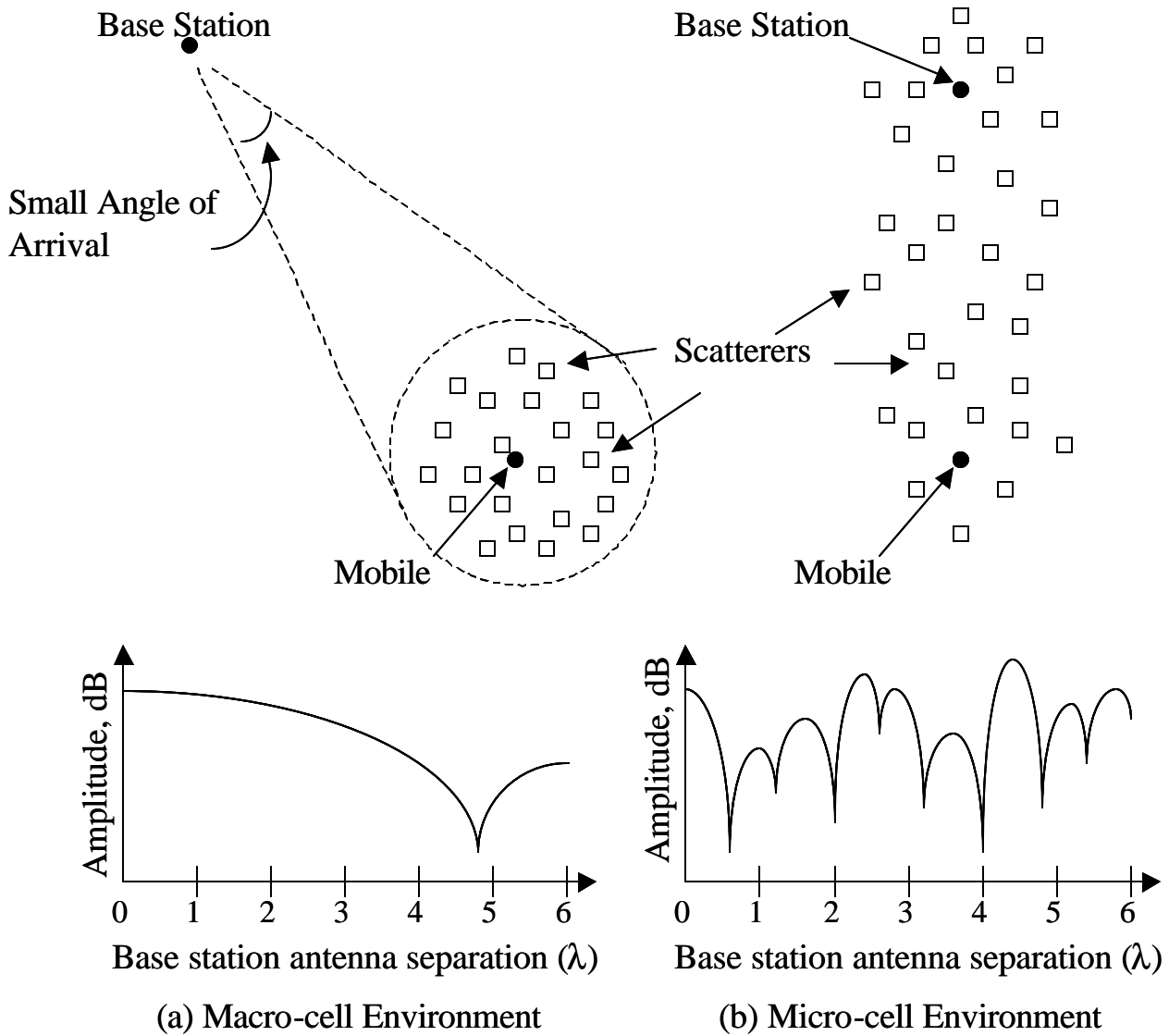


Figure 2.2 Fading rate of the received envelope as a function of distance in macro and micro-cellular channels.

2.3.4 Diversity Combining Techniques

There are several schemes for connecting or using diversity branches to improve system performance. The main techniques in use are *selection*, *equal gain*, and *maximal ratio combining*. When using selection diversity, the receiver monitors the signal-to-noise ratio of all branches and selects and uses the information from the branch with the largest SNR. Equal gain combining requires the receiver to coherently sum the signals received through all channels in order to increase the available signal-to-noise ratio at the receiver. The most effective of these three is maximal ratio combining because as its output it presents the receiver with a signal-to-noise ratio that is the direct sum of all individual SNRs in the branches. One of the drawbacks of maximal ratio combining is that the signal level and noise power at each branch need to be correctly estimated for all instances in time. This is fairly unrealistic in a practical system but the gains of this combining technique can be approached even if the required receiver estimations are not perfect for each branch. The following chapter examines these combining schemes in greater detail.

2.3.5 Diversity Gain

Diversity gain, G_D , is commonly used to quantify the gains achieved from a diversity system. Diversity gain is a function of envelope correlation, branch signal-to-noise ratio distribution (environment), number of branches, reliability or CDF percentage, and combining technique. The gain is usually measured as an improvement of signal-to-noise ratio over the strongest branch in the diversity system. In single branch systems, the signal level that is exceeded for a certain percentage of a time (or reliability) can be obtained from the cumulative distribution function of the envelope. A reliability of 90 percent refers to the signal level above which 90 percent of the time the signal is found and is equivalent to the 10 percent (100-90) level on the CDF curve. The signal after branch combining is examined for the signal level at the same reliability and the diversity gain is the increase in the level of signal after combining over the branch with the largest

SNR. Diversity gain by itself doesn't mean much unless quoted together with the reliability or CDF value at which the gain was measured. The advantage of using diversity gain is that it integrates all the diversity system and environment variables into one comparative measure. The mathematical formulations of diversity gain will be addressed in more detail in Chapter 8.

2.3.6 Interpretation of Diversity Measurements, and Extraction of Statistics

As mentioned earlier, diversity measurements are performed by transmitting a tone at a specific frequency and measuring the received envelope behavior as the receiver moves along the propagation environment. Wider bandwidth signals will have the same channel gain as single frequency measurements as long as both fall within the frequency range over which the channel is flat and slow fading. Slow fading ensures that the channel does not affect the modulation of the wider bandwidth signal and flat guarantees that the channel only introduces delay and applies a constant complex gain to the transmitted signal. Under these conditions, the broader band signal is not distorted and can only be signal-to-noise ratio limited when the channel attenuates the signal severely. The performance of the wider bandwidth signal hence depends on its symbol amplitude and shape and on the noise introduced by the channel.

Figure 2.3 shows example envelopes measured by a two-branch polarization diversity system under test at a frequency of 2.05 GHz [5]. The receiver uses vertical and horizontally polarized antennas as part of a two-branch polarization diversity system. Both antennas are identical dipoles receiving a constant wave from a stationary transmitter with a vertically polarized antenna. The direct radio path is blocked and the propagation environment is similar to that of a micro-cellular channel.

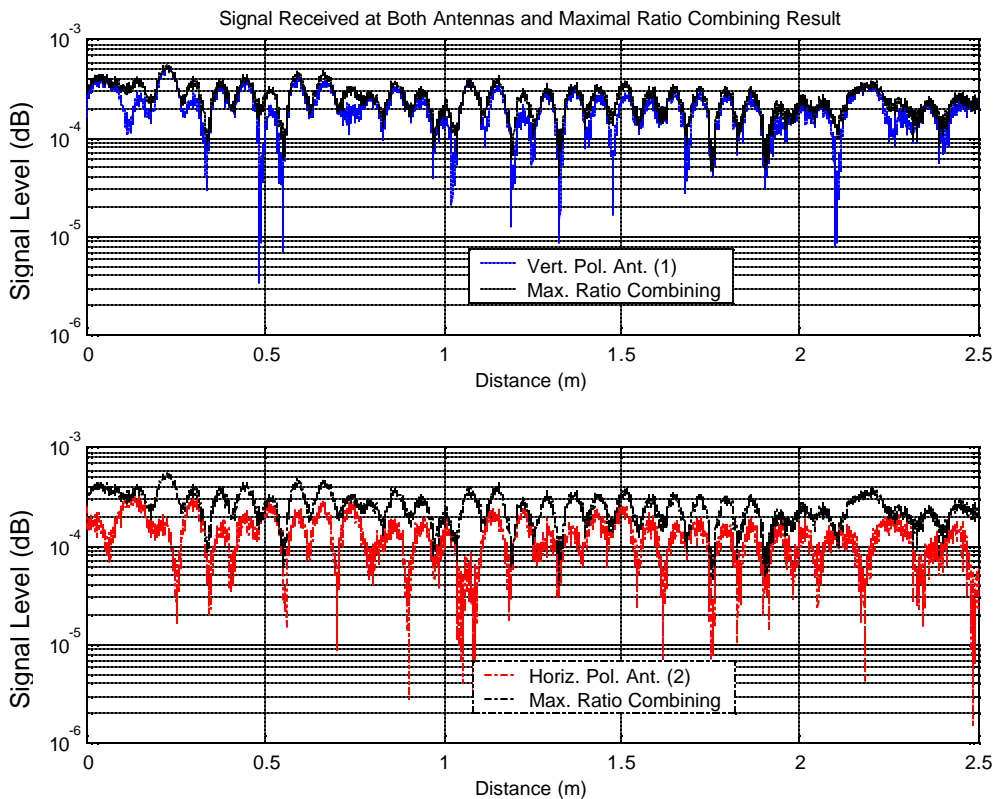


Figure 2.3 Envelopes received by a two-branch polarization diversity system using maximal ratio combining at 2.05 GHz. The upper (lower) plot shows the signal received by vertically (horizontally) polarized receive antenna compared to the combined output.

In this example the multipath components are arriving from approximately a 180° angle spread at the receiver. The solid line on both envelope graphs is identical and represents the maximal ratio combined signal of both branches. The top plot shows the variation of the envelope of the vertically polarized antenna over distance while the bottom plot that of the horizontally polarized element. The separation between fades in both channels is approximately once every wavelength ($\lambda=15$ cm) which is due to the angle spread of the multipath components. A 360° angle spread usually produces a fade approximately every $\lambda/2$. It can be clearly seen that the combined signal does not fade as severely as any of the envelopes in the two branches. A reason for this effect is the envelope correlation

between both branches in this example is $r=0.155$. The correlation between polarization diversity branches is usually lower than that of spatial diversity systems for a given antenna separation [2]; but unlike spatial diversity systems, polarization diversity usually experiences higher power imbalances between branches (or high differences in mean SNR). In this example the differences in mean signal-to-noise ratio between branches is 3.9 dB.

The cumulative distribution function of the signals gives a better indication of how much gain is actually achieved through diversity. Figure 2.4 shows the cumulative distribution function (CDF) of the individual branches and that of the combined signal of the diversity system in Figure 2.3. The CDF curves give a better indication of what fraction of time the signal is below a certain signal level. The diversity gain value can be directly read from the CDF curves. To illustrate how to read the CDF curves, the signal levels on antenna 1 and antenna 2 equal or exceed -96 and -89 dB for 99% of the time (ordinate value of 10^{-2}). The combined signal, constructed by applying maximal ratio combining to both branches, is equal or exceeds -82 dB for 99% of the time. Diversity gain is a measure of improvement in signal level over the strongest branch at a given reliability after diversity combining. It is found by measuring the horizontal distance between the combined signal and the largest branch for a given cumulative distribution value which in this case is 7 dB at the 1% CDF level. The diversity gain at the 10% CDF level (90% reliability) is 3.5 dB. From this example, it can be clearly seen that diversity gain is highly dependent on the reliability level. The CDF curves show that there is a very large improvement after combining at the lower end of the CDF curve which correspond to the signal levels when the received SNR is at its lowest. This is the desired effect and means that the combined signal experiences fewer deep fades than a single branch system.

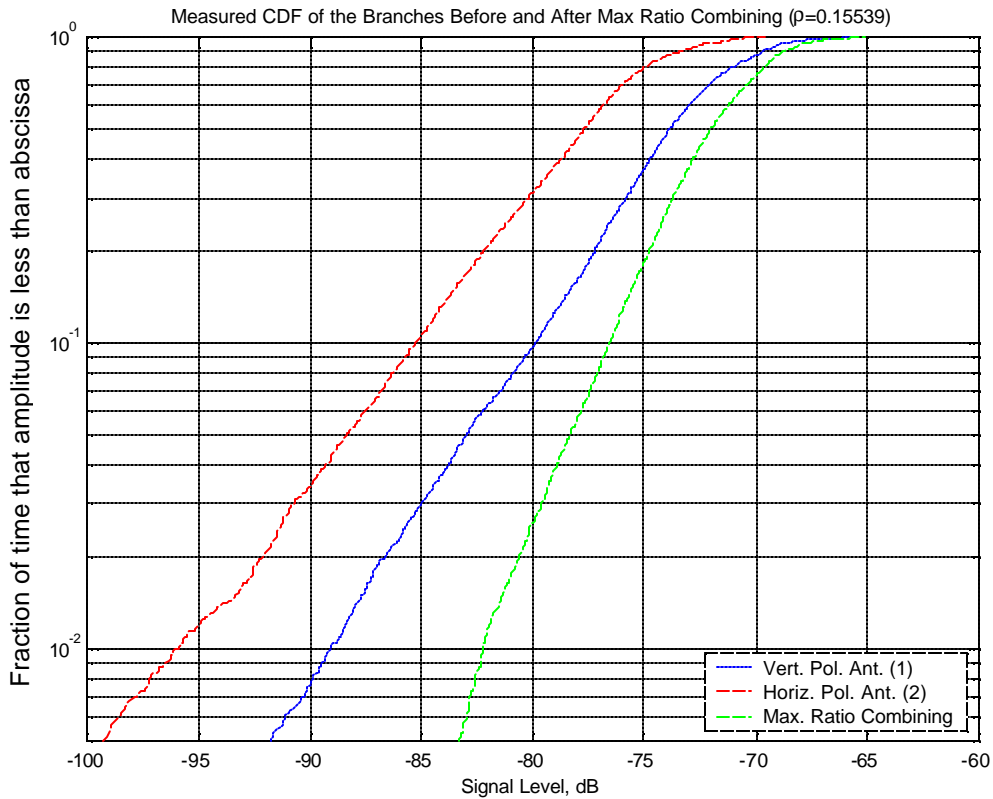


Figure 2.4 Cumulative distribution function of a two-branch polarization diversity system at 2.05 GHz for the example shown in Figure 2.3.

2.3.7 Additional Factors Affecting Diversity Systems

The environment has a considerable effect on the envelope correlation between the branches of a two-branch diversity system. At PCS frequencies (1850-1990 MHz), antennas on a hand set due to size constraint can be placed approximately half a wavelength apart or less. Depending on the angle spread this separation might be too small to achieve low correlation between the branches for all environments. When a second antenna element is introduced in the proximity of another, there is often coupling between both elements. Measurements show that the coupling can be significant at

separations less than half a wavelength distorting the antenna patterns of both elements due to this effect. The distorted antenna patterns function in part as a pattern diversity system in addition to the spatial diversity. This effect helps decorrelate the signals received at both elements even further allowing for close separations of the elements. More on this topic can be found in [3].

Diversity usually improves the signal-to-noise ratio but there are few instances when diversity can perform worse. This happens with equal gain combining when a branch introduces proportionally more noise than signal. This phenomenon will be addressed in more detail in a Chapter 4.

References:

- [1] W. C. Jakes, Ed., *Microwave Mobile Communications*, Wiley, New York, NY, 1974. (reprint IEEE Press, New York, 1993.)
- [2] A.M.D. Turkmani, A.A. Arowogolu, P.A. Jefford, and C.J. Kellent, "An Experimental Evaluation of Performance of Two-Branch Space and Polarization Diversity Schemes at 1800 MHz," *IEEE Trans. Veh. Tech.*, vol. 44, no.2, pp. 318-326, May 1995.
- [3] C. B. Dietrich, Jr., K. Dietze, J. R. Nealy, and W. L. Stutzman, "Spatial, Polarization, and Pattern Diversity for Wireless Handheld Terminals," *IEEE Antennas and Propagation*, *accepted for publication*.
- [4] W. C.-Y. Lee and Y. S. Yeh, "Polarization Diversity System for Mobile Radio," *IEEE Trans. On Communications*, vol. com-20, no.5, pp. 912-923, October 1972.
- [5] C. B. Dietrich, *Adaptive Arrays and Diversity Antenna Configurations for Handheld Wireless Communication Terminals*. PhD thesis, Virginia Polytechnic Institute and State University, 2000.

Chapter 3

Combining Schemes and the Rayleigh Channel

As mentioned in Chapter 2, diversity is an effective method for increasing the received signal-to-noise ratio of a wireless communication system in a flat fading channel. Diversity branches can be established through frequency, time, antenna, or any combination of these diversity mechanisms. Regardless of what methods are used to achieve diversity, the branch outputs can be processed using schemes such as selection, equal gain, or maximal ratio combining. The combining technique affects the performance of a diversity system and determines the attainable output signal-to-noise ratio.

The second part of this chapter will present a probabilistic approach to examine the makeup of Rayleigh fading channels. The assumptions that lead to a received envelope that is Rayleigh distributed will give an insight on what type of environments manifest this type of fading. Throughout this chapter, the assumptions that the signal of interest undergoes flat and slow fading will be made.

3.1 Diversity Combining Schemes

3.1.1 Selection Diversity

The principal diversity combining techniques are selection diversity, maximal ratio combining, and equal gain combining. Selection diversity, shown in Figure 3.1, is the simplest of these methods. From a collection of antennas, the branch that receives the signal with the largest signal-to-noise ratio at any time is selected and connected to the demodulator. As one would expect, the larger the number of available branches the higher the probability of having a larger signal-to-noise ratio (SNR) at the output. The remainder of this report will focus on two branch diversity systems in Rayleigh fading channels. Consequently all figures and derivations are presented with these parameters in mind.

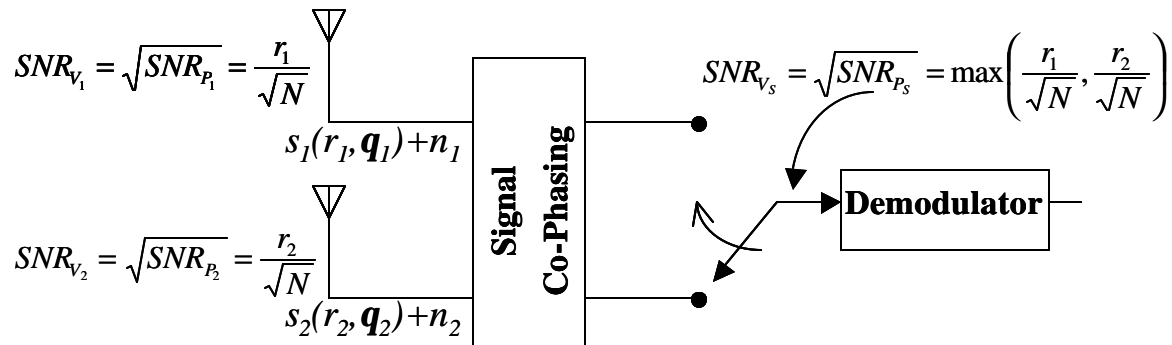


Figure 3.1 Block diagram of a two-branch selection diversity system for equal noise powers in both branches.

The inputs to the branches in Figure 3.1 are the Rayleigh signals s_1 and s_2 . The signals s_1 and s_2 are received with amplitudes r_1 and r_2 and with phases \mathbf{q}_1 and \mathbf{q}_2 respectively. The analysis that follows will primarily focus on the magnitude of the received envelopes (r_1 ,

r_2) since the value of these variables determines the strength of the received signals. s_1 and s_2 are assumed to be time synchronized and contain the same transmitted information but are received at the receiver with different strengths and phases due to the propagation effects of the channel. Both branches are corrupted by additive noise sources n_1 and n_2 respectively. n_1 and n_2 are identically distributed white Gaussian noise sources uncorrelated with each other and any of the input signals s_1 and s_2 . n_1, n_2 contain the lumped effects of all environmental and receiver noise sources which because of their number and distribution follow the central limit theorem and can be modeled as Gaussian. The noise sources arriving from the surroundings combine at each antenna differently and together with the receiver noise, which is unique for each receiver, ensures that signals n_1 and n_2 are very much uncorrelated. Both noise sources have unrestricted spectral content and are in similar environments (with identical antenna and receiver temperatures) and therefore the statistics for n_1 and n_2 are expected to be equivalent with a zero mean and a variance, or noise power, of N . The noise power can be evaluated by taking the expected value ($E[\cdot]$) of the noise signal squared or

$$P_N = E[n_1^2] = E[n_2^2] = \int_{-\infty}^{\infty} n_{1,2}^2 f_{N_{1,2}}(n_{1,2}) dn_{1,2} = N \quad (3.1)$$

$$f_{N_{1,2}}(n_{1,2}) = \frac{1}{\sqrt{2pN}} e^{-\frac{n_{1,2}^2}{2N}}$$

The first moment of the probability density function corresponds to the average signal level and is given by

$$E[n_1] = E[n_2] = \int_{-\infty}^{\infty} n_{1,2} f_{N_{1,2}}(n_{1,2}) dn_{1,2} = 0 \quad (3.2)$$

where $f_{N_{1,2}}(n_{1,2})$ is the probability density function of the noise in either of the branches. Additionally, each noise source is independent of either of the received signals s_1 and s_2 since the value of one noise variable does not in any way imply or restrict the value of any of the two signals. The signals r_1 and r_2 are assumed to vary much slower than the

noise such that during a short period of time these two received signals are relatively constant while the noise undergoes several random fluctuations (Fig. 3.3).

At a given instant (t_0) and receiver location, the receiver receives a signal with amplitude $r_1(t_0)$ and $r_2(t_0)$ at both branches. The strength of the received signals together with the noise power at that particular time determines the quality of the received information at that instant. The modulation/demodulation technique also affects the performance of a communication system and can usually be quantified from the knowledge of the received signal to noise ratio. If there is no noise and no inter-symbol-interference, an ideal receiver could correctly decipher the signal as long as a non-zero signal was received. In a flat fading environment, which is when the use of diversity is the most effective, the reliability (or quality) of the received information can be predicted from the SNR available at the demodulator stage.

At any given time the received signal power is defined, as is commonly done in communication systems, as the envelope squared or the power delivered to a 1Ω resistor. The signals $s_1(t_0)$ and $s_2(t_0)$ are corrupted by white noise over their duration which has an average power, or second moment, of N as given in (3.1). The signal-to-noise ratio at the input of each diversity branch is the ratio of instantaneous signal power to noise power, or $SNR_{P_{1,2}}(t_0)$. The subscripts 1 and 2 refer to channel, or branch, 1 and 2 of the diversity system. At time t_0 , the SNR_P received by each antenna element is therefore given by

$$SNR_{P_{1,2}}(t_0) = \frac{Power_{Signal}(t_0)}{Power_{Noise}(t_0)} = \frac{r_{1,2}(t_0)^2}{E[n_{1,2}^2]} = \frac{r_{1,2}(t_0)^2}{N} \quad (3.3)$$

The above result is the instantaneous signal-to-noise ratio at around the time t_0 over a period when the received envelopes are constant. In actuality, in a dynamic environment, the received signal envelopes do not remain constant for all time but instead fluctuate randomly. The $SNR_{P_{1,2}}$ is therefore also a random variable that depends on the distributions of the variables r_1 and r_2 over all events and which have statistics that are a function of the characteristics of the channel. Since the noise power, N , is assumed to be

constant; the characteristics of the distribution of $SNR_{P_{1,2}}$ depends directly on the distribution of the envelopes squared or $r_{1,2}^2$. The value of N (because of its invariance to time and location) does not alter the shape of the probability density function of $SNR_{P_{1,2}}$, it only contributes to the variance and therefore determines how wide the form is stretched. In practice, the distributions of r_1 and r_2 are determined through extensive site measurements.

What is almost exclusively measured when evaluating the performance of diversity system in a given channel are the received signal envelopes of the diversity branches or r_1 and r_2 . The success of the communications link is evaluated based on the distribution of the envelope statistics so it will be useful to express, especially when comparing theory to measured data, the result of the mathematics in terms of the voltage signal-to-noise ratio ($SNR_{V_{1,2}}$) instead of the power signal-to-noise ratio ($SNR_{P_{1,2}}$). The input voltage signal-to-noise ratio, or $SNR_{V_{1,2}}$, is the square root of the power SNR and is expressed as

$$SNR_{V_{1,2}} = \sqrt{SNR_{P_{1,2}}} = \frac{r_{1,2}}{\sqrt{N}} \quad (3.4)$$

The advantage of expressing the results in terms of the $SNR_{V_{1,2}}$ is that the distribution of this variable is proportional to the probability density function of the received envelopes. As mentioned earlier, the shape of the distributions SNR_{V_1} and SNR_{V_2} is going to be similar to the shapes of the received envelopes (r_1 and r_2) and the average signal and noise power will determine the variance of the probability density function.

Figure 3.1 shows the two-branch selection diversity system under analysis. For this configuration, the receiver monitors the signal-to-noise ratio of both channels and connects the branch with the largest SNR at any instant in time to the demodulator. In order to prevent phase discontinuities when the receiver switches between both branches, this occurs when one signal falls below the other and the receiver switches to the strongest branch, the signals in both channels are constantly co-phased. The voltage and

power signal-to-noise ratio (SNR_{V_S} and SNR_{P_S}) after selection combining is simply the maximum of both branches or equivalently

$$\begin{aligned} SNR_{P_S} &= \max(SNR_{P_1}, SNR_{P_2}) = \max\left(\frac{r_1^2}{N}, \frac{r_2^2}{N}\right) = \frac{1}{N} \max(r_1^2, r_2^2) \\ SNR_{V_S} &= \sqrt{SNR_{P_S}} = \max\left(\frac{r_1}{\sqrt{N}}, \frac{r_2}{\sqrt{N}}\right) = \frac{1}{\sqrt{N}} \max(r_1, r_2) \end{aligned} \quad (3.5)$$

The SNR_{P_S} and SNR_{V_S} are the output signal-to-noise ratios of the two-branch selection diversity system. The purpose of this report is to develop the means to quantify the gain of an ideal two-branch diversity combining scheme in a Rayleigh fading channel. The gain of the diversity configuration in Fig. 3.1 over a single branch receiver can be evaluated by examining the increase in signal-to-noise ratio from before to after selection combining. The factor including the noise variance $1/N$ (or $1/\sqrt{N}$ in the case of voltage SNR's), is present as a multiplicative constant in both the combined signal and the individual branch signal to noise ratios as can be seen in (3.5) and (3.3, 3.4) respectively. The gain (as a ratio) is independent of the value N since this constant divides out when evaluating improvement. The gain of the selection diversity system therefore only depends on the distributions of r_1 and r_2 in the case where both branches have equal noise power. This property can also be observed in systems that use maximal ratio and equal gain combining.

When performing gain measurements in an operational situation, the signal envelopes r_1 and r_2 are used as inputs to the diversity combiner and the output is obtained by selecting the maximum of both signal levels. This procedure does not account for noise power and is equivalent to evaluating the input and output SNR_V when the noise power is assumed to be unity; using $N=1$ in (3.5) gives

$$\begin{aligned} SNR_{V_{1,2}} |_{N=1} &= r_{1,2} \\ SNR_{V_S} |_{N=1} &= \sqrt{SNR_{P_S} |_{N=1}} = \max(r_1, r_2) \end{aligned} \quad \text{Selection Diversity (3.6)}$$

As stated earlier, this is sufficient information when examining the improvement of the diversity system over a single branch receiver in form of a gain parameter. In order to simplify the expression by one variable, the assumptions that $N=1$ will be made throughout this report. This procedure will comply with what is commonly done with measurements. It is important to note that no information is lost when setting the average noise power to unity since the envelopes r_1 and r_2 can also be interpreted as the input $SNR_{V_{1,2}}$ which includes the effects of N (3.4). Under these conditions ($N=1$), the input signal r_1 , for example, is not only the distribution of the amplitude of the signal but also the input SNR_{V_1} of branch 1 . In subsequent analysis, references will be made to branch signal power instead of average signal-to-noise ratio since these two values are equivalent when the assumptions that N is 1 are made.

A variation of selection diversity is *switched diversity*. Under this combining scheme, the receiver does not monitor all branches simultaneously as in selection diversity. The receiver begins connected to a branch and monitors its signal-to-noise ratio, if the SNR is above a certain threshold it stays connected to that branch. As soon as the SNR drops below the acceptable limit, the receiver picks the next available branch and measures its received SNR. If the SNR is acceptable, the receiver stays connected to the antenna otherwise it moves to a new branch and the process is repeated. The advantage of using the switched combining scheme is that it requires only a single receiver.

The equations for $SNR_{P_{1,2}}$ and $SNR_{V_{1,2}}$, (3.3) and (3.4), are the input signal-to-noise ratios at both branches that will also be used for the maximal ratio and equal gain diversity schemes.

3.1.2 Maximal Ratio Combining

Maximal ratio combining takes better advantage of all the diversity branches in the system. Fig. 3.2 shows this configuration for a two-branch diversity system. Both

branches are weighted by their respective instantaneous voltage-to-noise ratios. The branches are then co-phased prior to summing in order to insure that all branches are added in phase for maximum diversity gain. The summed signals are then used as the received signal and connected to the demodulator. Maximal ratio combining will always perform better than either selection diversity or equal gain combining because it is an optimum combiner [4]. The information on all channels is used with this technique to get a more reliable received signal. The disadvantage of maximal ratio is that it is complicated and requires accurate estimates of the instantaneous signal level and average noise power to achieve optimum performance with this combining scheme. The advantage is that improvements can be achieved with this configuration even when both branches are completely correlated.

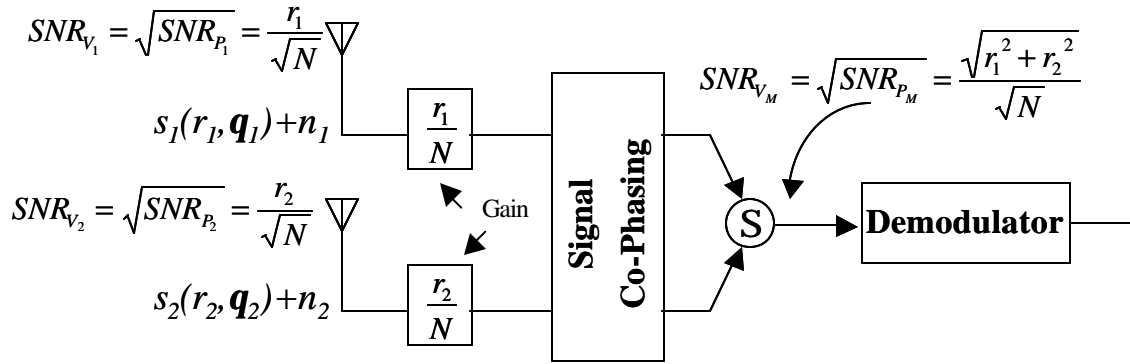


Figure 3.2. Block diagram of a two-branch maximal ratio combiner for equal noise powers in both branches.

The inputs to the maximal ratio combiner (Fig. 3.2) are both Rayleigh distributed signals (with envelopes r_1 and r_2) with additive independent noise voltage sources n_1 and n_2 . n_1 and n_2 are zero mean white Gaussian random variables with a variance of N ; see (3.1). As before, the input voltage signal-to-noise ratios are given by (3.3) and (3.4) are repeated here

$$SNR_{P_{1,2}} = \frac{r_{1,2}^2}{N} \quad (3.7)$$

$$SNR_{V_{1,2}} = \sqrt{SNR_{P_{1,2}}} = \frac{r_{1,2}}{\sqrt{N}}$$

The SNR after maximal ratio combining (MRC) requires the evaluation of the instantaneous signal power and noise power. The amplitude of the signal of interest after MRC at a given time t_0 , $V_{S,M}(t_0)$, can be evaluated by multiplying the received signal envelopes r_1 and r_2 , at t_0 , by their instantaneous voltage to noise power ratios which when summed gives

$$V_{S,M}(t_0) = r_1(t_0) \left(\frac{r_1(t_0)}{N} \right) + r_2(t_0) \left(\frac{r_2(t_0)}{N} \right) = \frac{r_1(t_0)^2 + r_2(t_0)^2}{N} \quad (3.8)$$

The instantaneous signal power after maximal ratio combining, $P_{S,M}(t_0)$, is defined as the signal squared or equivalently

$$P_{S,M}(t_0) = V_{S,M}(t_0)^2 = \left(\frac{r_1(t_0)^2 + r_2(t_0)^2}{N} \right)^2 \quad (3.9)$$

The noise component after MRC at t_0 , $V_{N,M}(t_0)$, is also multiplied by the gains in both branches and evaluates after co-phasing and branch addition to

$$V_{N,M}(t_0) = n_1 \left(\frac{r_1(t_0)}{N} \right) + n_2 \left(\frac{r_2(t_0)}{N} \right) = \frac{n_1 r_1(t_0) + n_2 r_2(t_0)}{N} \quad (3.10)$$

In this report, one of the assumptions is that the signal changes considerably slower than the noise. This assumption ensures that during the demodulation stage, the channel has not changed such that the received signals, $s_1(t_0)$ and $s_2(t_0)$, remain steady while the noise sources, n_1 and n_2 , which are of infinite frequency content, vary randomly over the duration of the steady received signals. This occurs when the channel exhibits slow fading conditions and the signal modulation is unaffected during the demodulation of the

message. Figure 3.3 describes such an example where a signal with amplitude r_x is constant over a period of time around the time t_0 while the noise n_x experiences several fluctuations. The instantaneous signal power over this interval is simply the envelope squared, or $r_x(t_0)^2$. The noise power, on the other hand, for a given event $r_x(t_0)$ is a stochastic variable whose power can be evaluated by computing the second moment of the probability density function of n_x . The noise power is given by

$$P_N = E[n_x^2] = \int_{-\infty}^{\infty} n_x^2 f_{N_x}(n_x) dn_x = N_x \quad (3.11)$$

where $E[\cdot]$ is the expected value operator and $f_{N_x}(n_x)$ is the probability density function of n_x . The subscript x can refer to the signals at either the individual branches or at the output of the diversity combiner.

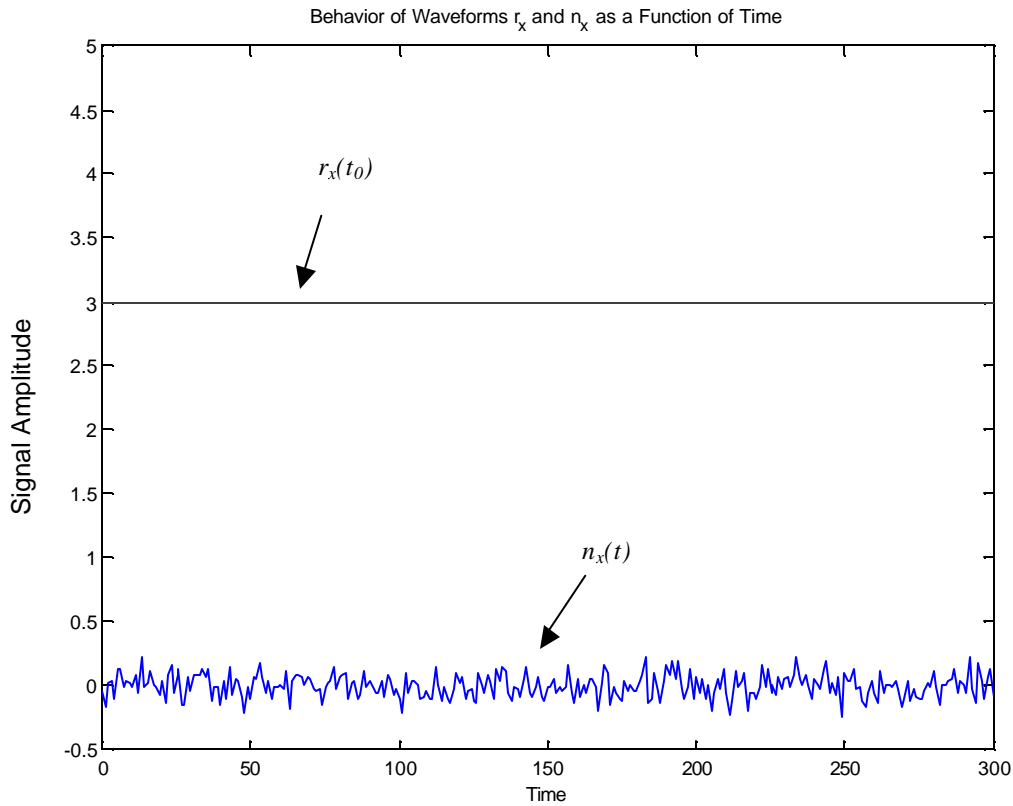


Figure 3.3 Behavior of the signal envelope r_x and the noise signal n_x around the time t_0 over a duration when the envelope r_x remains constant.

Similarly, at the output of the maximal ratio combiner, the signal power for a given event $r_1(t_0)$ and $r_2(t_0)$ is given by (3.9) while the output noise power, $P_{N,M}$, can be found by evaluating the expected value of the noise voltage squared expression in (3.10) or

$$P_{N,M}(t_0) = E[V_{N,M}(t_0)^2] = E\left[\frac{n_1^2 r_1(t_0)^2}{N^2} + \frac{2n_1 n_2 r_1(t_0) r_2(t_0)}{N^2} + \frac{n_2^2 r_2(t_0)^2}{N^2}\right] \quad (3.12)$$

$$P_{N,M}(t_0) = E\left[\frac{n_1^2 r_1(t_0)^2}{N^2}\right] + E\left[\frac{2n_1 n_2 r_1(t_0) r_2(t_0)}{N^2}\right] + E\left[\frac{n_2^2 r_2(t_0)^2}{N^2}\right]$$

The middle term evaluates to zero since each noise source is independent of all other signals and has a mean of zero. Simplifying (3.12) further, by noting that the expected value is performed given steady signals $r_1(t_0)$ and $r_2(t_0)$ which factor out of the operator as constants and produce the following result for the noise power at the output of the maximal ratio combiner at time t_0

$$P_{N,M}(t_0) = E\left[\frac{n_1^2 r_1(t_0)^2}{N^2}\right] + E\left[\frac{n_2^2 r_2(t_0)^2}{N^2}\right] \quad (3.13)$$

$$P_{N,M}(t_0) = \frac{r_1(t_0)^2}{N^2} E[n_1^2] + \frac{r_2(t_0)^2}{N^2} E[n_2^2] = \frac{r_1(t_0)^2 + r_2(t_0)^2}{N}$$

The output signal to noise ratio, $SNR_{P,M}$, at t_0 after maximal ratio combining is given by the ratio of signal to noise power or the division of (3.9) and (3.13) which gives

$$SNR_{P_M}(t_0) = \frac{Power_{Signal}}{Power_{Noise}} = \frac{P_{S,M}(t_0)}{P_{N,M}(t_0)} = \frac{V_{S,M}(t_0)^2}{E[V_{N,M}(t_0)^2]} \quad (3.14)$$

$$SNR_{P_M}(t_0) = \frac{r_1(t_0)^2 + r_2(t_0)^2}{N} = \frac{1}{N} (r_1(t_0)^2 + r_2(t_0)^2)$$

The output SNR_{V_M} , or the voltage signal-to-noise ratio after MRC, allows for a direct comparison between theory and measured data. The SNR_{V_M} is defined as the square root of the SNR_{P_M} and is given by

$$SNR_{V_M}(t_0) = \sqrt{SNR_{P_M}(t_0)} = \sqrt{\frac{r_1(t_0)^2 + r_2(t_0)^2}{N}} = \frac{1}{\sqrt{N}} \sqrt{r_1(t_0)^2 + r_2(t_0)^2} \quad (3.15)$$

As stated earlier, the goal of this research is to quantifying the improvement between systems using two-branch diversity over ones with just a single branch in a Rayleigh fading channel. As before, the gain (as a ratio) between the signal to noise ratio after maximal ratio combining and a single branch is independent of the noise power N . From (3.7) and (3.14) ((3.7) and (3.15) for the SNR_V) the factor $1/N$ ($1/\sqrt{N}$ for SNR_V) will cancel when dividing these two equations. The gain (as a ratio), again, is not a function of N and therefore depends solely on the distributions of r_1 and r_2 when both branches have equal noise power. In subsequent chapters, when examining the advantage of one configuration over the other the noise power (N) in both branches will be set to unity to simplify the output SNR expressions by one variable which in turn should not affect the final gain result. The equations for output SNR after diversity combining are derived in Chapter 5 and 6 with the branch noise power set to unity. The exact signal-to-noise ratios after combining can be computed from these expressions with the knowledge of N and by using the input SNR_{V_1} and SNR_{V_2} in place of r_1 and r_2 respectively for the expression of the output SNR.

The signal-to-noise ratio after two-branch maximal ratio combining with N set to unity can be computed from (3.14) and (3.15) and are given by

$$SNR_{P_M} |_{N=1} = r_1^2 + r_2^2 \quad \text{Maximal Ratio Combining} \quad (3.16)$$

$$SNR_{V_M} |_{N=1} = \sqrt{r_1^2 + r_2^2}$$

Finally the last diversity combining technique addressed in this report is equal gain combining.

3.1.3 Equal Gain Combining

Equal gain combining (EGC) can be viewed as a special case of maximal ratio combining (see Fig 3.4). In this scheme the gains of the branches are all set to a predetermined value and are not changed. As with the previous case, both branch signals are multiplied by the same branch gain (G) and the resulting signals are co-phased and summed. The resultant output signal is connected to the demodulator.

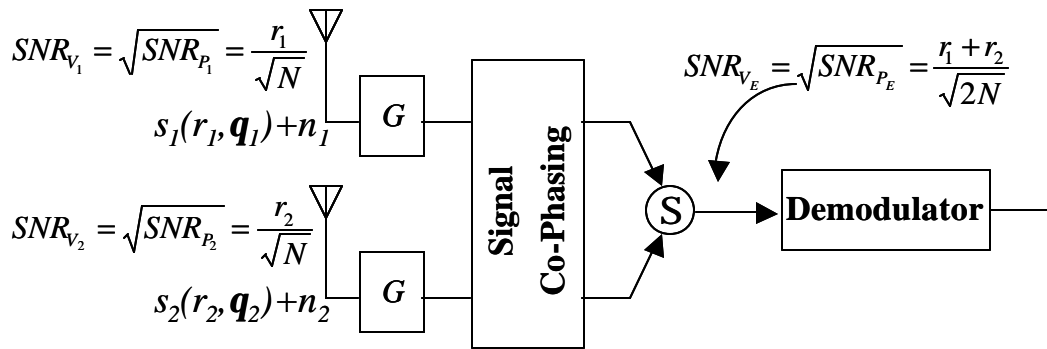


Figure 3.4 Block diagram of a two-branch equal gain combiner for equal noise powers in both branches.

As before, the signals arriving at both branches from the transmitter have envelopes given by r_1 and r_2 and have a distribution described by a Rayleigh probability density function. Both received signals are corrupted by white Gaussian noise sources n_1 and n_2 . Fig. 3.4 describes the equal gain combining technique in which all branches are pre-multiplied by G and then co-phased, such that the amplitude of the output signal is the direct addition of branch envelopes. The signal envelope after equal gain combining at a time t_0 is

$$V_{S,E}(t_0) = r_1(t_0)(G) + r_2(t_0)(G) = G(r_1(t_0) + r_2(t_0)) \quad (3.17)$$

The instantaneous signal power, $P_{S,E}(t_0)$, is given by the envelope squared or

$$P_{S,E}(t_0) = V_{S,E}(t_0)^2 = G^2(r_1(t_0) + r_2(t_0))^2 \quad (3.18)$$

The noise component after EGC for all time t , $V_{N,E}(t)$, also gets multiplied by the gain G in both branches and evaluates after co-phasing and branch addition to

$$V_{N,E}(t) = n_1(G) + n_2(G) = G(n_1 + n_2) \quad (3.19)$$

The noise power, on the other hand, for a given event $r_1(t_0)$ and $r_2(t_0)$ is a stochastic variable whose power can be evaluated by computing the second moment of the probability density function of $V_{N,E}$. The noise power, $P_{N,E}$, is given by (3.11) and with (3.19) becomes

$$\begin{aligned} P_{N,E}(t) &= E[V_{N,E}(t)^2] = E[G^2(n_1^2 + 2n_1n_2 + n_2^2)] \\ P_{N,E}(t) &= E[V_{N,E}(t)^2] = G^2 E[n_1^2] + 2G^2 E[n_1n_2] + G^2 E[n_2^2] \end{aligned} \quad (3.20)$$

The constant G^2 factors out of the expected value operator and the middle term involving the joint expectation of n_1 and n_2 evaluates to zero. The output noise power after equal gain combining evaluates to

$$P_{N,E}(t) = E[V_{N,E}(t)^2] = G^2 E[n_1^2] + G^2 E[n_2^2] = 2G^2 N \quad (3.21)$$

The instantaneous power signal-to-noise ratio is the ratio of signal to noise power and at t_0 evaluates to

$$\begin{aligned}
SNR_{P_E}(t_0) &= \frac{Power_{Signal}}{Power_{Noise}} = \frac{P_{S,E}(t_0)}{P_{N,E}(t)} = \frac{V_{S,E}(t_0)^2}{E[V_{N,E}(t)^2]} \\
SNR_{P_E}(t_0) &= \frac{G^2(r_1(t_0) + r_2(t_0))^2}{2G^2N} = \frac{1}{2N}(r_1(t_0) + r_2(t_0))^2
\end{aligned} \tag{3.22}$$

Similarly, the voltage signal-to-noise ratio, or $SNR_{V_E}(t_0)$, after equal gain combining can be computed from (3.22) and gives

$$SNR_{V_E}(t_0) = \sqrt{SNR_{P_E}} = \frac{1}{\sqrt{2N}}(r_1(t_0) + r_2(t_0)) \tag{3.23}$$

Since the value of G does not affect the output signal-to-noise ratio, this value is usually set to unity in practical applications. It is interesting to note that unlike selection diversity and maximal ratio combining, equal gain combining has the potential of performing worse after combining than selecting the branch with the largest signal-to-noise ratio. From (3.23) it can be seen that if the magnitude of r_2 at t_0 obeys the following constraint

$$r_2(t_0) < (\sqrt{2} - 1)r_1(t_0) \approx 0.414r_1(t_0) \tag{3.24}$$

the output signal-to-noise ratio after EGC, SNR_{V_E} , is less than the signal to noise ratio received at branch 1, or SNR_{V_1} . For these instances the use of equal gain combining actually deteriorates the SNR when compared to just picking the strongest branch. The signal-to-noise ratio after combining decreases under these circumstances because the second branch introduces proportionally more noise than signal to the output. This phenomenon will also be observed in the diversity gain plots presented in Chapter 8 for equal gain combining.

Section 3.1 introduced the three diversity combining mechanisms that are considered in this thesis (selection, equal gain, and maximal ratio combining). The performance of these combining schemes will be evaluated for Rayleigh fading channels. The Rayleigh

channel occurs often in multiple reflective non-dispersive environments such as the ones found in urban and indoor environments.

The following section describes a ray based multipath signal environment impinging on the receive antenna. The goal is to predict the probability density function of the received signal for this type of surroundings and under what assumptions the statistics become Rayleigh distributed. This analysis will give an insight on what type of environments manifest this type of fading.

3.2 Analysis of Rayleigh Fading Channels

Clarke [1] proposed a model where the signal received by an antenna element in a static environment from a constant wave transmitter can be modeled as a sum of a total of N multipath components as follows

$$\begin{aligned}
 E_z &= \sum_{n=1}^N A_n \cos(\mathbf{w}_c t + \mathbf{f}_n) \\
 E_z &= \sum_{n=1}^N A_n \cos \mathbf{f}_n \cos \mathbf{w}_c t - \sum_{n=1}^N A_n \sin \mathbf{f}_n \sin \mathbf{w}_c t \\
 E_z &= K_I \cos \mathbf{w}_c t - K_Q \sin \mathbf{w}_c t
 \end{aligned} \tag{3.25}$$

$$\begin{aligned}
 K_I &= \sum_{n=1}^N A_n \cos \mathbf{f}_n \\
 K_Q &= \sum_{n=1}^N A_n \sin \mathbf{f}_n
 \end{aligned} \tag{3.26}$$

where A_n is the amplitude of the individual multipath components and \mathbf{f}_n is the phase. Figure 3.5 depicts an example scenario in which five multipath components are arriving at the receiver from different angles in the azimuth plane.

The following paragraphs examine the above signal environment stochastically to evaluate the distribution of the received envelope at the antenna element. The signals are

assumed to arrive in the azimuth plane where the receiving antenna has an omnidirectional pattern. To simplify this analysis requires expanding the expression for the received signal and grouping the factors multiplying $\cos \mathbf{w}_c t$ and $\sin \mathbf{w}_c t$ into separate components as was done in (3.26). K_I corresponds to the factors multiplying the in-phase carrier, or $\cos \mathbf{w}_c t$, while K_Q is the summation of terms multiplying the quadrature carrier, or $\sin \mathbf{w}_c t$.

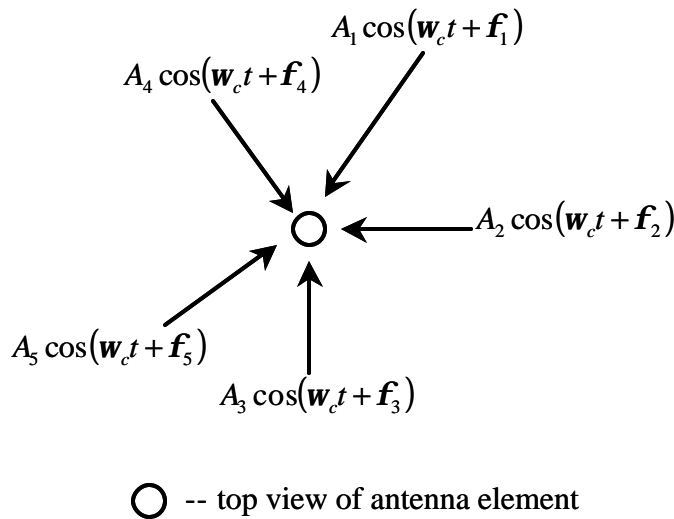


Figure 3.5. A scenario where five multipath components are arriving at an antenna element in the azimuth plane

The statistical distributions of the phases and amplitudes and their interrelationships determine the distribution of the received signal. The phase, \mathbf{f}_n , depends on a combination of factors including the distance and medium in which the signal travels as well as on the phase alterations that are introduced by objects obstructing the propagation path. The phase of a wave changes by 180° (or \mathbf{p}) for every half wavelength the signal travels (which corresponds to 7.5 cm at 2 GHz). As long as the distance covered by a traveling wave from the transmitter to the receiver is several wavelengths and/or its path is blocked by obstructions that introduce random phases, the phase of an impinging multipath component can take on any value and hence will be distributed with equal

likelihood between 0 and 2π . Additionally, if each of the arriving signal components travels along dissimilar paths and encounters unlike obstructions and propagation distances it is safe to expect that all components have phases that are independent of each other. As for the amplitudes, A_n , their distribution is a function of the traveled distance as well as the signal attenuation experienced by propagating through an environment with non-ideal reflections, transmission, and scattering. If as before, each multipath travels through different paths, all amplitude components are also expected to have statistics that are independent of each other. Summarizing, all amplitudes, A_n 's, and all phases, \mathbf{f}_n 's, are independent of each other or

$$E[A_n A_m] = E[A_n]E[A_m] \quad \forall n, m \text{ except when } m=n \quad (3.27)$$

$$E[\mathbf{f}_n \mathbf{f}_m] = E[\mathbf{f}_n]E[\mathbf{f}_m] \quad \forall n, m \text{ except when } m=n \quad (3.28)$$

The operator $E[\cdot]$ is the expected value of the term in the brackets. Additionally, from the received amplitude the phase of the wave cannot be implied or determined. Also, there is no association between the phase of one component and the amplitude on another component. These relations imply independence and can mathematically be expressed as

$$E[A_n \mathbf{f}_n] = E[A_n]E[\mathbf{f}_n] \quad \forall n \quad (3.29)$$

and

$$E[A_n \mathbf{f}_m] = E[A_n]E[\mathbf{f}_m] \quad \forall n, m \quad (3.30)$$

The interrelationships between the signal components arriving at the receive antenna will aid in determining the probability density function of the received envelope. As noted earlier, to simplify the analysis it is best to approach the problem by analyzing the terms associated with the in-phase and quadrature carrier as a group (K_I and K_Q).

The relationship between the in-phase and quadrature components, K_I and K_Q , will be useful in subsequent analysis and can be found by taking the joint expected value of these two random variables. The correlation between the K_I and K_Q components can be written as

$$E[K_I K_Q] = \int_{A_1} \dots \int_{A_N} \int_{\mathbf{f}_1} \dots \int_{\mathbf{f}_N} \sum_{n=1}^N A_n \cos \mathbf{f}_n \sum_{m=1}^N A_m \sin \mathbf{f}_m f_{A_1 \dots A_N \Phi_1 \dots \Phi_N}(A_1, \dots, A_N, \mathbf{f}_1, \dots, \mathbf{f}_N) dA_1 \dots dA_N d\mathbf{f}_1 \dots d\mathbf{f}_N \quad (3.31)$$

or equivalently

$$E[K_I K_Q] = \sum_{n=1}^N \sum_{m=1}^N \int \int \int \int A_n A_m \cos \mathbf{f}_n \sin \mathbf{f}_m f_{A_n A_m \Phi_n \Phi_m}(A_n, A_m, \mathbf{f}_n, \mathbf{f}_m) dA_n dA_m d\mathbf{f}_n d\mathbf{f}_m \quad (3.32)$$

after factoring out the summations and integrating out the non-dependent variables. As before, $E[\cdot]$ is the expected value operator. $f_{A_1 \dots A_N \Phi_1 \dots \Phi_N}(A_1, \dots, A_N, \mathbf{f}_1, \dots, \mathbf{f}_N)$ is the joint probability density of all A_n and \mathbf{f}_n while $f_{A_n A_m \Phi_n \Phi_m}(A_n, A_m, \mathbf{f}_n, \mathbf{f}_m)$ is the joint probability of A_n, A_m, \mathbf{f}_n , and \mathbf{f}_m .

As previously noted, all A_n 's are independent of each other and of any of the phases \mathbf{f}_n . With this in mind, equation (3.32) can be rewritten as follows

$$\begin{aligned} E[K_I K_Q] &= \sum_{n=1}^N \sum_{m=1}^N E[A_n A_m] \int \int \cos \mathbf{f}_n \sin \mathbf{f}_m f_{\Phi_n \Phi_m}(\mathbf{f}_n, \mathbf{f}_m) d\mathbf{f}_n d\mathbf{f}_m \\ E[K_I K_Q] &= \sum_{n=1}^N \sum_{m=1}^N E[A_n A_m] E[\cos \mathbf{f}_n \sin \mathbf{f}_m] \end{aligned} \quad (3.33)$$

$$E[K_I K_Q] = E[A_1^2] E[\cos \mathbf{f}_1 \sin \mathbf{f}_1] + E[A_1] E[A_2] E[\cos \mathbf{f}_1] E[\sin \mathbf{f}_2] + \dots + E[A_N^2] E[\cos \mathbf{f}_N \sin \mathbf{f}_N]$$

Concentrating on the expected values involving \mathbf{f}_n and \mathbf{f}_m the following results can be established:

$$\begin{aligned}
E[\cos \mathbf{f}_n] &= \int_0^{2\mathbf{p}} \cos \mathbf{f}_n f_{\Phi_n}(\mathbf{f}_n) d\mathbf{f}_n = \int_0^{2\mathbf{p}} \cos \mathbf{f}_n \frac{1}{2\mathbf{p}} d\mathbf{f}_n = 0 \\
E[\cos \mathbf{f}_n \sin \mathbf{f}_n] &= \int_0^{2\mathbf{p}} \cos \mathbf{f}_n \sin \mathbf{f}_n f_{\Phi_n}(\mathbf{f}_n) d\mathbf{f}_n = \int_0^{2\mathbf{p}} \cos \mathbf{f}_n \sin \mathbf{f}_n \frac{1}{2\mathbf{p}} d\mathbf{f}_n = 0
\end{aligned} \tag{3.34}$$

By substituting the results from (3.34) into the last equation of (3.33) it can be concluded that the in-phase component K_I and the quadrature component K_Q are uncorrelated or

$$E[K_I K_Q] = 0 \tag{3.35}$$

As stated earlier, K_I and K_Q are summations of random variables involving the probability density functions of all A_n 's and \mathbf{f}_n 's as described by (3.26).

The purpose of this analysis is to find the distribution of the received envelope by the antenna element. The result can be found by summing the effects of all the individual multipath components. To simplify this analysis requires the introduction of two variables, H_n and T_n , which are defined as

$$\begin{aligned}
H_n &= A_n \cos \mathbf{f}_n \\
T_n &= A_n \sin \mathbf{f}_n
\end{aligned} \tag{3.36}$$

which are the in-phase and quadrature components of each individual multipath components. K_I and K_Q can be rewritten as

$$\begin{aligned}
K_I &= \sum_{n=1}^N H_n \\
K_Q &= \sum_{n=1}^N T_n
\end{aligned} \tag{3.37}$$

Equation (3.37) suggests that the probability density function of K_I , $f_{K_I}(K_I)$, is a result of the summation of N random variables having a probability distribution given by $f_{H_n}(H_n)$.

The probability density function $f_{H_n}(H_n)$ has a mean that is

$$E[H_n] = E[A_n \cos \mathbf{f}_n] = E[A_n] \int_0^{2\mathbf{p}} \cos \mathbf{f}_n \frac{1}{2\mathbf{p}} d\mathbf{f}_n = 0 \quad (3.38)$$

and a variance given by

$$E[H_n^2] = E[A_n^2 \cos^2 \mathbf{f}_n] = E[A_n^2] \int_0^{2\mathbf{p}} \cos^2 \mathbf{f}_n \frac{1}{2\mathbf{p}} d\mathbf{f}_n = \frac{1}{2} E[A_n^2] \quad (3.39)$$

Similarly, the random variables that make up K_Q , have a probability density function described by $f_{T_n}(T_n)$ and have a mean and variance given by

$$E[T_n] = E[A_n \sin \mathbf{f}_n] = E[A_n] \int_0^{2\mathbf{p}} \sin \mathbf{f}_n \frac{1}{2\mathbf{p}} d\mathbf{f}_n = 0 \quad (3.40)$$

$$E[T_n^2] = E[A_n^2 \sin^2 \mathbf{f}_n] = E[A_n^2] \int_0^{2\mathbf{p}} \sin^2 \mathbf{f}_n \frac{1}{2\mathbf{p}} d\mathbf{f}_n = \frac{1}{2} E[A_n^2] \quad (3.41)$$

It can also be shown that any two of the stochastic variables H_n and T_n are independent and uncorrelated of each other

$$\begin{aligned} E[H_n H_m] &= E[H_n] E[H_m] = 0 \\ E[T_n T_m] &= E[T_n] E[T_m] = 0 \end{aligned} \quad \forall m, n \text{ except when } m=n \quad (3.42)$$

Summarizing, the random variables K_I and K_Q are independent of each other and are the result of the summation of N independent random variables (H_n and T_n) that have a mean of zero and a variance of $\frac{1}{2} E[A_n^2]$. A summation of N independent random variables creates a new signal whose probability density function (pdf) can be computed by convolving the pdf's of all N random variables [2] as follows

$$\begin{aligned}
f_{K_I}(K_I) &= f_{H_1}(H_1) * f_{H_2}(H_2) * \dots * f_{H_N}(H_N) \\
f_{K_Q}(K_Q) &= f_{T_1}(T_1) * f_{T_2}(T_2) * \dots * f_{T_N}(T_N)
\end{aligned} \tag{3.43}$$

$$\begin{aligned}
E[K_I] &= E[K_Q] = \sum_{n=1}^N E[H_n] = \sum_{n=1}^N E[T_n] = 0 \\
E[K_I^2] &= E[K_Q^2] = \sum_{n=1}^N E[H_n^2] = \sum_{n=1}^N E[T_n^2] = \frac{1}{2} \sum_{n=1}^N E[A_n^2] = \mathbf{s}^2
\end{aligned} \tag{3.44}$$

where the * operator represents convolution. The central limit theorem states that as the number of random variables (N) increases, the probability density functions $f_{K_Q}(K_Q)$ and $f_{K_I}(K_I)$ approach a Gaussian probability density function. This occurs as long as the random variables H_n and T_n are zero mean and have individual variances that are small compared to the sum of all the variances [2]. In a multipath environment, about 5 or 6 multipath components (N) are needed to make the distributions of the random variables K_I and K_Q very much Gaussian when they are identically distributed. Additionally, as long as the variance of any individual component of A_n is much smaller than the sum of the variances of all the other components, or

$$E[A_n^2] \ll \sum_{n=1}^N E[A_n^2] \tag{3.45}$$

for all n not all the random variables H_n and T_n have to be identically distributed to produce a signal with a Gaussian distribution.

From the previous discussion, an antenna can be modeled as

$$E_z = K_I \cos \mathbf{v}_c t - K_Q \sin \mathbf{v}_c t \tag{3.46}$$

In an environment with multipath where all the arriving signals are identically distributed in amplitude and the number of these impinging waves (N) is large, the signals K_I and K_Q

will be Gaussian distributed with zero mean and equal variance. Mathematically, K_I and K_Q , have a probability density function given by

$$\begin{aligned} f_{K_I}(k_I) &= \frac{1}{\sqrt{2ps^2}} e^{-\frac{k_I^2}{2s^2}} \\ f_{K_Q}(k_Q) &= \frac{1}{\sqrt{2ps^2}} e^{-\frac{k_Q^2}{2s^2}} \end{aligned} \quad (3.47)$$

where s^2 is the variance of K_I and of K_Q .

From (3.35) it was found that both K_I and K_Q are uncorrelated and from (3.44) both signals have equal variance and are zero mean. In a flat fading channel, the envelope distribution of the signal received is important since the power of the received signal, which is related to the envelope and not the phase, has a direct influence on the signal-to-noise ratio. The envelope of the signal received by the antenna, or $|E_z|$, can be evaluated by taking the square root of the sum of squares as follows

$$|E_z| = r = \sqrt{K_I^2 + K_Q^2} \quad (3.48)$$

The probability density function of $|E_z|$ is a well known result in probability theory when K_I and K_Q are zero mean, equal variance, uncorrelated Gaussian random variables [2]. The probability density function of the signal r (or $|E_z|$) can be described by using a Rayleigh distribution and is given by

$$f_R(r) = \frac{r}{s^2} e^{-\frac{r^2}{2s^2}} \text{ for } r \geq 0 \quad (3.49)$$

where s^2 is the variance of K_I and of K_Q (3.44).

The value \mathbf{s} is a function of the average power of the envelope received by the antenna. Often the *cumulative distribution function (cdf)* of the received signal is examined which is the integral of (3.49) or the probability that the envelope is less than a certain value r . For a Rayleigh channel, the cdf is given by $F_R(r)$ and mathematically expressed as

$$F_R(r) = \int_{-\infty}^r f_R(r) dr = 1 - e^{-\frac{r^2}{2s^2}} \quad \text{for } r \geq 0 \quad (3.50)$$

In some cases there is a dominant multipath or direct line of sight component present such as the assumptions of (3.45) no longer hold. These types of channels can be usually modeled with a Ricean probability distribution. It could also be that not enough components are present in the signal environment for the central limit theorem to hold giving rise to non-Rayleigh characteristics. Rayleigh channels commonly occur in wireless communications and by the analysis presented in this chapter occur when multiple signals with equal distributed amplitudes and random phases impinge on the antenna. The remainder of this thesis will examine the performance of a two-branch diversity system in a Rayleigh channel because of its importance and the frequency of occurrence of this channel in practice.

The model discussed in this chapter is a two dimensional model that assumes that the incoming signals are limited to the azimuth plane in the presence of an omni directional antenna element. In reality, this model also applies to three-dimensional propagation with arbitrary antenna patterns. As far as the antenna is concerned, the signals received by it are still one-dimensional because its output is the superposition of scaled versions of the received signals as a function of time. With what strength the individual multipath components contribute to the output signal depends heavily on the propagation loss, the polarization mismatch, and the angle of arrival with respect to the antenna. For arbitrary arrival angles and non-uniform antenna patterns, the analysis is similar to the one described in this section except that the distributions of the amplitudes A_n need to account for more than just propagation loss but also polarization mismatch. Since the antenna pattern essentially weights each signal by the radiation pattern based on the angle of

arrival of the signal components, the distributions of the individual A_n 's will also be a function of the received angle. If the probability density functions of all A_n 's are still equally distributed (after accounting for angle of arrival effects on the antenna pattern, propagation loss, as well as any polarization mismatches) or follow equation (3.45), the received envelope will still exhibit Rayleigh behavior.

References:

- [1] R.H. Clarke, "A Statistical Theory of Mobile Radio Reception," *Bell Sys. Tech. J.*, 47, pp. 957-1000, July 1968.
- [2] Henry Stark and John W. Woods, *Probability, Random Processes, and Estimation Theory for Engineers*, Perentice Hall, Englewood Cliffs, NJ, 1994.
- [3] W. C. Jakes, Ed., *Microwave Mobile Communications*, Wiley, New York, NY, 1974. (reprint IEEE Press, New York, 1993.)
- [4] John G. Proakis, *Digital Communciations*, McGraw-Hill, New York, NY, 1995.

Chapter 4

Evaluation of the Joint Probability Density Function of Two Correlated and Unbalanced Rayleigh Signals

The focus of this report is to develop a theoretical model that will statistically predict the performance of a two-branch selection and maximal ratio combiner in a Rayleigh channel. In practice, the combining algorithm is applied in the time domain to the signals received at both diversity branches. The statistical performance, however, is evaluated by observing the rate of occurrence of the signal-to-noise ratio before and after combining. In this report, a probabilistic approach will be taken to predict the statistical distributions of the signal-to-noise ratio after two-branch selection and maximal ratio combining. In Chapter 8, the results of a measurement campaign are presented that verify the agreement between theoretical and measurement results.

In this chapter, a probabilistic approach is used to examine the effects of unbalanced branches and correlation on the performance of a two-branch diversity system in a Rayleigh fading channel. The analysis starts by decomposing the received signals into their in-phase and quadrature components as was done in Chapter 3. These components are random variables that have a Gaussian distribution as was previously shown (3.47).

The received signals in both branches can potentially be correlated and have unequal average received powers as was discussed in Chapter 2. An envelope correlation between both branch signals can be decomposed into a set of correlations relating the Gaussian subcomponents of both branches. This set of correlations, which includes the cross and auto correlations of all Gaussian subcomponents, when set correctly produce an equivalent received envelope correlation. Additionally, changing the Gaussian auto-correlations can set the average branch power of both Rayleigh branches. This chapter examines how the Gaussian inter-correlations affect the envelope correlation as well as the individual branch powers.

An expression for the joint probability density function (pdf) of both received Rayleigh signal envelopes, which can possibly be correlated and have unbalanced powers, will be developed in this chapter. The joint pdf will be used in the following chapters to develop an expression for the distribution of the signal-to-noise ratio after selection and maximal ratio combining in a Rayleigh channel. As a side note, the word moment, expected value, and correlation will be used interchangeably throughout the analysis to denote the same mathematical operation.

4.1 Separating Two Rayleigh Signals Into Gaussian Components

The signals received by two branches of the diversity system in a Rayleigh channel can be expressed as the sum of the in-phase, $\cos(\omega t)$, and quadrature, $\sin(\omega t)$ components. $S_1(t)$ is the signal received by antenna 1 while $S_2(t)$ is the signal received at antenna 2 and both are given by

$$\begin{aligned} S_1(t) &= A \cos(\omega t) + B \sin(\omega t) \\ S_2(t) &= C \cos(\omega t) + D \sin(\omega t) \end{aligned} \tag{4.1}$$

where A , B , C , and D are Gaussian random variables. As shown in the previous chapter, these four variables are required to be Gaussian in order to obtain Rayleigh fading signals in both branches. These two signals can also be expressed as

$$\begin{aligned} S_1(t) &= R_1 \cos(\omega t - \Theta_1) \\ S_2(t) &= R_2 \cos(\omega t - \Theta_2) \end{aligned} \quad (4.2)$$

where

$$\begin{aligned} R_1 &= \sqrt{A^2 + B^2}, R_2 = \sqrt{C^2 + D^2} \\ \Theta_1 &= \tan^{-1}\left(\frac{B}{A}\right), \Theta_2 = \tan^{-1}\left(\frac{D}{C}\right) \end{aligned} \quad (4.3)$$

From the above phase and amplitude notation, the Rayleigh signals R_1 and R_2 are the received envelopes at both branches and Θ_1 and Θ_2 are their respective phases.

When both branch signals envelopes are correlated, which occurs when both branch antennas are closely spaced, their joint expected value is not equal to the product of the expected values taken individually or

$$E[R_1 R_2] \neq E[R_1] E[R_2] \quad (4.4)$$

The operator $E[\cdot]$ represents the expected value of the term in the square brackets. A non-zero envelope correlation between two Rayleigh signals requires that one or more Gaussian subcomponents from both branches be inter-correlated such that

$$E[AD] \neq 0, E[AC] \neq 0, E[BD] \neq 0, \text{ and/or } E[BC] \neq 0 \quad (4.5)$$

When both branch envelopes are uncorrelated, their corresponding Gaussian cross-correlations (4.5) will be zero. This chapter will address the effects of correlation and power imbalance on the joint probability density function of both received envelopes r_1

and r_2 and how they relate back to the correlation of their Gaussian components in both branches.

4.1.1 Correlation Between the Gaussian Components of Two Rayleigh Signals

This section examines some conditions that need to be satisfied by both Rayleigh signals. Exploiting the branch inter-relationships leads to equations that relate the Gaussian subcomponents of both channels.

First of all, the moments between all Gaussian components A , B , C , and D should have statistics that are indifferent to the phase reference at both branches, or equivalently, the signals of (4.1) phase shifted by \mathbf{q}

$$\begin{aligned} S_1(t) &= \hat{A} \cos(\mathbf{w}t + \mathbf{q}) + \hat{B} \sin(\mathbf{w}t + \mathbf{q}) \\ S_2(t) &= \hat{C} \cos(\mathbf{w}t + \mathbf{q}) + \hat{D} \sin(\mathbf{w}t + \mathbf{q}) \end{aligned} \quad (4.6)$$

should have all joint moments of \hat{A} , \hat{B} , \hat{C} , and \hat{D} that are indifferent to the reference phase shift \mathbf{q} . This ensures that the statistics are analyzed independent of the effects of the carrier. The procedure that follows is similar to the one described by Pierce et al. [1]. The Gaussian variables in the second representation (4.6) can be solved in terms of the first (4.1) with the following result

$$\begin{aligned} \hat{A} &= A \cos \mathbf{q} - B \sin \mathbf{q} \\ \hat{B} &= A \sin \mathbf{q} + B \cos \mathbf{q} \\ \hat{C} &= C \cos \mathbf{q} - D \sin \mathbf{q} \\ \hat{D} &= C \sin \mathbf{q} + D \cos \mathbf{q} \end{aligned} \quad (4.6)$$

As stated earlier, the correlations between the Gaussian variables should be indifferent to the phase reference \mathbf{q} and hence the correlation between variables A and C in (4.1) should

be equivalent to the correlation between the variables \hat{A} and \hat{C} in (4.6). This mathematical relationship can be written as

$$E[\hat{A}\hat{C}] = E[AC] \quad (4.8)$$

where $E[\cdot]$ is the expected value operator. The correlation between \hat{A} and \hat{C} can be derived using the equalities presented in (4.7) which evaluates to

$$\begin{aligned} E[\hat{A}\hat{C}] &= E[(A \cos \mathbf{q} - B \sin \mathbf{q})(C \cos \mathbf{q} - D \sin \mathbf{q})] \\ E[\hat{A}\hat{C}] &= E[AC] \cos^2 \mathbf{q} + E[BD] \sin^2 \mathbf{q} - \{E[BC] + E[AB]\} \sin \mathbf{q} \cos \mathbf{q} \end{aligned} \quad (4.9)$$

The above equation is a function of the phase reference \mathbf{q} . The point at which the above equation becomes independent of the phase reference can be found by evaluating the derivative of $E[\hat{A}\hat{C}]$ with respect to \mathbf{q} and setting the resultant equation to zero as follows

$$\begin{aligned} \frac{dE[\hat{A}\hat{C}]}{d\mathbf{q}} &= -2E[AC] \cos \mathbf{q} \sin \mathbf{q} + 2E[BD] \sin \mathbf{q} \cos \mathbf{q} - \{E[BC] + E[AB]\} (\cos^2 \mathbf{q} - \sin^2 \mathbf{q}) \\ 0 &= -2 \cos \mathbf{q} \sin \mathbf{q} \{E[AC] - E[BD]\} - (\cos^2 \mathbf{q} - \sin^2 \mathbf{q}) \{E[BC] + E[AB]\} \end{aligned} \quad (4.10)$$

The solution to this equation represents the point at which the equation (4.8) is satisfied. By inspection, in order for the above equation to be satisfied for all \mathbf{q} , the statistics are independent of the reference phase only when the correlation between the variables A and C is equal to the correlation of the variables B and D . Also the joint expected value of variables B and C should be the negative of the joint expected value of A and B . These relationships can be mathematically written as

$$\begin{aligned} E[AC] &= E[BD] \\ E[BC] &= -E[AB] \end{aligned} \quad (4.11)$$

The equalities relating the remainder of the joint moments can be derived by applying a similar procedure of reference phase independence to the auto-correlations of the Gaussian signals. Evaluating the derivatives of the variances of the variables of A and C with respect to \mathbf{q} , and setting these equations to zero as was done in (4.10)

$$\frac{dE[\hat{A}^2]}{d\mathbf{q}} = 0, \frac{dE[\hat{C}^2]}{d\mathbf{q}} = 0 \quad (4.12)$$

produces an equation for which $E[\hat{A}^2]$ and $E[\hat{C}^2]$ is independent of \mathbf{q} . The solution of (4.12) requires that the variance of A be equal to the variance of B and the variance of the variable C should equal the variance of D .

$$\begin{aligned} E[A^2] &= E[B^2] \\ E[C^2] &= E[D^2] \end{aligned} \quad (4.13)$$

The above results establish the requirements for the Gaussian intra-branch correlations. The cross-correlation between the Gaussian variables within branch I (or $E[AB]$) can be computed by evaluating the second moment of the variable \hat{A} which from (4.7) yields

$$E[\hat{A}^2] = E[A^2]\cos^2 \mathbf{q} + E[B^2]\sin^2 \mathbf{q} - \{E[AB] + E[AB]\} \sin \mathbf{q} \cos \mathbf{q} \quad (4.14)$$

Substituting the equalities $E[\hat{A}^2] = E[A^2] = E[B^2]$ from (4.13) into (4.14) results in the following equation

$$0 = \{E[AB] + E[AB]\} \sin \mathbf{q} \cos \mathbf{q} \quad (4.15)$$

The above equation, as before, should be satisfied independent of the value of \mathbf{q} . Therefore the expected value of A and B should be equal to the negative of itself or

$$E[AB] = -E[AB] \quad (4.16)$$

The above equation can only be satisfied if the joint expected value of A and B is zero. The signals A and B , which are the Gaussian components of branch 1, should therefore be uncorrelated or

$$E[AB] = 0 \quad (4.17)$$

Applying a similar procedure to the variance of \hat{C}^2 (or $E[\hat{C}^2]$) leads to the equations from which the correlation between the Gaussian random variables for the second branch can be found. This leads to an identical result as in (4.17) where both individual components, C and D , of the received signal in branch 2 must be uncorrelated or

$$\begin{aligned} E[CD] &= -E[CD] \\ E[CD] &= 0 \end{aligned} \quad (4.18)$$

The requirements that both Gaussian components within each branch should have equal variance and be uncorrelated is also a necessary requirement for the received envelopes to be Rayleigh distributed as was discussed in Chapter 3.

To simplify the notation in subsequent analysis, the variables that will be used instead of the joint expected value operations are included in the summary of results in this section that follows:

$$\begin{aligned} E[A^2] &= E[B^2] = \mathbf{s}_1^2 \\ E[C^2] &= E[D^2] = \mathbf{s}_2^2 \\ E[AB] &= E[CD] = 0 \\ E[AC] &= E[BD] = \mathbf{a} \\ E[AD] &= -E[BC] = \mathbf{b} \end{aligned} \quad (4.19)$$

4.1.2 Joint Probability Density Function of Four Gaussian Variables

It is well known that two zero mean uncorrelated Gaussian distributed signals can be combined to create a signal that is Rayleigh distributed [2]. Hence four Gaussian distributed signals can be used to create two Rayleigh distributed signals. The inter-correlation between the individual Gaussian probability density functions controls the envelope correlation between the two Rayleigh signals as will be seen in Section 4.2.2.2. The auto-correlations of the Gaussian components sets the average power received by both branches. The joint probability density function, $P(X)$, of a set of N dimensional correlated Gaussian random variables is given in [2] and repeated here

$$P(X) = (2\mathbf{p})^{-N/2} |\mathbf{M}|^{-1/2} \exp\left(-\frac{1}{2} X\mathbf{M}^{-1} X^t\right) \quad (4.20)$$

$$X = [a \quad b \quad c \quad d]$$

The matrix \mathbf{M} contains the correlations of the Gaussian signals and the vector X contains the random variables. $|\mathbf{M}|$ represents the determinant of matrix \mathbf{M} and N is the number of Gaussian random processes. For four correlated Gaussian random variables (A , B , C , and D), the matrix \mathbf{M} becomes

$$\mathbf{M} = \begin{bmatrix} E[A^2] & E[AB] & E[AC] & E[AD] \\ E[BA] & E[B^2] & E[BC] & E[BD] \\ E[CA] & E[CB] & E[C^2] & E[CD] \\ E[DA] & E[DB] & E[DC] & E[D^2] \end{bmatrix} = \begin{bmatrix} \mathbf{s}_1^2 & 0 & \mathbf{a} & \mathbf{b} \\ 0 & \mathbf{s}_1^2 & -\mathbf{b} & \mathbf{a} \\ \mathbf{a} & -\mathbf{b} & \mathbf{s}_2^2 & 0 \\ \mathbf{b} & \mathbf{a} & 0 & \mathbf{s}_2^2 \end{bmatrix} \quad (4.21)$$

where the variables given in (4.19) have been substituted in place of the expectations.

The determinant of matrix \mathbf{M} , $|\mathbf{M}|$, evaluates to

$$\det(\mathbf{M}) = |\mathbf{M}| = (\mathbf{s}_1^2 \mathbf{s}_2^2 - \mathbf{a}^2 - \mathbf{b}^2)^2 \quad (4.22)$$

$$|\mathbf{M}|^{1/2} = \mathbf{s}_1^2 \mathbf{s}_2^2 - \mathbf{a}^2 - \mathbf{b}^2$$

and the inverse of matrix \mathbf{M} , \mathbf{M}^{-1} , can be found to be

$$\mathbf{M}^{-1} = \begin{bmatrix} \frac{\mathbf{s}_2^2}{|\mathbf{M}|^{1/2}} & 0 & -\frac{\mathbf{a}}{|\mathbf{M}|^{1/2}} & -\frac{\mathbf{b}}{|\mathbf{M}|^{1/2}} \\ 0 & \frac{\mathbf{s}_2^2}{|\mathbf{M}|^{1/2}} & \frac{\mathbf{b}}{|\mathbf{M}|^{1/2}} & -\frac{\mathbf{a}}{|\mathbf{M}|^{1/2}} \\ -\frac{\mathbf{a}}{|\mathbf{M}|^{1/2}} & \frac{\mathbf{b}}{|\mathbf{M}|^{1/2}} & \frac{\mathbf{s}_1^2}{|\mathbf{M}|^{1/2}} & 0 \\ -\frac{\mathbf{b}}{|\mathbf{M}|^{1/2}} & -\frac{\mathbf{a}}{|\mathbf{M}|^{1/2}} & 0 & \frac{\mathbf{s}_1^2}{|\mathbf{M}|^{1/2}} \end{bmatrix} \quad (4.23)$$

Substituting the equations (4.21), (4.22), and (4.23) into (4.20) results in the joint probability density function of the Gaussian variables A , B , C , and D . This joint pdf, $f_{ABCD}(a,b,c,d)$, evaluates to

$$f_{ABCD}(a,b,c,d) = \frac{1}{(2\mathbf{p})^2 (\mathbf{s}_1^2 \mathbf{s}_2^2 - \mathbf{a}^2 - \mathbf{b}^2)} e^{-\frac{1}{2(\mathbf{s}_1^2 \mathbf{s}_2^2 - \mathbf{a}^2 - \mathbf{b}^2)} [a^2 \mathbf{s}_2^2 - 2aca - 2ad\mathbf{b} + b^2 \mathbf{s}_2^2 + 2bc\mathbf{b} - 2bd\mathbf{a} + c^2 \mathbf{s}_1^2 + d^2 \mathbf{s}_1^2]} \quad (4.24)$$

were the four Gaussian variables represent the subcomponents of the received signals in branches 1 and 2 and are defined in (4.1). The variables \mathbf{a} , \mathbf{b} , \mathbf{s}_1 , and \mathbf{s}_2 represent the cross and auto correlations between the individual variables and are defined in (4.19).

4.2 Transforming a Four Dimensional Gaussian pdf into the Joint Probability Density of Two Rayleigh Signals

4.2.1 Joint Probability Density Function of Two Rayleigh Signals

The equation given in (4.24) represents the joint probability density function of four correlated Gaussian random variables a , b , c , and d . These four variables can be combined to create two Rayleigh distributed signals which in turn will also be correlated. The procedure that follows to construct Rayleigh signals from their Gaussian components is summarized in Figure 4.1.

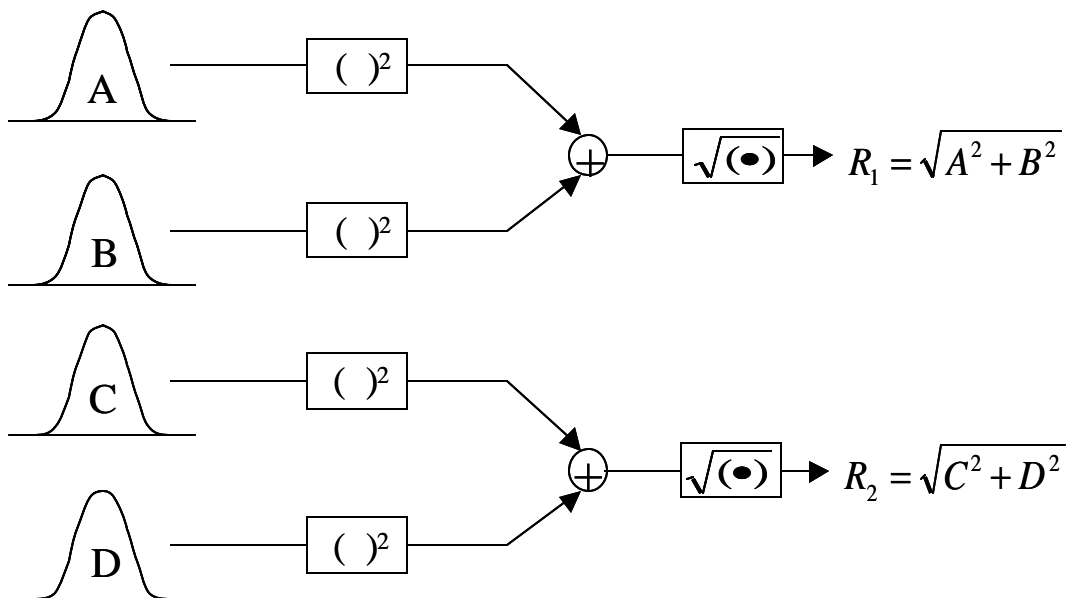


Figure 4.1 Diagram for transforming a four dimensional Gaussian pdf into the joint probability density function of two Rayleigh signals.

The received signal envelopes, r_1 and r_2 , can be constructed by performing the operations listed in Figure 4.1 on the Gaussian random variables. r_1 and r_2 , can be expressed as a function of their Gaussian components as follows

$$\begin{aligned} r_1^2 &= a^2 + b^2 \\ r_2^2 &= c^2 + d^2 \end{aligned} \quad (4.25)$$

The above equations can be re-written by introducing a secondary set of variables \mathbf{q}_1 and \mathbf{q}_2 that are defined as the phase variables in (4.2), the Gaussian variables can be re-written in terms of the phase and amplitude notation as follows:

$$\begin{aligned} a &= r_1 \cos \mathbf{q}_1 \\ b &= r_1 \sin \mathbf{q}_1 \\ c &= r_2 \cos \mathbf{q}_2 \\ d &= r_2 \sin \mathbf{q}_2 \end{aligned} \quad (4.26)$$

The above equations satisfy the equalities stated in (4.25). The 4-dimensional Gaussian joint probability density function of variables A , B , C , and D can be transformed into a pdf relating the variables R_1 , R_2 , \mathbf{Q}_1 , and \mathbf{Q}_2 using a jacobian transformation as stated in [2] using the expressions given in (4.26). The new joint probability density function, $f_{R_1 R_2 \mathbf{Q}_1 \mathbf{Q}_2}(r_1, r_2, \mathbf{q}_1, \mathbf{q}_2)$, results from the following operation

$$f_{R_1 R_2 \mathbf{Q}_1 \mathbf{Q}_2}(r_1, r_2, \mathbf{q}_1, \mathbf{q}_2) = \left| \tilde{\mathbf{J}} \right| f_{ABCD}(a, b, c, d) \quad (4.27)$$

where $\tilde{\mathbf{J}}$ is the jacobian and is defined as

$$\tilde{\mathbf{j}} = \begin{vmatrix} \frac{\partial a}{\partial r_1} & \frac{\partial a}{\partial r_2} & \frac{\partial a}{\partial \mathbf{q}_1} & \frac{\partial a}{\partial \mathbf{q}_2} \\ \frac{\partial b}{\partial r_1} & \frac{\partial b}{\partial r_2} & \frac{\partial b}{\partial \mathbf{q}_1} & \frac{\partial b}{\partial \mathbf{q}_2} \\ \frac{\partial c}{\partial r_1} & \frac{\partial c}{\partial r_2} & \frac{\partial c}{\partial \mathbf{q}_1} & \frac{\partial c}{\partial \mathbf{q}_2} \\ \frac{\partial d}{\partial r_1} & \frac{\partial d}{\partial r_2} & \frac{\partial d}{\partial \mathbf{q}_1} & \frac{\partial d}{\partial \mathbf{q}_2} \end{vmatrix} = \begin{vmatrix} \cos \mathbf{q}_1 & 0 & -r_1 \sin \mathbf{q}_1 & 0 \\ \sin \mathbf{q}_1 & 0 & r_1 \cos \mathbf{q}_1 & 0 \\ 0 & \cos \mathbf{q}_2 & 0 & -r_2 \sin \mathbf{q}_2 \\ 0 & \sin \mathbf{q}_2 & 0 & r_2 \cos \mathbf{q}_2 \end{vmatrix} \quad (4.28)$$

The magnitude of the jacobian evaluates to

$$|\tilde{\mathbf{j}}| = r_1 r_2 \quad (4.29)$$

Substituting (4.24) and (4.29) into (4.27) and expanding the result leads to the joint pdf of the received envelopes and phases at both branches or equivalently

$$f_{R_1 R_2 \Theta_1 \Theta_2}(r_1, r_2, \mathbf{q}_1, \mathbf{q}_2) = \frac{r_1 r_2}{(2p)^2 (\mathbf{s}_1^2 \mathbf{s}_2^2 - \mathbf{a}^2 - \mathbf{b}^2)} e^{-\frac{1}{2(\mathbf{s}_1^2 \mathbf{s}_2^2 - \mathbf{a}^2 - \mathbf{b}^2)} \left[r_1^2 \cos^2 \mathbf{q}_1 \mathbf{s}_2^2 - 2r_1 \cos \mathbf{q}_1 r_2 \cos \mathbf{q}_2 \mathbf{a} - 2r_1 \cos \mathbf{q}_1 r_2 \cos \mathbf{q}_2 \mathbf{b} \right.} \quad (4.30)$$

$$\left. + r_1^2 \sin^2 \mathbf{q}_1 \mathbf{s}_2^2 + 2r_1 \sin \mathbf{q}_1 r_2 \cos \mathbf{q}_2 \mathbf{b} - 2r_1 \sin \mathbf{q}_1 r_2 \sin \mathbf{q}_2 \mathbf{a} \right.}$$

$$\left. + \mathbf{s}_1^2 r_2^2 \cos^2 \mathbf{q}_2 + \mathbf{s}_1^2 r_2^2 \sin^2 \mathbf{q}_2 \right]$$

Applying trigonometric identities to the exponent of the above equation simplifies the expression further and the results becomes

$$f_{R_1 R_2 \Theta_1 \Theta_2}(r_1, r_2, \mathbf{q}_1, \mathbf{q}_2) = \frac{r_1 r_2}{(2p)^2 (\mathbf{s}_1^2 \mathbf{s}_2^2 - \mathbf{a}^2 - \mathbf{b}^2)} e^{-\frac{1}{2(\mathbf{s}_1^2 \mathbf{s}_2^2 - \mathbf{a}^2 - \mathbf{b}^2)} \left[\mathbf{s}_2^2 r_1^2 + \mathbf{s}_1^2 r_2^2 - 2r_1 r_2 \sqrt{\mathbf{a}^2 + \mathbf{b}^2} \cos(\mathbf{q}_1 - \mathbf{q}_2 + \tan^{-1}(\mathbf{b}/\mathbf{a})) \right]} \quad (4.31)$$

which describes the joint probability density function of the received envelopes and phases (r_1 , r_2 , \mathbf{q}_1 , and \mathbf{q}_2) as defined in (4.2). The remainder of this thesis will examine the performance of diversity systems under the assumption of optimum conditions or that the phases are tracked perfectly in both branches. Hence the effects of \mathbf{Q}_1 and \mathbf{Q}_2 are not material to the analysis. The effects of phase estimation errors can be evaluated by using the complete expression given in (4.31). To eliminate the dependence of phase on the

joint probability density function given in (4.31), the phase variables can be integrated out of the distribution as follows

$$f_{R_1 R_2}(r_1, r_2) = \int_0^{2p} \int_0^{2p} f_{R_1 R_2 \Theta_1 \Theta_2}(r_1, r_2, \mathbf{q}_1, \mathbf{q}_2) d\mathbf{q}_1 d\mathbf{q}_2 \quad (4.32)$$

The resulting distribution will be independent of phase and purely a function of the received envelopes R_1 and R_2 . Performing the above integration involves solving the expression

$$f_{R_1 R_2}(r_1, r_2) = \frac{r_1 r_2 e^{-\frac{1}{2(\mathbf{s}_1^2 \mathbf{s}_2^2 - \mathbf{a}^2 - \mathbf{b}^2)}[\mathbf{s}_1^2 r_2^2 + \mathbf{s}_2^2 r_1^2]}}{(2p)^2 (\mathbf{s}_1^2 \mathbf{s}_2^2 - \mathbf{a}^2 - \mathbf{b}^2)} \int_0^{2p} \int_0^{2p} e^{\frac{r_1 r_2 \sqrt{\mathbf{a}^2 + \mathbf{b}^2}}{(\mathbf{s}_1^2 \mathbf{s}_2^2 - \mathbf{a}^2 - \mathbf{b}^2)} [\cos(\mathbf{q}_1 - \mathbf{q}_2 + \tan^{-1}(\mathbf{b}/\mathbf{a}))]} d\mathbf{q}_1 d\mathbf{q}_2 \quad (4.33)$$

$$f_{R_1 R_2}(r_1, r_2) = \frac{r_1 r_2 e^{-\frac{1}{2(\mathbf{s}_1^2 \mathbf{s}_2^2 - \mathbf{a}^2 - \mathbf{b}^2)}[\mathbf{s}_1^2 r_2^2 + \mathbf{s}_2^2 r_1^2]}}{(2p)^2 (\mathbf{s}_1^2 \mathbf{s}_2^2 - \mathbf{a}^2 - \mathbf{b}^2)} Z_1$$

where Z_1 is the integral

$$Z_1 = \int_0^{2p} \int_0^{2p} e^{K [\cos(\mathbf{q}_1 - \mathbf{q}_2 + \tan^{-1}(\mathbf{b}/\mathbf{a}))]} d\mathbf{q}_1 d\mathbf{q}_2 \quad (4.34)$$

and the constant K in Z_1 is

$$K = \frac{r_1 r_2 \sqrt{\mathbf{a}^2 + \mathbf{b}^2}}{(\mathbf{s}_1^2 \mathbf{s}_2^2 - \mathbf{a}^2 - \mathbf{b}^2)} \quad (4.35)$$

The solution of the expression given in (4.33) requires the evaluation of the integral Z_1 .

The integral Z_1 can be solved by applying a transformation of variables of the form

$$\mathbf{q} = \mathbf{q}_1 - \mathbf{q}_2 + \tan^{-1}\left(\frac{\mathbf{b}}{\mathbf{a}}\right) \quad (4.36)$$

such that the integral Z_I can be re-written as a function of the new variable \mathbf{q} as follows

$$Z_1 = \int_0^{2p} \left[\int_{-\mathbf{q}_2 + \tan^{-1}(\mathbf{b}/\mathbf{a})}^{2p - \mathbf{q}_2 + \tan^{-1}(\mathbf{b}/\mathbf{a})} e^{K \cos \mathbf{q}} d\mathbf{q} \right] d\mathbf{q}_2 \quad (4.37)$$

The term in the brackets in the above equation can be expanded as a sum of separate integrals over the span of the integration limits such that Z_I can be re-written as

$$Z_1 = \int_0^{2p} \left[\int_{-\mathbf{q}_2 + \tan^{-1}(\mathbf{b}/\mathbf{a})}^0 e^{K \cos \mathbf{q}} d\mathbf{q} + \int_0^p e^{K \cos \mathbf{q}} d\mathbf{q} + \int_p^{2p} e^{K \cos \mathbf{q}} d\mathbf{q} + \int_{2p}^{2p - \mathbf{q}_2 + \tan^{-1}(\mathbf{b}/\mathbf{a})} e^{K \cos \mathbf{q}} d\mathbf{q} \right] d\mathbf{q}_2 \quad (4.38)$$

Noting that the two middle terms are equivalent and the two end terms cancel each other out, reduces the integral Z_I to

$$Z_1 = \int_0^{2p} \left[2 \int_0^p e^{K \cos \mathbf{q}} d\mathbf{q} \right] d\mathbf{q}_2 \quad (4.39)$$

Using the well know integral of the modified Bessel function of order zero, $I_0(K)$, given in [3] as

$$I_0(K) = \frac{1}{p} \int_0^p e^{K \cos \mathbf{q}} d\mathbf{q} \quad (4.40)$$

and replacing this result into (4.39) yields

$$Z_1 = \int_0^{2p} (2p) I_0(K) d\mathbf{q}_2 = (2p)^2 I_0(K) \quad (4.41)$$

for Z_I . Replacing the solution of Z_I back into (4.33) produces the final result for the joint probability density function of the received envelopes, r_1 and r_2 , in a correlated and unbalanced Rayleigh fading channel. The distribution $f_{R_1 R_2}(r_1, r_2)$ becomes

$$f_{R_1 R_2}(r_1, r_2) = \frac{r_1 r_2}{(\mathbf{s}_1^2 \mathbf{s}_2^2 - \mathbf{a}^2 - \mathbf{b}^2)} e^{-\frac{1}{2(\mathbf{s}_1^2 \mathbf{s}_2^2 - \mathbf{a}^2 - \mathbf{b}^2)}[\mathbf{s}_2^2 r_1^2 + \mathbf{s}_1^2 r_2^2]} I_0\left(\frac{r_1 r_2 \sqrt{\mathbf{a}^2 + \mathbf{b}^2}}{(\mathbf{s}_1^2 \mathbf{s}_2^2 - \mathbf{a}^2 - \mathbf{b}^2)}\right) \quad (4.42)$$

$$r_1, r_2 \geq 0$$

where $I_0(\cdot)$ is the modified Bessel function of order zero. The above equation describes the distributions of both Rayleigh variables as a function of the Gaussian auto and cross-correlations (\mathbf{s}_1 , \mathbf{s}_2 , \mathbf{a} , and \mathbf{b}). In the following section, the Rayleigh branch power and envelope correlation will be related back to the Gaussian correlations.

4.2.2 Relating the Gaussian Correlations to the Rayleigh Envelope Correlation and Branch power

4.2.2.1 Branch Power

The joint probability density function of the signal envelopes r_1 and r_2 was developed in the previous section. The resulting equation for $f_{R_1 R_2}(r_1, r_2)$ is given in (4.42) and is expressed as a function of \mathbf{a} , \mathbf{b} , \mathbf{s}_1 , and \mathbf{s}_2 which are the moments relating the Gaussian variables A , B , C , and D and are defined in (4.19). The probability density function of the individual branches can be computed by integrating out the dependence of the opposite variable on the joint probability density function as follows

$$\begin{aligned}
f_{R_1}(r_1) &= \int_0^{\infty} f_{R_1 R_2}(r_1, r_2) dr_2 = \frac{r_1}{2} e^{-\frac{r_1^2}{2\mathbf{s}_1^2}} \quad r_1 \geq 0 \\
f_{R_2}(r_2) &= \int_0^{\infty} f_{R_1 R_2}(r_1, r_2) dr_1 = \frac{r_2}{2} e^{-\frac{r_2^2}{2\mathbf{s}_2^2}} \quad r_2 \geq 0
\end{aligned} \tag{4.43}$$

The outcome of the above integrals describe the distribution of the individual branch signals $f_{R_1}(r_1)$ and $f_{R_2}(r_2)$. The results of both probability density functions are Rayleigh distributed as expected. The statistics of both received envelopes are also independent of the variables \mathbf{a} and \mathbf{b} which are the cross-correlations of the components of the received signals. This result is intuitive since the functions $f_{R_1}(r_1)$ and $f_{R_2}(r_2)$ describe the properties of r_1 and r_2 individually independent of one another. The average branch power, or variance, is the second moment of the probability density function. The average signal envelope, $E[R_{1,2}]$, and variance, $E[R_{1,2}^2]$, can be computed from the envelope distributions given in (4.43) which yields

$$\begin{aligned}
E[R_1] &= \bar{r}_1 = \int_0^{\infty} r_1 f_{R_1}(r_1) dr_1 = \sqrt{\frac{\mathbf{p}}{2}} \mathbf{s}_1 \\
E[R_1^2] &= \int_0^{\infty} r_1^2 f_{R_1}(r_1) dr_1 = 2\mathbf{s}_1^2
\end{aligned} \tag{4.44}$$

similarly for branch 2

$$\begin{aligned}
E[R_2] &= \bar{r}_2 = \int_0^{\infty} r_2 f_{R_2}(r_2) dr_2 = \sqrt{\frac{\mathbf{p}}{2}} \mathbf{s}_2 \\
E[R_2^2] &= \int_0^{\infty} r_2^2 f_{R_2}(r_2) dr_2 = 2\mathbf{s}_2^2
\end{aligned} \tag{4.45}$$

The equations given in (4.44) and (4.45) relate the mean and the second moment (average power) of the received envelopes r_1 and r_2 to the Gaussian auto-correlations or variances

$(\mathbf{s}_1^2$ and \mathbf{s}_2^2). The remaining statistic to be determined is how the Gaussian cross and auto correlations relate to the envelope correlation of the received signals. This relationship will be derived in the following section.

4.2.2.2 Envelope Correlation (r)

The envelope correlation, r , is defined as the expected value of the demeaned variables r_1 and r_2 over the square root of the product of the individual envelope variances as follows

$$\begin{aligned} r &= \frac{E[(r_1 - \bar{r}_1)(r_2 - \bar{r}_2)]}{\sqrt{E[(r_1 - \bar{r}_1)^2]E[(r_2 - \bar{r}_2)^2]}} \\ r &= \frac{E[r_1 r_2] - E[r_1]E[r_2]}{\sqrt{(E[r_1^2] - E[r_1]^2)(E[r_2^2] - E[r_2]^2)}} \end{aligned} \quad (4.46)$$

The overbar over the variables r_1 and r_2 represents the mean as defined in (4.44) and (4.45). All expectations in (4.46) have been derived previously except for the correlation of r_1 and r_2 ($E[r_1 r_2]$). The joint expected value of both variables is defined as

$$E[r_1 r_2] = \int_0^\infty \int_0^\infty r_1 r_2 f_{R_1 R_2}(r_1, r_2) dr_1 dr_2 \quad (4.47)$$

and can be computed by integrating the function

$$E[r_1 r_2] = \int_0^\infty \int_0^\infty \frac{r_1^2 r_2^2}{(\mathbf{s}_1^2 \mathbf{s}_2^2 - \mathbf{a}^2 - \mathbf{b}^2)} e^{-\frac{1}{2(\mathbf{s}_1^2 \mathbf{s}_2^2 - \mathbf{a}^2 - \mathbf{b}^2)}[\mathbf{s}_2^2 r_1^2 + \mathbf{s}_1^2 r_2^2]} I_0\left(\frac{r_1 r_2 \sqrt{\mathbf{a}^2 + \mathbf{b}^2}}{(\mathbf{s}_1^2 \mathbf{s}_2^2 - \mathbf{a}^2 - \mathbf{b}^2)}\right) dr_1 dr_2 \quad (4.48)$$

To simplify the notation, the following variables will be used in place of some of the constants

$$\begin{aligned} H &= \mathbf{s}_1^2 \mathbf{s}_2^2 - \mathbf{a}^2 - \mathbf{b}^2 \\ J &= \sqrt{\mathbf{a}^2 + \mathbf{b}^2} \end{aligned} \quad (4.49)$$

so that equation (4.48) can be re-written in simplified form as

$$E[r_1 r_2] = \int_0^\infty \int_0^\infty \frac{r_1^2 r_2^2}{H} e^{-\frac{1}{2H}[\mathbf{s}_2^2 r_1^2 + \mathbf{s}_1^2 r_2^2]} I_0\left(\frac{r_1 r_2 J}{H}\right) dr_1 dr_2 \quad (4.50)$$

The solution of a variation of the inside integral of (4.50) can found in the table of integrals given in [4]. The integral shown in (4.50) can be re-written in the same form as the integral given in [4] by performing the following change of variables on r_1 :

$$x = r_1^2, \quad \frac{dx}{dr_1} = 2r_1 \quad (4.51)$$

re-writing (4.50) in terms of the new variable x produces the integral

$$E[r_1 r_2] = \int_0^\infty \frac{r_2^2}{2H} e^{-\frac{1}{2H}[\mathbf{s}_1^2 r_2^2]} \int_0^\infty \sqrt{x} e^{-\frac{1}{2H}[\mathbf{s}_2^2 x]} I_0\left(\frac{\sqrt{x} r_2 J}{H}\right) dx dr_2 \quad (4.52)$$

The solution of the inside integral as found in [4] taken with respect to the variable x is given by

$$\int_0^\infty x^{m-\frac{1}{2}} e^{-hx} I_{2n}(2e\sqrt{x}) dx = \frac{\Gamma(\mathbf{m}+\mathbf{n}+1/2)}{\Gamma(2\mathbf{n}+1)} e^{-1} e^{\frac{e^2}{2h}} \mathbf{h}^{-m} M_{-m\mathbf{n}}\left(\frac{e^2}{\mathbf{h}}\right) \quad (4.53)$$

$$\text{Re}(\mathbf{m}+\mathbf{n}+1/2) > 0$$

Where $I_{2n}(\cdot)$ is the modified Bessel function of order $2\mathbf{n}$; $\Gamma(\cdot)$ is the gamma function, and finally $M_{-m\mathbf{n}}(\cdot)$ is the Whittaker function. The values of the variables \mathbf{h} , \mathbf{e} , \mathbf{m} and \mathbf{n} , given in (4.53), correspond for the integral of interest, given in (4.52), to

$$\mathbf{h} = \frac{\mathbf{s}_2^2}{2H}, \quad \mathbf{e} = \frac{r_2 J}{2H}, \quad \mathbf{m} = 1, \quad \mathbf{n} = 0 \quad (4.54)$$

From the above equalities, it can be seen that the constraint given in (4.53) over which the solution of integral is valid is satisfied for the integral given in (4.52) and therefore the correlation between the variables r_1 and r_2 reduces to the solution of a single integral over the variable r_1 as follows

$$E[r_1 r_2] = \int_0^\infty \frac{2Hr_2 \Gamma(3/2)}{J \mathbf{s}_2^2 \Gamma(1)} e^{-\frac{1}{2H}[\mathbf{s}_1^2 r_2^2]} e^{\frac{r_2^2 J^2}{4H \mathbf{s}_2^2}} M_{-1,0} \left(\frac{r_2^2 J^2}{2H \mathbf{s}_2^2} \right) dr_2 \quad (4.55)$$

The above integral can be solved by introducing the auxiliary variable y and performing the following change of variables:

$$y = \frac{r_2^2 J^2}{2H \mathbf{s}_2^2}, \quad \frac{dy}{dr_2} = \frac{J^2 r_2}{H \mathbf{s}_2^2} \quad (4.56)$$

The integral (4.55) can be written as a function of the new variable y reducing the integral to the following form

$$E[r_1 r_2] = \frac{2H^2 \Gamma(3/2)}{J^3 \Gamma(1)} \int_0^\infty e^{-y \left[\frac{\mathbf{s}_1^2 \mathbf{s}_2^2 - 1}{J^2} \right]} M_{-1,0}(y) dy \quad (4.57)$$

As before, the solution of the above integral can be found in integral tables of [4] and is given by

$$\int_0^\infty e^{-st} t^h M_{mn}(t) dt = \frac{\Gamma(\mathbf{h} + \mathbf{n} + 3/2)}{(1/2 + s)^{\mathbf{h} + \mathbf{n} + 3/2}} F \left(\mathbf{h} + \mathbf{n} + 3/2, -\mathbf{m} + \mathbf{n} + 1/2; 2\mathbf{n} + 1; \frac{2}{(2s + 1)} \right) \quad (4.58)$$

$$\text{Re}(\mathbf{h} + \mathbf{m} + 3/2) > 0, \text{Re}(s) > \frac{1}{2}$$

where $M_{mn}(\cdot)$ is the Whittaker function, $\Gamma(\cdot)$ is the gamma function, and $F(l, m; n; o)$ is the hypergeometric function as defined in (4.63) and [4]. From (4.58), the values of the variables \mathbf{h} , \mathbf{n} , \mathbf{m} and s given equate for the integral of interest in (4.57) to

$$\mathbf{h} = 0, \quad \mathbf{m} = -1, \quad \mathbf{n} = 0, \quad s = \frac{\mathbf{s}_1^2 \mathbf{s}_2^2}{J^2} - \frac{1}{2} \quad (4.59)$$

The constraint over which the solution of the integral in (4.58) are valid is satisfied and using the following results of the gamma function

$$\Gamma(1) = 1, \quad \Gamma\left(\frac{3}{2}\right) = \sqrt{\frac{\mathbf{p}}{2}} \quad (4.60)$$

reduces the integral in (4.57) to

$$E[r_1 r_2] = \frac{(\mathbf{s}_1^2 \mathbf{s}_2^2 - \mathbf{a}^2 - \mathbf{b}^2)^2 \mathbf{p}}{2(\mathbf{s}_1^2 \mathbf{s}_2^2)^{3/2}} F\left(\frac{3}{2}, \frac{3}{2}; 1; \frac{\mathbf{a}^2 + \mathbf{b}^2}{\mathbf{s}_1^2 \mathbf{s}_2^2}\right) \quad (4.61)$$

The above equation relates the correlation between both received signal envelopes to their respective Gaussian correlations. The above result is evaluated in terms of the hypergeometric function which has a solution that is not commonly found in ordinary tables or computer programs. (4.61) can be re-written as a function of the more readily available elliptic integral by noting that equation (4.61) can be manipulated using equations found in [4] to produce the equivalent result

$$E[r_1 r_2] = \frac{\mathbf{p}(\mathbf{s}_1 \mathbf{s}_2 + \sqrt{\mathbf{a}^2 + \mathbf{b}^2})}{2} F\left(-\frac{1}{2}, \frac{1}{2}; 1; \frac{4\sqrt{\mathbf{a}^2 + \mathbf{b}^2} \mathbf{s}_1 \mathbf{s}_2}{(\mathbf{s}_1 \mathbf{s}_2 + \sqrt{\mathbf{a}^2 + \mathbf{b}^2})^2}\right) \quad (4.62)$$

The hypergeometric function from [4] is the solution of the integral

$$F(\mathbf{h}, \mathbf{e}; \mathbf{g}, z) = \frac{\Gamma(\mathbf{g})}{\Gamma(\mathbf{e})\Gamma(\mathbf{g} - \mathbf{e})} \int_0^1 t^{\mathbf{e}-1} (1-t)^{\mathbf{g}-\mathbf{e}-1} (1-tz)^{-\mathbf{h}} dt \quad (4.63)$$

while the complete elliptic integral of the second kind given in [4] is expressed as

$$E(k) = \int_0^1 \frac{\sqrt{1-k^2x^2}}{\sqrt{1-x^2}} dx \quad (4.64)$$

The complete elliptic integral of the second kind and the hypergeometric function as can be seen from (4.64) and (4.63) are related by the equation

$$F\left(-\frac{1}{2}, \frac{1}{2}; 1; H\right) = \frac{2}{\mathbf{p}} E(\sqrt{H}) \quad (4.65)$$

As a side note, the definition of the complete elliptic integral of the second kind is expressed somewhat differently in some references from the one given in (4.64). The modulus of the expression in the brackets of the elliptic integral is sometimes the variable k^2 instead of just k . For consistency, the definition of the elliptic integral used in this report is given in (4.64).

Finally, substituting (4.65) into (4.62) produces the joint expected value of both received envelopes, $E[r_1 r_2]$, as a function of the complete elliptic integral of the second kind or

$$E[r_1 r_2] = \left(\mathbf{s}_1 \mathbf{s}_2 + \sqrt{\mathbf{a}^2 + \mathbf{b}^2} \right) E \left(\frac{2(\mathbf{a}^2 + \mathbf{b}^2)^{1/4} \sqrt{\mathbf{s}_1 \mathbf{s}_2}}{\mathbf{s}_1 \mathbf{s}_2 + \sqrt{\mathbf{a}^2 + \mathbf{b}^2}} \right) \quad (4.66)$$

The envelope correlation between the variables r_1 and r_2 is given in (4.46). Substituting this result and (4.44), (4.45), and (4.66) into the equation of envelope correlation given in (4.46) results in the following expression for \mathbf{r} in a Rayleigh fading channel

$$\mathbf{r} = \frac{E[r_1 r_2] - (\mathbf{p}/2)\mathbf{s}_1 \mathbf{s}_2}{\mathbf{s}_1 \mathbf{s}_2 (2 - \mathbf{p}/2)} \quad (4.67)$$

The envelope correlation, \mathbf{r} , is a parameter that is extensively used in literature that involve measurement results. Most papers that perform theoretical analysis, on the other hand, express the probability distributions in terms of the power envelope correlation (\mathbf{r}_p) because this variable is easily computed theoretically. For completeness, the power envelope correlation for the joint correlated Rayleigh channel is derived next.

4.2.2.3 Power Envelope Correlation (\mathbf{r}_p)

The definition of the power envelope correlation is similar to the envelope correlation given in (4.46) except that the correlation is performed on r_1^2 and r_2^2 instead of the variables r_1 and r_2 . The definition of \mathbf{r}_p is the following:

$$\mathbf{r}_p = \frac{E\left[\left(r_1^2 - \overline{r_1^2}\right)\left(r_2^2 - \overline{r_2^2}\right)\right]}{\sqrt{E\left[\left(r_1^2 - \overline{r_1^2}\right)^2\right]}E\left[\left(r_2^2 - \overline{r_2^2}\right)^2\right]} \quad (4.68)$$

$$\mathbf{r}_p = \frac{E[r_1^2 r_2^2] - E[r_1^2]E[r_2^2]}{\sqrt{\left(E[r_1^4] - E[r_1^2]^2\right)\left(E[r_2^4] - E[r_2^2]^2\right)}}$$

The expected value of r_1^2 and r_2^2 are given in (4.44) and (4.45) and the fourth moment of the probability density function, $E[r_{1,2}^4]$, can be computed by integrating the weighted probability density functions of r_1 and r_2 as follows

$$E[R_1^4] = \int_0^{\infty} r_1^4 f_{R_1}(r_1) dr_1 = 8\mathbf{s}_1^4 \quad (4.69)$$

$$E[R_2^4] = \int_0^{\infty} r_2^4 f_{R_2}(r_2) dr_2 = 8\mathbf{s}_2^4$$

The term that has not been evaluated in equation (4.68) is the joint envelope squared correlation of r_1 and r_2 that can be computed by evaluating the double integral

$$E[r_1^2 r_2^2] = \int_0^{\infty} \int_0^{\infty} r_1^2 r_2^2 f_{R_1 R_2}(r_1, r_2) dr_1 dr_2 \quad (4.70)$$

where $f_{R_1 R_2}(r_1, r_2)$ is given in (4.42). Evaluating the above equation using the integration tables given in [4] yields

$$E[r_1^2 r_2^2] = 4(\mathbf{a}^2 + \mathbf{b}^2 + \mathbf{s}_1^2 \mathbf{s}_2^2) \quad (4.71)$$

Substituting the equations given in (4.69), (4.71), (4.44), and (4.45) into (4.68) results in an power envelope correlation given by

$$\mathbf{r}_p = \frac{\mathbf{a}^2 + \mathbf{b}^2}{\mathbf{s}_1^2 \mathbf{s}_2^2} \quad (4.72)$$

As can be seen from the above equation, the expression for the power envelope correlation is simpler than that of the envelope correlation. This is the reason most theoretical work is expressed in terms of this variable. The variables \mathbf{r}_p and \mathbf{r} as can be seen from (4.72) and (4.67) are related by the equation

$$\mathbf{r} = \frac{(1 + \sqrt{\mathbf{r}_p}) E\left(\frac{2\mathbf{r}_p^{1/4}}{1 + \sqrt{\mathbf{r}_p}}\right) - \mathbf{p}/2}{2 - \mathbf{p}/2} \quad (4.73)$$

were $E(\cdot)$ is the complete elliptic integral of the second kind as defined in (4.64). The following section will summarize the results derived in this chapter and present some example joint probability density functions of r_1 and r_2 .

4.3 Summary of Results and Examples

In this chapter, the joint probability density function of two Rayleigh correlated and unbalanced signals was developed. The distribution of $f_{R_1 R_2}(r_1, r_2)$ as a function of the power envelope correlation, \mathbf{r}_P , is given by

$$f_{R_1 R_2}(r_1, r_2) = \frac{r_1 r_2}{\mathbf{s}_1^2 \mathbf{s}_2^2 (1 - \mathbf{r}_P)} e^{-\frac{1}{2\mathbf{s}_1^2 \mathbf{s}_2^2 (1 - \mathbf{r}_P)} [\mathbf{s}_2^2 r_1^2 + \mathbf{s}_1^2 r_2^2]} I_0 \left(\frac{r_1 r_2 \sqrt{\mathbf{r}_P}}{\mathbf{s}_1 \mathbf{s}_2 (1 - \mathbf{r}_P)} \right) \quad (4.74)$$

$$\mathbf{r}_P < 1, r_1, r_2 \geq 0$$

The envelope correlation \mathbf{r} for the corresponding value of \mathbf{r}_P can be computed using (4.73).

All the expressions given in this thesis are a function of \mathbf{a} , \mathbf{b} , \mathbf{s}_1 , and \mathbf{s}_2 . The variables \mathbf{s}_1 and \mathbf{s}_2 , as shown in (4.44) and (4.45), determine the average power of channel 1 and 2 respectively. The random variable R_1 has a second moment of $2\mathbf{s}_1^2$ while the average power of R_2 is $2\mathbf{s}_2^2$. The cross correlations \mathbf{a} and \mathbf{b} (defined in 4.19) correlate the signals r_1 and r_2 and can be chosen arbitrarily to produce any given envelope correlation (\mathbf{r}) as described by (4.66) and (4.67). There are no conditions set on \mathbf{a} or \mathbf{b} , only that they in combination produce a given envelope correlation. The expressions in this paper are given as a function of \mathbf{a} and \mathbf{b} for completeness but both variables can be set equal to each other to reduce the complexity of all the analytical expressions by one variable. It

should also be noted that the envelope correlation (\mathbf{r}) does not uniquely describe the relationships between both received signals because there is a large (infinite) combination of \mathbf{a} and \mathbf{b} that produce the same equivalent envelope correlation (\mathbf{r}) as can be seen from (4.66) and (4.72).

The shape of the joint probability density function of R_1 and R_2 , $f_{R_1R_2}(r_1, r_2)$, varies significantly with the envelope correlation coefficient \mathbf{r} . In all cases, the marginal probability density functions, $f_{R_1}(r_1)$ and $f_{R_2}(r_2)$ as defined in (4.43), remain the same regardless of the correlation between both branches. Figure 4.2 shows both the marginal and joint probability density functions when both received signals are uncorrelated. For example purposes, branch 1 has an average power of 2 while the second branch has an average power of 4.5. That corresponds to

$$\begin{aligned} E[R_1^2] &= 2\mathbf{s}_1^2 = 2 \\ E[R_2^2] &= 2\mathbf{s}_2^2 = 4.5 \\ \mathbf{r} = \mathbf{r}_p &= 0 \end{aligned} \tag{4.75}$$

As a contrast, Figure 4.3 shows both the marginal and joint probability density functions for an envelope correlation of 0.8. As before, branch 1 and branch 2 have average powers of 2 and 4.5 respectively. This corresponds to

$$\begin{aligned} E[R_1^2] &= 2\mathbf{s}_1^2 = 2 \\ E[R_2^2] &= 2\mathbf{s}_2^2 = 4.5 \\ \mathbf{r} &= 0.8 \\ \mathbf{r}_p &= 0.8189 \end{aligned} \tag{4.76}$$

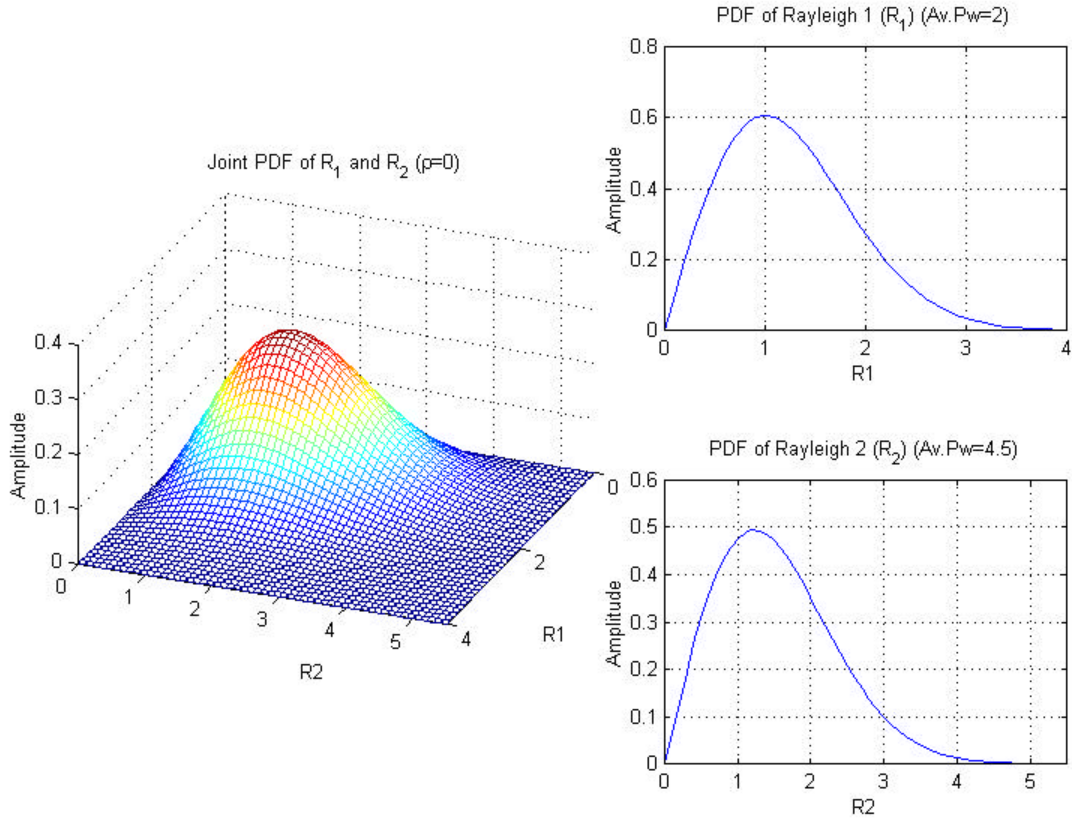


Figure 4.2 Joint probability density function of R_1 and R_2 and their marginal probabilities for an envelope correlation of zero.

From Figure 4.2 and 4.3 it can be seen that the amplitude of $f_{R_1 R_2}(r_1, r_2)$ approaches infinity as the envelope correlation approaches unity. In order to maintain the required volume of unity, the function compresses itself along a line with a slope that is the ratio of both average branch powers (as \mathbf{r} approaches 1). Both branches are completely correlated when $\mathbf{s}_1^2 \mathbf{s}_2^2 = \mathbf{a}^2 + \mathbf{b}^2$ as can be seen from (4.67). For partially correlated signals, $\mathbf{a}^2 + \mathbf{b}^2$ will always be less than $\mathbf{s}_1^2 \mathbf{s}_2^2$.

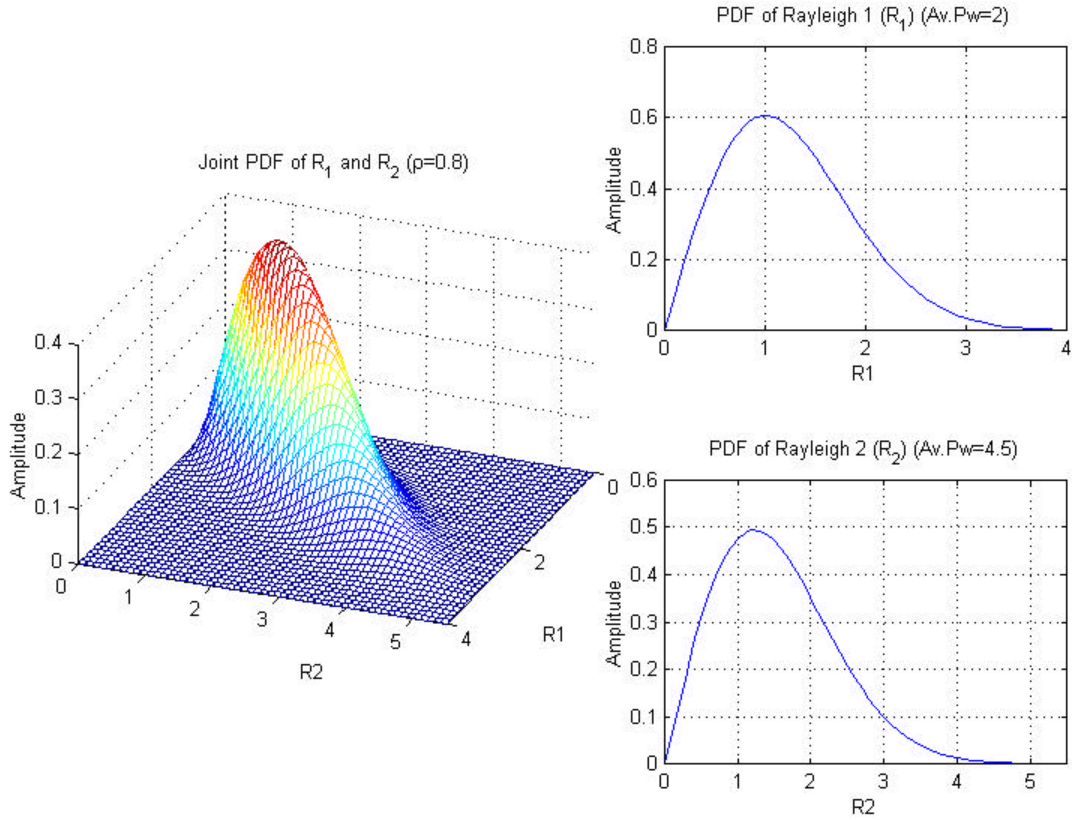


Figure 4.3 Joint probability density function of R_1 and R_2 and their marginal probabilities for an envelope correlation of 0.8.

In the following chapter, the joint probability density function in (4.74) will be used to evaluate the performance of a two-branch selection diversity system for the Rayleigh channel. The probability density function of the signal-to-noise ratio after selection diversity will be derived next as a means to establish a norm to compare improvement between diversity combining algorithms.

References:

- [1] J. N. Pierce and S. Stein, "Multiple Diversity with Nonindependent Fading," *Proceedings of the IRE*, pp. 89-104 Jan. 1960.
- [2] Henry Stark and John W. Woods, *Probability, Random Processes, and Estimation Theory for Engineers*, Perentice Hall, Englewood Cliffs, NJ, 1994.
- [3] Milton Abramowitz and Irene Stegun, *Handbook of Mathematical Functions with Formulas, Graphs, and Mathematical Tables*, U.S. Govt. Print. Off., Washington, 1972.
- [4] I. S. Gradshteyn and I. M. Ryzhik, *Table of Integrals, Series, and Products*, Academic Press Inc., San Diego, CA, 1994.

Chapter 5

Two-Branch Selection Diversity In a Rayleigh Channel

In this chapter, the probability density function of the SNR after two-branch selection diversity is developed for the correlated and unbalanced Rayleigh channel. In the previous chapter, the joint probability density function of both received signals was derived as a function of envelope correlation and average branch power. The process of selection diversity will be applied to the joint envelope distribution to arrive at the probability density function of the output SNR.

The probability density function of the SNR for a dual selection diversity system has also been analyzed in [3] and [4]. In both cases, the result has been left in integral form. In this chapter, an expression for the SNR will be given that does not require numerical integration

5.1 Introduction

A two-branch selection diversity system was discussed in Chapter 3 and is shown in Figure 3.1. This system has an instantaneous output voltage signal-to-noise ratio given in (3.5) and repeated here

$$SNR_{V_s} = \sqrt{SNR_{P_s}} = \frac{1}{\sqrt{N}} \max(r_1, r_2) \quad (5.1)$$

To reduce the number of variables in the equations, the noise power N can be set to unity.

This operation is equivalent to replacing $\frac{r_1}{\sqrt{N}} = SNR_{V_1}$ by r_1 and $\frac{r_2}{\sqrt{N}} = SNR_{V_2}$ by r_2 .

The SNR_{V_1} and SNR_{V_2} are the branch voltage signal-to-noise ratios defined in (3.4).

As also noted in Chapter 3, the distributions of SNR_{V_1} and r_1 (SNR_{V_2} and r_2) have pdfs with the same shape except they differ in variance because the constant N in general is not always unity. The output voltage signal-to-noise ratio after selection combining, SNR_{V_s} , with N set to 1 can be computed from (5.11) to give

$$SNR_{V_s} \Big|_{N=1} = \sqrt{SNR_{P_s}} \Big|_{N=1} = \max(r_1, r_2) \quad (5.2)$$

The voltage signal-to-noise ratio provides a direct comparison metric between measured and theoretical statistics since both are functions of the received envelope instead of the received envelope squared. The probability density function for both the SNR_V and the SNR_P after selection combining will be developed in the Sections 5.2 and 5.3, respectively. The distributions of both these signal-to-noise ratios are related by a simple transformation function.

As noted earlier, the envelopes r_1 and r_2 over all events are random variables and at any given time have a distribution described by the Rayleigh probability density function

(4.43). The distribution of the voltage signal-to-noise ratio after selection diversity, SNR_{V_S} , therefore depends on the distributions of r_1 and r_2 and their correlation.

5.2 Probability Density Function of the SNR_{V_S}

The probability density function of the voltage SNR after selection diversity with N set to unity will be derived in this section. As mentioned in section 5.1, the signal to noise ratio as a function of N can always be computed from this expression by performing a change of variables of the form

$$\begin{aligned} r_1 &\Rightarrow \frac{r_1}{\sqrt{N}} \\ r_2 &\Rightarrow \frac{r_2}{\sqrt{N}} \end{aligned} \tag{5.3}$$

which will be carried out at the end of this section. The reason, as explained in Chapter 3, for deriving the result for a noise power of unity is to find a distribution that directly relates to what is done with measurement data. The combining algorithm is applied to measured envelope data, instead of SNR, and the performance improvement is evaluated as a function of a gain parameter. Improvement is determined by comparing the distribution of signal-to-noise ratio after combining to that of a single branch system. The gain (i.e. diversity gain which is discussed in Chapter 8) parameter of an equivalent system when combining is applied to only the envelopes is the same as the SNR gain when both branches have equal noise power as was discussed in Chapter 3. Since only the relative and not the actual SNR is required, this performance metric does not require computing the noise power of the diversity branches.

The output of a selection diversity system has a signal-to-noise ratio equal to that of the strongest branch. The output SNR of the selection combiner will be that of branch I when this branch has the highest signal to noise ratio of both branches. Under these conditions, the second branch has an SNR less than or equal to that of branch I . Assuming equal branch powers (so the branch with the largest envelope is also the branch with the largest SNR), when the envelope of the signal at the output of the combiner is the value s it can be concluded that the envelope r_1 is also the value s and r_2 is less than or equal to s . This event corresponds to the line labeled I_1 on Figure 5.1. The second alternative is when the signal-to-noise ratio of branch 2 is larger than that of branch I . The output signal envelope will be s when r_2 is s and r_1 can possibly be any value less than or equal to s . The line I_2 in Figure 5.1 reflects the second possibility. Hence, any joint event of r_1 and r_2 that lies along the lines I_1 and I_2 in Figure 5.1 will produce an output envelope from the selection diversity system of s .

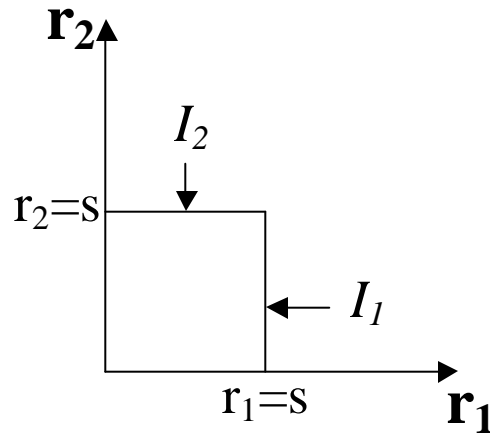


Figure 5.1. Values of r_1 and r_2 that produce an envelope value of s at the output of the selection combiner.

The distribution of the frequency of occurrence given an event r_1 and r_2 is described by the joint probability density function $f_{R_1 R_2}(r_1, r_2)$ (4.42). The event that the envelope after the selection combiner is a value s , is the sum (or integral) of all the events over r_1 and r_2 that produce s at the output. This corresponds to the integration of $f_{R_1 R_2}(r_1, r_2)$ along the

lines described in Figure 5.1. This new probability density function, $f_S(s)$, describes the distribution of the output envelope s and is derived from the distribution of r_1 and r_2 . Mathematically, this process can be written as

$$f_S(s) = \int_0^s f_{R_1 R_2}(r_1, r_2) \Big|_{r_1=s} dr_2 + \int_0^s f_{R_1 R_2}(r_1, r_2) \Big|_{r_2=s} dr_1 \quad (5.4)$$

$$f_S(s) = I_1 + I_2$$

where I_1 and I_2 correspond to the integrals along the I_1 and I_2 line respectively in figure 5.1. The integral I_1 after substituting (4.42) into (5.4) can be expanded as

$$I_1 = \int_0^s \frac{sr_2}{(\mathbf{s}_1^2 \mathbf{s}_2^2 - \mathbf{a}^2 - \mathbf{b}^2)} e^{-\frac{1}{2(\mathbf{s}_1^2 \mathbf{s}_2^2 - \mathbf{a}^2 - \mathbf{b}^2)} [\mathbf{s}_2^2 s^2 + \mathbf{s}_1^2 r_2^2]} I_0 \left(\frac{sr_2 \sqrt{\mathbf{a}^2 + \mathbf{b}^2}}{(\mathbf{s}_1^2 \mathbf{s}_2^2 - \mathbf{a}^2 - \mathbf{b}^2)} \right) dr_2$$

$$I_1 = \frac{se^{-\frac{1}{2(\mathbf{s}_1^2 \mathbf{s}_2^2 - \mathbf{a}^2 - \mathbf{b}^2)} [\mathbf{s}_2^2 s^2]}}{(\mathbf{s}_1^2 \mathbf{s}_2^2 - \mathbf{a}^2 - \mathbf{b}^2)} \int_0^s r_2 e^{-\frac{1}{2(\mathbf{s}_1^2 \mathbf{s}_2^2 - \mathbf{a}^2 - \mathbf{b}^2)} [\mathbf{s}_1^2 r_2^2]} I_0 \left(\frac{sr_2 \sqrt{\mathbf{a}^2 + \mathbf{b}^2}}{(\mathbf{s}_1^2 \mathbf{s}_2^2 - \mathbf{a}^2 - \mathbf{b}^2)} \right) dr_2 \quad (5.5)$$

A solution of the above integral can found in [1]. The integral shown in (5.5) can be rewritten in the same form as the integral given in [1] by performing the following change of variables on r_2 :

$$j = \frac{\mathbf{s}_1}{\sqrt{2(\mathbf{s}_1^2 \mathbf{s}_2^2 - \mathbf{a}^2 - \mathbf{b}^2)}} r_2, \quad \frac{dj}{dr_2} = \frac{\mathbf{s}_1}{\sqrt{2(\mathbf{s}_1^2 \mathbf{s}_2^2 - \mathbf{a}^2 - \mathbf{b}^2)}} \quad (5.6)$$

which produces an equivalent integral in terms of the variable j

$$I_1 = \frac{2se^{-\frac{1}{2(\mathbf{s}_1^2 \mathbf{s}_2^2 - \mathbf{a}^2 - \mathbf{b}^2)} [\mathbf{s}_2^2 s^2]}}{\mathbf{s}_1^2} \int_0^{\frac{s\mathbf{s}_1}{\sqrt{2(\mathbf{s}_1^2 \mathbf{s}_2^2 - \mathbf{a}^2 - \mathbf{b}^2)}}} j e^{-j^2} I_0 \left(2 \frac{s\sqrt{\mathbf{a}^2 + \mathbf{b}^2} j}{\sqrt{2\mathbf{s}_1^2 (\mathbf{s}_1^2 \mathbf{s}_2^2 - \mathbf{a}^2 - \mathbf{b}^2)}} \right) dj \quad (5.7)$$

The solution of this integral as found in [1] taken with respect to the variable t is given by

$$\int_0^b t e^{-t^2} I_0(2rt) dt = \frac{e^{r^2}}{2} (1 - J(x, y)) \quad (5.8)$$

$$J(x, x) = \frac{1}{2} [1 + e^{-2x} I_0(2x)] \quad \text{for } h = 1$$

$$J(x, y) = e^{-(x+y)} \sum_{k=0}^{\infty} h^k I_k(x) \quad \text{for } h < 1$$

$$J(x, y) = 1 - e^{-(x+y)} \sum_{k=1}^{\infty} h^{-k} I_k(x) \quad \text{for } h > 1$$

where the constants \mathbf{x} , \mathbf{h} , y , and x are described by

$$\mathbf{x} = 2(xy)^{\frac{1}{2}}, \mathbf{h} = \left(\frac{y}{x}\right)^{\frac{1}{2}}, x = \mathbf{b}^2, y = \mathbf{r}^2 \quad (5.9)$$

Additionally, the integral I_2 has a similar form as I_1 in (5.5) and is given by

$$I_2 = \frac{se^{-\frac{1}{2(\mathbf{s}_1^2 \mathbf{s}_2^2 - \mathbf{a}^2 - \mathbf{b}^2)}[\mathbf{s}_1^2 \mathbf{s}_2^2]}}{(\mathbf{s}_1^2 \mathbf{s}_2^2 - \mathbf{a}^2 - \mathbf{b}^2)} \int_0^s r_1 e^{-\frac{1}{2(\mathbf{s}_1^2 \mathbf{s}_2^2 - \mathbf{a}^2 - \mathbf{b}^2)}[\mathbf{s}_2^2 r_1^2]} I_0\left(\frac{sr_2 \sqrt{\mathbf{a}^2 + \mathbf{b}^2}}{(\mathbf{s}_1^2 \mathbf{s}_2^2 - \mathbf{a}^2 - \mathbf{b}^2)}\right) dr_1 \quad (5.10)$$

and hence its solution can also be computed from (5.8).

The final results for the probability density function of $f_S(s)$ is the summation of the terms involving the integrals I_1 and I_2 . By substituting the values of the integrals of interest in (5.7) and (5.10) for the constants in (5.9) gives rise to the following distribution of the SNR_{V_S} at the output of the selection combiner for a noise power of unity:

$$f_S(s) = \frac{s}{\mathbf{s}_1} e^{-\frac{s^2}{2\mathbf{s}_1^2}} [1 - J_1(x_1, y_1)] + \frac{s}{\mathbf{s}_2} e^{-\frac{s^2}{2\mathbf{s}_2^2}} [1 - J_2(x_2, y_2)] \quad s \geq 0, \mathbf{r}_p < 1 \quad (5.11)$$

$$\text{if } \mathbf{h}_{1,2} = 1, x_{1,2} = y_{1,2} \quad J_{1,2}(x_{1,2}, x_{1,2}) = \frac{1}{2} [1 + e^{-2x_{1,2}} I_0(2x_{1,2})]$$

$$\text{if } \mathbf{h}_{1,2} < 1 \quad J_{1,2}(x_{1,2}, y_{1,2}) = e^{-(x_{1,2} + y_{1,2})} \sum_{k=0}^{\infty} \mathbf{h}_{1,2}^k I_k(\mathbf{x})$$

$$\text{if } \mathbf{h}_{1,2} > 1 \quad J_{1,2}(x_{1,2}, y_{1,2}) = 1 - e^{-(x_{1,2} + y_{1,2})} \sum_{k=1}^{\infty} \mathbf{h}_{1,2}^{-k} I_k(\mathbf{x})$$

$$\mathbf{h}_{1,2} = \frac{\mathbf{s}_1 \mathbf{s}_2 \sqrt{\mathbf{r}_p}}{\mathbf{s}_{1,2}^2}, \quad x_{1,2} = \frac{s^2 \mathbf{s}_{1,2}^2}{2\mathbf{s}_1^2 \mathbf{s}_2^2 (1 - \mathbf{r}_p)}, \quad y_{1,2} = \frac{s^2 \mathbf{r}_p}{2\mathbf{s}_{1,2}^2 (1 - \mathbf{r}_p)}, \quad \mathbf{x} = \frac{s^2 \sqrt{\mathbf{r}_p}}{\mathbf{s}_1 \mathbf{s}_2 (1 - \mathbf{r}_p)}$$

\mathbf{r}_p is the power envelope correlation given in (4.72) and describes the relationship between the Rayleigh signals. The corresponding value of the envelope correlation, \mathbf{r} , can be computed from (4.73). The function $f_S(s)$ in (5.11) describes the distribution of $SNR_{V_S/N=1}$ and is valid for envelope and power envelope correlations less than unity. As can be seen from (5.11), when r_1 and r_2 are perfectly correlated ($\mathbf{r}_p = \mathbf{r} = 1$) the variables \mathbf{x} , x , and y become infinite and the above equation is no longer valid. Under the special case when both envelope signals r_1 and r_2 are perfectly correlated, both antennas receive envelopes that peak and fade at the same time. In a selection diversity system, the receiver picks the branch with the largest received envelope which under the assumption of completely correlated signals corresponds to the branch with the largest average envelope power. The $f_S(s)$ for the special case when $\mathbf{r}_p = \mathbf{r} = 1$ becomes

$$f_S(s) = \frac{s}{\max(\mathbf{s}_1^2, \mathbf{s}_2^2)} e^{-\frac{s^2}{2\max(\mathbf{s}_1^2, \mathbf{s}_2^2)}} \quad s \geq 0, \mathbf{r} = \mathbf{r}_p = 1 \quad (5.12)$$

This representation is equivalent to connecting the branch with the largest average power directly to the receiver at all times.

As mentioned earlier, $f_S(s)$ describes the probability density function of the output SNR_V of the selection combiner with the noise power set to unity ($SNR_{V_S/N=1}$). The distribution of s was derived from r_1 and r_2 using the relationship

$$s = SNR_{V_S} \Big|_{N=1} = \sqrt{SNR_{P_S}} \Big|_{N=1} = \max(r_1, r_2) \quad (5.13)$$

For completeness, the distribution of the output SNR_V after selection diversity as a function of the noise power N ($f_{S_N}(s_N)$) can be found from $f_S(s)$ by applying the following change of variables

$$s_N = SNR_{V_S} = \frac{1}{\sqrt{N}} \max(r_1, r_2) = \frac{1}{\sqrt{N}} s \quad (5.14)$$

The variables s_N and s are related by the multiplicative constant $\frac{1}{\sqrt{N}}$. From probability theory [2] it is well known that the distribution of s_N can be found by performing a simple exchange of variables of the form

$$f_{s_N}(s_N) = \sqrt{N} f_S(\sqrt{N} s_N) \quad (5.15)$$

to arrive at the distribution of the output voltage signal-to-noise ratio given in (5.1). Since performing the above substitution is trivial, the result of the distribution of the output voltage signal-to-noise ratio for an arbitrary value of N will not be performed here. In the following section, the distribution of the power signal-to-noise ratio at the output of the two-branch selection diversity system will be developed.

5.3 Probability Density Function of the SNR_{PS}

The power signal-to-noise ratio (SNR_P) as defined in Chapter 3 is the voltage signal-to-noise ratio squared or

$$SNR_P = SNR_v^2 \quad (5.16)$$

As a reminder, the SNR_P , is defined in Chapter 3 as the ratio of signal power to noise power. In this section, the distribution of the SNR_P at the output of the selection combiner will be derived for a noise power of unity. This variable z is equivalent to

$$z = SNR_{P_s} \Big|_{N=1} = \left(SNR_{V_s} \Big|_{N=1} \right)^2 = \max(r_1^2, r_2^2) = s^2 \quad (5.17)$$

The distribution of the variable s was developed in the previous section and as can be seen from the above equation, z can be computed by squaring the variable s .

Probabilistically, the probability density function of z , $f_z(z)$, can be computed from the distribution of s , $f_s(s)$, through a simple transformation [2]. The probability density function of s is given in (5.11) and (5.12) and the distribution of z can be computed from

$$f_z(z) = \frac{1}{2\sqrt{z}} f_s(\sqrt{z}) + \frac{1}{2\sqrt{z}} f_s(-\sqrt{z}) \quad (5.18)$$

Since the probability density of s is zero for all values less than zero, the second term of the above equation is zero reducing (5.18) to

$$f_z(z) = \frac{1}{2\sqrt{z}} f_s(\sqrt{z}) \quad (5.19)$$

Performing the substitution of (5.11) into (5.19), results in the probability of $SNR_{P_S/N=1}$ described by the variable z and is given by

$$f_Z(z) = \frac{1}{2\mathbf{s}_1^2} e^{-\frac{z}{2\mathbf{s}_1^2}} [1 - J_1(x_1, y_1)] + \frac{1}{2\mathbf{s}_2^2} e^{-\frac{z}{2\mathbf{s}_2^2}} [1 - J_2(x_2, y_2)] \quad z \geq 0, \mathbf{r}_p < 1 \quad (5.20)$$

$$\text{if } \mathbf{h}_{1,2} = 1, x_{1,2} = y_{1,2} \quad J_{1,2}(x_{1,2}, x_{1,2}) = \frac{1}{2} [1 + e^{-2x_{1,2}} I_0(2x_{1,2})]$$

$$\text{if } \mathbf{h}_{1,2} < 1 \quad J_{1,2}(x_{1,2}, y_{1,2}) = e^{-(x_{1,2} + y_{1,2})} \sum_{k=0}^{\infty} \mathbf{h}_{1,2}^k I_k(\mathbf{x})$$

$$\text{if } \mathbf{h}_{1,2} > 1 \quad J_{1,2}(x_{1,2}, y_{1,2}) = 1 - e^{-(x_{1,2} + y_{1,2})} \sum_{k=1}^{\infty} \mathbf{h}_{1,2}^{-k} I_k(\mathbf{x})$$

$$\mathbf{h}_{1,2} = \frac{\mathbf{s}_1 \mathbf{s}_2 \sqrt{\mathbf{r}_p}}{\mathbf{s}_{1,2}^2}, \quad x_{1,2} = \frac{z \mathbf{s}_{1,2}^2}{2\mathbf{s}_1^2 \mathbf{s}_2^2 (1 - \mathbf{r}_p)}, \quad y_{1,2} = \frac{z \mathbf{r}_p}{2\mathbf{s}_{1,2}^2 (1 - \mathbf{r}_p)}, \quad \mathbf{x} = \frac{z \sqrt{\mathbf{r}_p}}{\mathbf{s}_1 \mathbf{s}_2 (1 - \mathbf{r}_p)}$$

and when both branches are perfectly correlated the probability density function of z is described by

$$f_Z(z) = \frac{1}{2 \max(\mathbf{s}_1^2, \mathbf{s}_2^2)} e^{-\frac{z}{2 \max(\mathbf{s}_1^2, \mathbf{s}_2^2)}} \quad z \geq 0, \mathbf{r} = \mathbf{r}_p = 1 \quad (5.21)$$

The above results, (5.20) and (5.21), are valid for the special case when N is 1. However, the distribution of the output signal-to-noise ratio for an arbitrary value of noise power is an important theoretical result. For completeness, the distribution of the output SNR_P after selection diversity as a function of the noise power N ($f_{Z_N}(z_N)$) can be found from $f_Z(z)$ by applying the following change of variables

$$z_N = SNR_{P_S} = \frac{1}{N} \max(r_1^2, r_2^2) = \frac{1}{N} z \quad (5.22)$$

The variables z_N and z are related by the multiplicative constant $\frac{1}{N}$. From probability theory [2] it is well known that the distribution of z_N can be found by performing a simple exchange of variables of the form

$$f_{z_N}(z_N) = Nf_z(Nz_N) \quad (5.23)$$

to arrive at the distribution of the output power signal-to-noise ratio given in (5.22). The distribution of the output voltage signal-to-noise ratio for an arbitrary value of N can be computed from (5.20) and (5.21) by replacing z by Nz_N and multiplying the resultant distribution by N .

The following section examines some examples of the cumulative distributions after selection combining to give an appreciation of how envelope correlation affects the performance of a selection diversity system.

5.4 Selection Diversity Example

The performance of the selection diversity system depends greatly on the branch envelope correlation as will be seen in the following example. Examining the cumulative distribution function before and after combining gives an idea on how much improvement can be achieved through diversity combining. What is especially important in communication systems is to decrease the occurrence of low received signal levels because it is during these instances that the message is most likely demodulated incorrectly. The improvement at the lower ends of the CDF curve from before to after combining is therefore especially important. The following example shows the cumulative distribution function of the SNR_V of both Rayleigh branches and the distribution of the voltage signal-to-noise ratio at the output of the selection combiner with a noise power set to unity.

The values for the average power of r_1 and r_2 and the correlation are the same as the one used in the example given in relationship with Figure 4.3. The values are given in (4.76) and are repeated here as

$$\begin{aligned} E[r_1^2] &= 2\mathbf{s}_1^2 = 2 \\ E[r_2^2] &= 2\mathbf{s}_2^2 = 4.5 \\ \mathbf{r} &= 0.8 \quad (\mathbf{r}_p = 0.8189) \end{aligned} \tag{5.24}$$

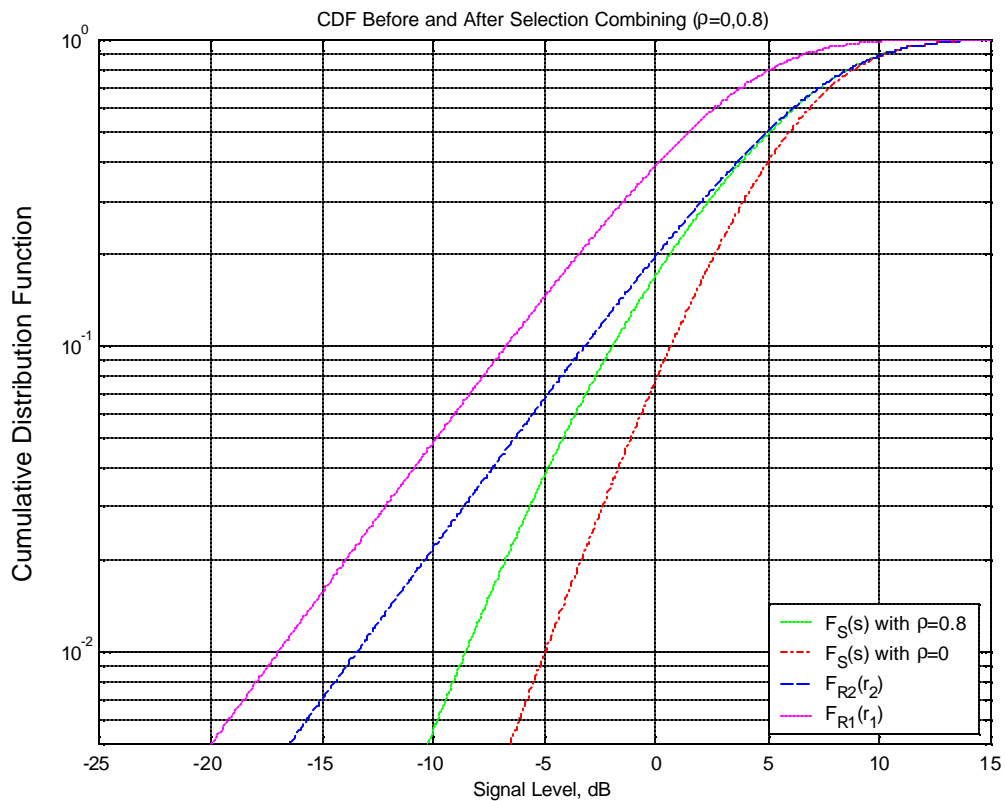


Figure 5.2 Cumulative distribution function of r_1 , r_2 , and s for an envelope correlation of 0.8 and 0.

Figure 5.2 shows an example cumulative distribution function after maximal ratio combining for an average branch power of 2 for the first branch and 4.5 for the second branch and an envelope correlation of 0.8. The CDF curve that would result from a selection diversity combining for uncorrelated branches is included for comparison in Figure 5.2. The cumulative distribution function significantly degrades as the envelope correlation approaches unity, the CDF curve after selection diversity approaches the distribution of the largest branch as r approaches unity. This effect is also demonstrated by equation (5.12).

The following chapter examines the performance a two-branch maximal ratio combiner. The probability density function of the signal to noise ratio after maximal ratio combining will be developed for the Rayleigh fading channel.

References:

- [1] Yudell L. Luke, *Integrals of Bessel Functions*, McGraw-Hill, New York, NY, 1962
- [2] Henry Stark and John W. Woods, *Probability, Random Processes, and Estimation Theory for Engineers*, Perentice Hall, Englewood Cliffs, NJ, 1994.
- [3] F. Adachi, K. Ohno, and M. Ikura, "Postdetection Selection Diversity Reception with Correlated, Unequal Average Power Rayleigh Fading Signals for $\pi/4$ -shift QDPSK Mobile Radio," *IEEE Trans. Vehic. Tech.*, vol. 41, pp. 199-210, May 1992.
- [4] M. K. Simon, M.-S. Alouini, "A Unified Performance Analysis of Digital Communications with Dual Selective Combining Diversity over Correlated Rayleigh and Nakagami-m Fading Channels," *IEEE Trans. on Commun.*, vol. 47, no. 1, pp. 33-43, Jan. 1999.

Chapter 6

Two-Branch Maximal Ratio Combining In a Rayleigh Channel

In this chapter, the probability density function of the SNR after two-branch maximal ratio combining will be developed for the correlated and unbalanced Rayleigh channel. From the joint probability density function of both received signals developed in Chapter 4 the distribution of the SNR_V and SNR_P after maximal ratio combining will be derived as a function of correlation and average branch power.

Maximal ratio combining for the correlated and unbalanced Rayleigh fading channel have also been considered in [3-6]. All results in [3-6] are expressed as a function of power envelope correlation, r_p . The envelope correlation, r , can be computed from r_p by using (4.73). In [7] and [8], an expression for the probability density function after maximal ratio combining is presented as a function of the eigen values of the correlation matrix.

6.1 Introduction

The two-branch maximal ratio combiner was analyzed in Chapter 3. Figure 3.2 shows a block diagram of the combining scheme which has an instantaneous output voltage signal-to-noise ratio given by (3.15) as

$$SNR_{V_M} = \sqrt{SNR_{P_M}} = \frac{1}{\sqrt{N}} \sqrt{r_1^2 + r_2^2} \quad (6.1)$$

As in the previous chapter, the distribution of the signal-to-noise ratio for a noise power of unity will be developed first. This probability density function with N set to 1 can be used directly as a comparison metric between theoretical and experimental results. The combining algorithm, when evaluating a diversity system, is applied to the extracted envelope data, instead of SNR, and the performance is evaluated as a function of a gain parameter. Diversity gain (see Chapter 8) depends only on the distribution of r_1 and r_2 and their correlation (and not on N) for equal noise powers in the branches. Once the distribution for a unity noise power is derived, the distribution for an arbitrary noise power can be computed by performing a trivial substitution of variables (6.23) and (6.35).

6.2 Distribution of the SNR_{V_M}

6.2.1 Probability Density Function of the SNR_{V_M}

The probability density function of the voltage SNR after maximal ratio combining with N set to unity will be derived in this section. The variable m describes this function and is defined as

$$m = SNR_{V_M} \Big|_{N=1} = \sqrt{SNR_{P_M} \Big|_{N=1}} = \sqrt{r_1^2 + r_2^2} \quad (6.2)$$

Geometrically, a two-branch maximal ratio combining system has an output voltage signal-to-noise ratio equal to that of the hypotenuse of a right triangle with the individual branch SNR_V on each side. For a noise power of unity, the sides of the triangle correspond to the envelopes r_1 and r_2 . Hence, all combinations of r_1 and r_2 that lie along the quarter circle in Figure 6.1 produce an output value of m after maximal ratio combining for a noise power of unity. The likelihood of all possible events of r_1 and r_2 that in combination produce a value m determines the probability density function $f_M(m)$. To arrive at the distribution $f_M(m)$ requires summing, or integrating, the probability density of all joint events r_1 and r_2 that generate m .

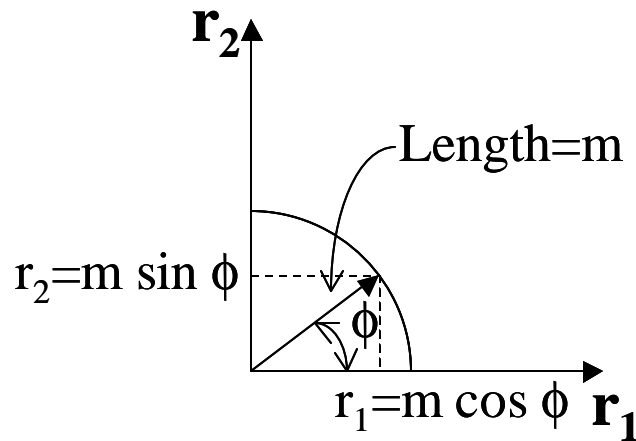


Figure 6.1. Values of r_1 and r_2 that produce a value m at the output of the maximal ratio combiner.

This integration is quite involved in the Cartesian coordinate system because it involves integrating $f_{R_1 R_2}(r_1, r_2)$ (which is a function of an exponential and a Bessel function) along the contours of a quarter circle. An alternative and equivalent method is to perform a change of variables into the m and ϕ space through the use of the Jacobian as was done in

Chapter 4 and described in [1]. This transformation is equivalent to evaluating the integration in the original space but by using this procedure it creates a probability density function which is not only a function of the variable m but also \mathbf{f} . Since only the distribution of m is of interest, the variable \mathbf{f} can be integrated out of the joint density function to develop an expression for $f_M(m)$.

The variables r_1 and r_2 can be written as a function of the variables \mathbf{f} and m as can be seen from Figure 6.1 as follows

$$\begin{aligned} r_1 &= m \cos \mathbf{f} \\ r_2 &= m \sin \mathbf{f} \end{aligned} \quad (6.3)$$

The above equations satisfy (6.2). As mentioned earlier, the new probability density function $f_{M\mathbf{F}}(m, \mathbf{f})$, which contains the variable of interest m , can be derived from $f_{R_1 R_2}(r_1, r_2)$ using a Jacobian which is defined as

$$\tilde{J} = \begin{vmatrix} \frac{\partial r_1}{\partial m} & \frac{\partial r_1}{\partial \mathbf{f}} \\ \frac{\partial r_2}{\partial m} & \frac{\partial r_2}{\partial \mathbf{f}} \end{vmatrix} = \begin{vmatrix} \cos \mathbf{f} & -m \sin \mathbf{f} \\ \sin \mathbf{f} & m \cos \mathbf{f} \end{vmatrix} = m \cos^2 \mathbf{f} + m \sin^2 \mathbf{f} = m \quad (6.4)$$

Making use of the Jacobian, the probability density function of $f_{M\mathbf{F}}(m, \mathbf{f})$ can be computed by direct substitution into the equation

$$f_{M\mathbf{F}}(m, \mathbf{f}) = |\tilde{J}| f_{R_1 R_2}(r_1, r_2) \quad (6.5)$$

which produces the joint probability density function

$$f_{M\Phi}(m, \mathbf{f}) = \frac{m^3 \cos \mathbf{f} \sin \mathbf{f}}{\mathbf{s}_1^2 \mathbf{s}_2^2 - \mathbf{a}^2 - \mathbf{b}^2} e^{-\frac{1}{2(\mathbf{s}_1^2 \mathbf{s}_2^2 - \mathbf{a}^2 - \mathbf{b}^2)} [\mathbf{s}_2^2 m^2 \cos^2 \mathbf{f} + \mathbf{s}_1^2 m^2 \sin^2 \mathbf{f}]} I_0 \left(\frac{m^2 \cos \mathbf{f} \sin \mathbf{f} \sqrt{\mathbf{a}^2 + \mathbf{b}^2}}{\mathbf{s}_1^2 \mathbf{s}_2^2 - \mathbf{a}^2 - \mathbf{b}^2} \right) \quad (6.6)$$

$m \geq 0$

The dependence of the above distribution on \mathbf{f} is of no interest to the problem at hand and can be integrated out. The above distribution can be put into a form that can be more readily integrated with respect to the variable \mathbf{f} as follows

$$f_{M\Phi}(m, \mathbf{f}) = \frac{m^3 \sin 2\mathbf{f}}{2(\mathbf{s}_1^2 \mathbf{s}_2^2 - \mathbf{a}^2 - \mathbf{b}^2)} e^{-\frac{1}{2(\mathbf{s}_1^2 \mathbf{s}_2^2 - \mathbf{a}^2 - \mathbf{b}^2)} \left[\mathbf{s}_1^2 m^2 + \frac{\mathbf{s}_2^2 m^2 - \mathbf{s}_1^2 m^2}{2} + \frac{\mathbf{s}_2^2 m^2 - \mathbf{s}_1^2 m^2}{2} \cos 2\mathbf{f} \right]} I_0 \left(\frac{m^2 \sin 2\mathbf{f} \sqrt{\mathbf{a}^2 + \mathbf{b}^2}}{2(\mathbf{s}_1^2 \mathbf{s}_2^2 - \mathbf{a}^2 - \mathbf{b}^2)} \right) \quad (6.7)$$

which was computed using the trigonometric identities

$$\begin{aligned} \sin x \cos x &= \frac{1}{2} \sin 2x \\ \cos^2 x &= \frac{1}{2} (1 + \cos 2x) \end{aligned} \quad (6.8)$$

The distribution given in (6.7) is a function of two random variables \mathbf{f} and m but only the probability density of the latter is of interest. The marginal probability density function of just the variable m can be computed by integrating out the dependence of the variable \mathbf{f} on $f_{M\Phi}(m, \mathbf{f})$. The variable \mathbf{f} ranges from 0 to $\mathbf{P}/2$ as can be seen from Figure 6.1, so this integral can be mathematically written as

$$f_M(m) = \int_0^{\mathbf{P}/2} f_{M\Phi}(m, \mathbf{f}) d\mathbf{f} \quad (6.9)$$

Substituting the joint probability given in (6.7) into the above equation produces the integral to

$$f_M(m) = Q \int_0^{p/2} \sin 2f e^{\frac{1}{2(s_1^2 s_2^2 - a^2 - b^2)} \left[\frac{s_2^2 m^2 - s_1^2 m^2}{2} \cos 2f \right]} I_0 \left(\frac{m^2 \sin 2f \sqrt{a^2 + b^2}}{2(s_1^2 s_2^2 - a^2 - b^2)} \right) df \quad (6.10)$$

$$Q = \frac{m^3}{2(s_1^2 s_2^2 - a^2 - b^2)} e^{-\frac{1}{2(s_1^2 s_2^2 - a^2 - b^2)} \left[s_1^2 m^2 + \frac{s_2^2 m^2 - s_1^2 m^2}{2} \right]}$$

where the function Q is a constant with respect to the variable f . The solution of the above integral can be achieved by applying the following change of variables on f .

$$\begin{aligned} u &= \cos 2f \\ \frac{du}{df} &= -2 \sin 2f \\ \sin 2f &= \pm \sqrt{1 - \cos^2 2f}, \text{ over the interval} \\ &\text{of interest, } \sin 2f = \sqrt{1 - u^2} \end{aligned} \quad (6.11)$$

The motivation for performing this substitution is to transform the integral in a form that can be more readily found in an integral table. The function (6.10) can be re-written in terms of the variable u in the following manner

$$f_M(m) = \frac{Q}{2} \int_{-1}^1 e^{\frac{1}{2(s_1^2 s_2^2 - a^2 - b^2)} \left[\frac{s_2^2 m^2 - s_1^2 m^2}{2} u \right]} I_0 \left(\frac{m^2 \sqrt{1 - u^2} \sqrt{a^2 + b^2}}{2(s_1^2 s_2^2 - a^2 - b^2)} \right) du \quad (6.12)$$

The solution of the above equation can be found in [2] under the integral

$$\int_{-1}^1 e^{-ax} I_0(b\sqrt{1-x^2}) dx = (a^2 + b^2)^{-1/2} \left(e^{\sqrt{a^2 + b^2}} - e^{-\sqrt{a^2 + b^2}} \right) \quad (6.13)$$

$$a > 0, b \geq 0, \text{ or } a \geq 0, b > 0$$

The above result requires that both the constants b and a be positive and if one of them is zero, the other should be larger than zero. For the integral in question, (6.12), these constants equate to

$$a = \frac{\mathbf{s}_2^2 m^2 - \mathbf{s}_1^2 m^2}{4(\mathbf{s}_1^2 \mathbf{s}_2^2 - \mathbf{a}^2 - \mathbf{b}^2)}, \quad b = \frac{m^2 \sqrt{\mathbf{a}^2 + \mathbf{b}^2}}{2(\mathbf{s}_1^2 \mathbf{s}_2^2 - \mathbf{a}^2 - \mathbf{b}^2)} \quad (6.14)$$

By inspection, the value of b will always be larger or equal to zero. The variable a , on the other hand will be nonnegative only when the average branch power of branch 2 is larger or equal to the average power in branch 1 ($\mathbf{s}_2^2 \geq \mathbf{s}_1^2$). Hence, based on the values of a and b , the solution will only be valid for an arbitrary correlation when branch 2 is larger than branch 1 ($2\mathbf{s}_2^2 > 2\mathbf{s}_1^2$), or under the special case when the average powers are equal ($2\mathbf{s}_2^2 = 2\mathbf{s}_1^2$), the correlation between both branches has to be nonzero for (6.13) to apply. The previous statements guarantee that a and b are not zero at the same time and that a always be non-negative. From (6.13), it can be seen if these two provisions are not met, the equation (6.13) will be singular and therefore not valid.

After several algebraic manipulations, using the values of a and b given in (6.14) results in the following equation for the probability density function of m at the output of the maximal ratio combiner

$$f_M(m) = \frac{m e^{-\frac{m^2(\mathbf{s}_1^2 + \mathbf{s}_2^2)}{4\mathbf{s}_1^2 \mathbf{s}_2^2 (1-r_p)}}}{\sqrt{(\mathbf{s}_2^2 - \mathbf{s}_1^2)^2 + 4\mathbf{s}_1^2 \mathbf{s}_2^2 r_p}} \left[e^{\frac{m^2 \sqrt{(\mathbf{s}_2^2 - \mathbf{s}_1^2)^2 + 4\mathbf{s}_1^2 \mathbf{s}_2^2 r_p}}{4\mathbf{s}_1^2 \mathbf{s}_2^2 (1-r_p)}} - e^{-\frac{m^2 \sqrt{(\mathbf{s}_2^2 - \mathbf{s}_1^2)^2 + 4\mathbf{s}_1^2 \mathbf{s}_2^2 r_p}}{4\mathbf{s}_1^2 \mathbf{s}_2^2 (1-r_p)}} \right] \quad (6.15)$$

$$m \geq 0; r_p, r < 1$$

for $\mathbf{s}_2 \geq \mathbf{s}_1$ except when both, $\mathbf{s}_1 = \mathbf{s}_2$ and $\mathbf{a} = \mathbf{b} = 0$ ($r = r_p = 0$)

As stated earlier, (6.15) is valid for $\mathbf{s}_1 \leq \mathbf{s}_2$ as long as both \mathbf{a} and \mathbf{b} are not equal to zero ($r = r_p = 0$). For the case when \mathbf{a} and \mathbf{b} are both zero, the average power in branch 2 must exceed the power in branch 1 for (6.15) to apply. The above equation does not account for the case when both received signals are uncorrelated and have the same average power ($\mathbf{a} = \mathbf{b} = 0$ in (6.14)). If both average branch powers are equal, $\mathbf{s} = \mathbf{s}_1 = \mathbf{s}_2$, and uncorrelated, $\mathbf{a} = \mathbf{b} = 0$, (6.10) simplifies to

$$f_M(m) = \int_0^{P/2} f_{M\Phi}(m, \mathbf{f}) d\mathbf{f} = \int_0^{P/2} \frac{m^3 \sin 2\mathbf{f}}{2\mathbf{s}^4} e^{-\frac{m^2}{2\mathbf{s}^2}} d\mathbf{f} = \frac{m^3}{2\mathbf{s}^4} e^{-\frac{m^2}{2\mathbf{s}^2}} \quad (6.16)$$

$$m \geq 0$$

valid for $\mathbf{s}_1 = \mathbf{s}_2 = \mathbf{s}$ and $\mathbf{a} = \mathbf{b} = 0$ ($\mathbf{r} = \mathbf{r}_p = 0$)

The above equation for the probability density function of signal m at the output of the maximal ratio combiner is valid only for equal branch powers that are completely uncorrelated. Both equations presented above, (6.15) and (6.16), are not applicable when branches are completely correlated. So finally, under the special case when both branches are perfectly correlated ($\mathbf{r} = \mathbf{r}_p = I$), the variable r_1 can be represented as

$$r_1 = \mathbf{s}_1 r \quad (6.17)$$

where r has a probability density function $f_R(r)$ given by

$$f_R(r) = r e^{-\frac{r^2}{2}} \quad r \geq 0 \quad (6.18)$$

The probability density function of the variable r_1 as described by (6.17), $f_{R_1}(r_1)$, can be found to match the distribution given in (4.43) after performing the necessary transformation of variables. When both branches are perfectly correlated, the received envelopes peak and fade at the same time. This means that the envelopes r_1 and r_2 have the same underlying random variable but can possibly differ in amplitude because \mathbf{s}_1 and \mathbf{s}_2 are not necessarily equal. Consequently r_2 can also be expressed as a function of r when both branches are perfectly correlated as

$$r_2 = \mathbf{s}_2 r \quad (6.19)$$

where r is described by (6.18). As with $f_{R_1}(r_1)$, it can be shown, that the definition in (6.19) still produces the probability density function $f_{R_2}(r_2)$ given by (4.43). For $\mathbf{r}=I$, the variable m given in (6.2) can be re-written as

$$m|_{\mathbf{r}=I} = \sqrt{r_1^2 + r_2^2} = \sqrt{(\mathbf{s}_1 r)^2 + (\mathbf{s}_2 r)^2} = \sqrt{\mathbf{s}_1^2 + \mathbf{s}_2^2} r \quad (6.20)$$

The above equation of m is a scaled version of the variable r and therefore has a similar shape as the underlying variable $f_R(r)$. The probability of m for perfectly correlated branches becomes

$$f_M(m) = \frac{m}{(\mathbf{s}_1^2 + \mathbf{s}_2^2)} e^{-\frac{m^2}{2(\mathbf{s}_1^2 + \mathbf{s}_2^2)}} m^{\mathfrak{a}0} \text{ and } \mathbf{r} = \mathbf{r}_p = 1 \quad (6.21)$$

which can be evaluated in a similar fashion as (6.17) and (6.19). The above equations describe the probability density function of the variable m at the output of the maximal ratio combiner for all combinations of envelope correlation and average branch powers. For completeness, the distribution of the output SNR_V after maximal ratio combining as a function of the noise power N ($f_{M_N}(m_N)$) can be found from $f_M(m)$ by applying the following change of variables

$$m_N = SNR_{V_M} = \sqrt{SNR_{P_M}} = \frac{1}{\sqrt{N}} \sqrt{r_1^2 + r_2^2} = \frac{1}{\sqrt{N}} m \quad (6.22)$$

The variables m_N and m are related by the multiplicative constant $\frac{1}{\sqrt{N}}$. From probability theory [1] it is well known that the distribution of m_N can be found by performing an exchange of variables of the form

$$f_{M_N}(m_N) = \sqrt{N} f_M(\sqrt{N} m_N) \quad (6.23)$$

to arrive at the distribution of the output voltage signal-to-noise ratio for an arbitrary value of N defined by (6.22). This substitution is easily computed from the probability density function of m . In the following section, the cumulative distribution function of the voltage signal-to-noise ratio will be derived at the output of the two-branch maximal ratio combiner.

6.2.2 Cumulative Distribution Function of the SNR_{V_M}

In probability theory, the cumulative distribution function (CDF) is defined as the probability that an occurred event is below or equal to a given value. It is related to the probability density function in the following manner

$$F_M(m) = \int_{-\infty}^m f_M(x) dx \quad (6.24)$$

In the previous section, the probability density function of m was derived for all possible combinations of average branch powers and correlation. The resulting three equations were valid over different intervals and should therefore be integrated separately. These equations are given listed under (6.15), (6.16), and (6.21). Integrating the first equation of $f_M(m)$ given in (6.15) as described in (6.24) results in the cumulative distribution function

$$F_M(m) = 1 - \frac{e^{-\frac{m^2(\mathbf{s}_1^2 + \mathbf{s}_2^2)}{4\mathbf{s}_1^2\mathbf{s}_2^2(1-r_p)}}}{2\sqrt{(\mathbf{s}_2^2 - \mathbf{s}_1^2)^2 + 4\mathbf{s}_1^2\mathbf{s}_2^2r_p}} \left[e^{\frac{m^2\sqrt{(\mathbf{s}_2^2 - \mathbf{s}_1^2)^2 + 4\mathbf{s}_1^2\mathbf{s}_2^2r_p}}{4\mathbf{s}_1^2\mathbf{s}_2^2(1-r_p)}} \left(\sqrt{(\mathbf{s}_2^2 - \mathbf{s}_1^2)^2 + 4\mathbf{s}_1^2\mathbf{s}_2^2r_p} + (\mathbf{s}_1^2 + \mathbf{s}_2^2) \right) + e^{-\frac{m^2\sqrt{(\mathbf{s}_2^2 - \mathbf{s}_1^2)^2 + 4\mathbf{s}_1^2\mathbf{s}_2^2r_p}}{4\mathbf{s}_1^2\mathbf{s}_2^2(1-r_p)}} \left(\sqrt{(\mathbf{s}_2^2 - \mathbf{s}_1^2)^2 + 4\mathbf{s}_1^2\mathbf{s}_2^2r_p} - (\mathbf{s}_1^2 + \mathbf{s}_2^2) \right) \right] \quad (6.25)$$

$$m \geq 0; \mathbf{r}, \mathbf{r}_p < 1$$

for $\mathbf{s}_2 \geq \mathbf{s}_1$ except when both, $\mathbf{s}_2 = \mathbf{s}_1$ and $\mathbf{a} = \mathbf{b} = 0$ ($\mathbf{r} = \mathbf{r}_p = 0$)

which is valid over the same conditions as (6.15). This result was computed by performing a change of variables prior to integration. Integration by parts can be used to compute the cumulative distribution function of $f_M(m)$ given in (6.16) which is valid when both average branch powers are equal and at the same time are uncorrelated. The resulting $F_M(m)$ corresponding to the probability density function given in (6.16) becomes

$$F_M(m) = 1 - \left(1 + \frac{m^2}{2\mathbf{s}^2}\right) e^{-\frac{m^2}{2\mathbf{s}^2}} m^{\mathfrak{A}0}, \text{ valid for } \mathbf{s}_2 = \mathbf{s}_1 = \mathbf{s} \text{ and } \mathbf{a} = \mathbf{b} = 0 \text{ (} \mathbf{r} = 0 \text{)} \quad (6.26)$$

And finally, the cumulative distribution function for perfectly correlated signals produces a cumulative distribution given by

$$F_M(m) = 1 - e^{-\frac{m^2}{2(\mathbf{s}_1^2 + \mathbf{s}_2^2)}} m^{\mathfrak{A}0} \text{ and } \mathbf{r} = \mathbf{r}_p = 1 \quad (6.27)$$

An example of the application of (6.25), (6.26), and (6.27) will be given in section 6.4. These cumulative distribution functions will also be used in Chapter 8 where comparisons between measured and theoretical data are made.

6.3 Probability Density Function of the SNR_{PM}

The power signal-to-noise ratio is a useful distribution because this variable is proportional to the symbol energy to noise ratio (E_S/N_0) in flat fading channel. From the distribution of E_S/N_0 , the average probability of symbol error for digital modulations can be determined as will be seen in Chapter 7. The power signal-to-noise ratio (SNR_p) as defined in Chapter 3 is the voltage signal-to-noise ratio squared or

$$\text{SNR}_p = \text{SNR}_v^2 \quad (6.28)$$

The SNR_P is defined as the ratio of signal power to noise power. As was done in Section 6.2, the SNR_P at the output of the maximal ratio combiner will be derived for a noise power of unity. This variable y is equivalent to

$$y = SNR_{P_M} \Big|_{N=1} = \left(SNR_{V_M} \Big|_{N=1} \right)^2 = r_1^2 + r_2^2 = m^2 \quad (6.29)$$

The variable y can be computed by squaring the random variable m . This is a similar problem to the one that was already addressed in section 5.3. The probability density function of m is given in (6.15), (6.16), and (6.21) and distribution of y can be found by using the transformation given in (5.19). $f_Y(y)$ can be computed from

$$f_Y(y) = \frac{1}{2\sqrt{y}} f_M(\sqrt{y}) \quad (6.30)$$

Replacing (6.15) into (6.30), results in the probability of $SNR_{P_M/N=1}$ described by the variable y and is given by

$$f_Y(y) = \frac{e^{-\frac{y(\mathbf{s}_1^2 + \mathbf{s}_2^2)}{4\mathbf{s}_1^2 \mathbf{s}_2^2 (1-r_p)}}}{2\sqrt{(\mathbf{s}_2^2 - \mathbf{s}_1^2)^2 + 4\mathbf{s}_1^2 \mathbf{s}_2^2 r_p}} \left[e^{\frac{y\sqrt{(\mathbf{s}_2^2 - \mathbf{s}_1^2)^2 + 4\mathbf{s}_1^2 \mathbf{s}_2^2 r_p}}{4\mathbf{s}_1^2 \mathbf{s}_2^2 (1-r_p)}} - e^{-\frac{y\sqrt{(\mathbf{s}_2^2 - \mathbf{s}_1^2)^2 + 4\mathbf{s}_1^2 \mathbf{s}_2^2 r_p}}{4\mathbf{s}_1^2 \mathbf{s}_2^2 (1-r_p)}} \right] \quad (6.31)$$

$$y \geq 0; r_p, r < 1$$

for $\mathbf{s}_2 \geq \mathbf{s}_1$ except when both, $\mathbf{s}_1 = \mathbf{s}_2$ and $\mathbf{a} = \mathbf{b} = 0$ ($\mathbf{r} = r_p = 0$)

and is valid for correlated signals when branch 2 has an average power that is larger or equal to that of branch 1. In the case both signals are uncorrelated ($\mathbf{a} = \mathbf{b} = 0$), the average power in branch 2 must exceed the power in branch 1 for (6.31) to apply. When both branches are at the same time uncorrelated and have equal average branch powers, $f_Y(y)$ is determined by substituting (6.16) into (6.30) which produces

$$f_Y(y) = \frac{y}{4\mathbf{s}^4} e^{-\frac{y}{2\mathbf{s}^2}} \quad (6.32)$$

$$y \geq 0$$

valid for $\mathbf{s}_1 = \mathbf{s}_2 = \mathbf{s}$ and $\mathbf{a} = \mathbf{b} = 0$ ($\mathbf{r} = \mathbf{r}_p = 0$)

Finally by plugging (6.21) in (6.30), the probability density function $f_Y(y)$ becomes

$$f_Y(y) = \frac{1}{2(\mathbf{s}_1^2 + \mathbf{s}_2^2)} e^{-\frac{y}{2(\mathbf{s}_1^2 + \mathbf{s}_2^2)}} \quad y \geq 0 \text{ and } \mathbf{r} = \mathbf{r}_p = 1 \quad (6.33)$$

when both branches are perfectly correlated. The variable y describes the distribution of the output SNR_p for a noise power of unity. In general, the noise power is not always unity and the distribution for an arbitrary value of N is easily computed from $f_Y(y)$. The distribution of the output SNR_p after maximal ratio combining as a function of the noise power N ($f_{Y_N}(y_N)$) can be found from $f_Y(y)$ by applying the following change of variables

$$y_N = SNR_{p_M} = \frac{1}{N} (r_1^2 + r_2^2) = \frac{1}{N} y \quad (6.34)$$

The variables y_N and y are related by the multiplicative constant $\frac{1}{N}$. As done in section

5.3, the distribution of y_N can be found by performing a substitution of variables of the form

$$f_{Y_N}(y_N) = N f_Y(N y_N) \quad (6.35)$$

to arrive at the distribution of the output power signal-to-noise ratio given in equation (6.34). Performing the above substitution is straightforward so the expression of the distribution of y_N will not be evaluated here.

The following section examines the cumulative distribution after maximal ratio combining for the same example described in Section 4.3.

6.4 Maximal Ratio Combining Example

The performance of the maximal ratio combiner in the Rayleigh channel depends greatly on the branch envelope correlation and average branch power imbalance. The improvements in the cumulative distribution function before and after combining gives an idea on how much gain can be achieved by using this combining algorithm. The following example shows the cumulative distribution function of the SNR_V of both Rayleigh branches and the distribution of the voltage signal-to-noise ratio at the output of the maximal ratio combiner for a noise power of unity.

The values for the average power of r_1 and r_2 and the correlation are the same as the ones used in the example given in relationship with Figure 4.3. The following values were used for the example

$$\begin{aligned} E[r_1^2] &= 2\mathbf{s}_1^2 = 2 \\ E[r_2^2] &= 2\mathbf{s}_2^2 = 4.5 \\ \mathbf{r} &= 0.8 (\mathbf{r}_p = 0.8189) \end{aligned} \tag{6.36}$$

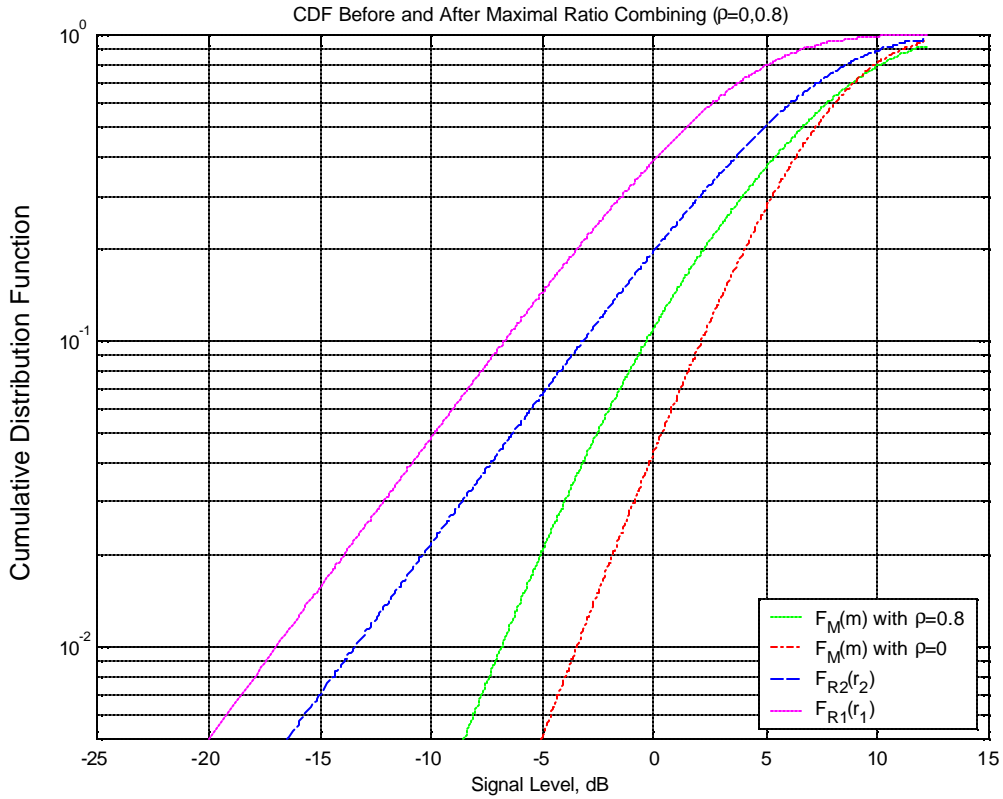


Figure 6.2 Cumulative distribution function of r_1 , r_2 , and m for an envelope correlation of 0.8 and 0.

In Figure 6.2, the individual Rayleigh branch signals defined in (4.43) are plotted with the distribution at the output of the maximal ratio combiner, $F_M(m)$, for uncorrelated branches and an envelope correlation of 0.8 as described by (6.25). The average branch powers of both signals are given in (6.36). Maximal ratio combining will always outperform selection diversity at both instantaneously level and in the statistical sense. This result can be observed by comparing the curves in Figures 5.2 and 6.2 which compare both diversity combining schemes under the same conditions. The curves represent the distribution of the voltage signal-to-noise ratio for a noise power of 1. If the value of the noise power N was known, all curves would just shift to the left or right by the same amount depending on the value of N . The horizontal distance separating all four

curves in Figure 6.2 are unaffected by the value of N and hence the diversity gain (Chapter 8) will remain the same.

References:

- [1] Henry Stark and John W. Woods, *Probability, Random Processes, and Estimation Theory for Engineers*, Perentice Hall, Englewood Cliffs, NJ, 1994.
- [2] I. S. Gradshteyn and I. M. Ryzhik, *Table of Integrals, Series, and Products*, Academic Press Inc., San Diego, CA, 1994.
- [3] Emad K. Al-Hussaini and Abdel Aziz M. Al-Bassiouni, "Performance of MRC Diversity Systems for the Detection of Signals with Nakagami Fading," *IEEE Trans. Commun.*, vol. COM-33, no. 12, pp. 1315-1319, Dec. 1985.
- [4] Francois Patenaude, John H. Lodge, and Jean-Yves Chouinard, "Noncoherent Diversity Reception Over Nakagami-Fading Channels," *IEEE Trans. Commun.*, vol. 46, no. 8, pp. 985-991, Aug. 1998.
- [5] Q. T. Zhang, "Exact Analysis of Postdetection Combining for DPSK and NFSK System Over Arbitrarily Correlated Nakagami Channels," *IEEE Trans. Commun.*, vol. 46, no. 11, pp. 1459-1467, Nov. 1998.
- [6] Pierfrancesco Lombardo, Gennaro Fedele, and Murli Mohan Rao, "MRC Performance for Binary Signals in Nakagami Fading with General Branch Correlation," *IEEE Trans. Commun.*, vol. 47, no. 1, pp. 44-52, Jan. 1999.
- [7] O. Norklit and R.G. Vaughan, "Method to Determine Effective Number of Diversity branches," *Global Communications Conference 1998*, vol. 1, pp. 138-141, 1998.
- [8] M. Z. Win, J. H. Winters, "On Maximal Ratio Combining in Correlated Nakagami channels with unequal fading parameters and SNR's among branches: an Analytic Framework," *Wireless Communications and Networking Conference*, vol. 3, pp. 1058-1064, 1999.

Chapter 7

Performance of Coherent BPSK and QPSK in a Rayleigh Channel with a Two Branch Diversity Maximal Ratio Combiner

The previous chapters analyzed the performance of diversity combining on narrowband signals in a Rayleigh fading channel. The analysis was performed with the assumptions that the message contained only a single frequency tone. In this chapter the narrowband results derived in the Chapters 4-6 will be extended to encompass wideband signals for slow channels that have a flat frequency response over the bandwidth of the message.

7.1 Introduction

The performance of two digital modulation schemes will be evaluated in this chapter for a flat and slow fading channel. The symbol error rate of coherent BPSK (Binary Phase Shift Keying) and coherent QPSK (Quadrature Phase Shift Keying) will be derived for a

two-branch maximal ratio combiner in a correlated and unbalanced Rayleigh channel.

Both these digital modulation schemes are heavily used in present wireless communication networks and their performance in the Rayleigh channel can be evaluated analytically.

Section 7.2 examines the channel model for which the average symbol error probabilities will be derived. In Section 7.3, the symbol error rate of QPSK and BPSK will be related to the envelope distribution of the received signal. The performance of both these digital modulations will also be examined in this section for a single branch antenna system. In Sections 7.4, an exact expression for the average symbol error rate of BPSK and QPSK after two-branch maximal ratio combining will be developed.

7.2 Channel model

As mentioned in Chapter 2, the antenna receives a signal that is a superposition of several versions of the transmitted signal that arrive at the receiver with different time delays. In general, these channels can introduce flat or frequency selective fading. A flat fading channel occurs when all the frequency components of the signal of interest are equally affected in amplitude by the channel and only a linear phase over frequency is introduced. A flat fading channel translates into an environment in which the multipath components arrive at the receiver at approximately the same time (t_0). The resultant sum of all the multipath components can be expressed as follows in the time domain

$$r(t) = \sum_{i=1}^L a_i s(t - t_0) = s(t - t_0) \sum_{i=1}^L a_i = \mathbf{a} s(t - t_0) \quad (7.1)$$

$$\sum_{i=1}^L a_i = \mathbf{a}$$

and in the frequency domain as

$$s(t) \Leftrightarrow S(f), r(t) = \mathbf{a}s(t - t_0) \Leftrightarrow R(f) = \mathbf{a}S(f)e^{-j2\pi ft_0} \quad (7.2)$$

a_i are the complex weights associated with each multipath component and \mathbf{a} represents the distribution of the amplitude and phase of the received signal which is a result of the addition of multiple reflections. If all a_i are equally distributed and large in number, the resulting \mathbf{a} is Rayleigh distributed as was shown in Chapter 3. The instantaneous value of \mathbf{a} determines the instantaneous amplitude of the received symbol regardless of the bandwidth of the message as long as the channel is flat. From the spectral representation of $r(t)$ in (7.2) one can see that all frequency components of the signal of interest ($s(t)$) are affected equally in amplitude by the channel (they are all scaled by \mathbf{a}) and have a linear phase. According to the discussions in Chapter 2, this type of channel introduces flat fading. A frequency selective channel, on the other hand, has multipath components that do not arrive at the receiver at the same time. These types of channels require equalization to combat inter-symbol-interference before diversity can be applied to increase the signal-to-noise ratio. The expressions presented here for the symbol error probability were all derived under the assumptions of a flat and slow fading channel. A channel is slow fading when the channel has not changed during the arrival of a transmitted symbol. This means that there are no notable amplitude and phase modulations on the symbol arising from the time varying nature of the channel. Hence, the channel varies slowly compared to the symbol data rate.

7.3 Symbol Error Rate of Coherent QPSK and BPSK in the Rayleigh Channel

The optimum receiver in the presence of additive white Gaussian noise has been extensively analyzed in textbooks [1]. This section gives a review of the symbol error probabilities of coherent BPSK and QPSK in the presence of AWGN. From these results, the average probabilities of symbol error are derived for both modulations in the Rayleigh channel. An example of a maximum likelihood receiver for QPSK is shown in Figure 7.1.

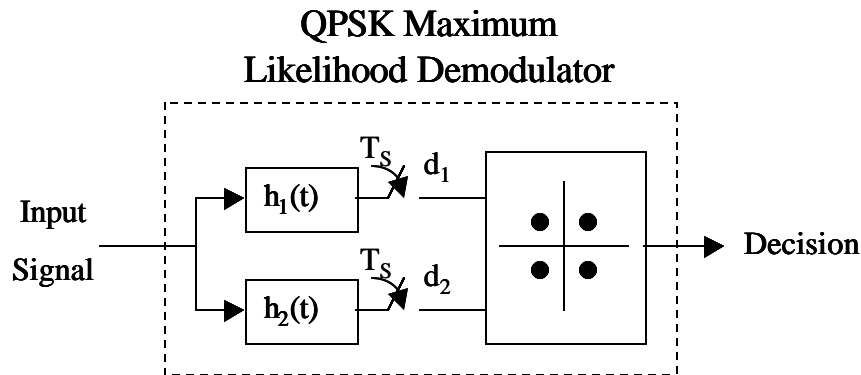


Figure 7.1 Optimal receiver for QPSK in the presence of AWGN

The receiver consists of two matched filters, h_1 and h_2 , which are matched to the in-phase and quadrature components of the received signal. The receiver makes a decision of what symbol was transmitted based on the region where d_1 and d_2 falls on the constellation diagram. The regions are picked in a way that the symbol error probability is minimized. The probability of symbol error, P_{AWGN}^e , in the presence of AWGN is usually expressed as a function of the ratio E_s/N_0 which is a measure of signal to noise ratio. E_s is the average symbol energy and $1/2 N_0$ is the variance of the Gaussian noise. A BPSK signal can only take on one of two possible values, so for this modulation, the symbol error probability and the bit error probability can be used interchangeably and the symbol energy E_s is equal to the bit energy E_b . The probability of symbol error, P^e , for an AWGN channel using an optimal coherent BPSK receiver is given by [1]

$$P_{AWGN,BPSK}^e = Q\left(\sqrt{\frac{2E_b}{N_0}}\right) = Q\left(\sqrt{\frac{2E_s}{N_0}}\right) \quad (7.3)$$

where Q is the Q-function. QPSK, on the other hand, has four distinct levels and hence each symbol can be represented by two bits. The symbol energy is related to the bit energy in the following manner

$$E_s = 2E_b \quad (7.4)$$

Equivalently, the probability of symbol error for coherent QPSK in an additive white Gaussian noise for a given E_s/N_0 ratio is given in [1] as

$$P_{AWGN,QPSK}^e = 2Q\left(\sqrt{\frac{E_s}{N_0}}\right) - \left[Q\left(\sqrt{\frac{E_s}{N_0}}\right)\right]^2 \quad (7.5)$$

In a fading channel, E_s (the energy of the symbol) is a random variable proportionally distributed to the envelope squared. Similarly, the ratio E_s/N_0 is proportional to the power signal to noise ratio in a channel that is frequency non-selective. E_s/N_0 and the SNR_P are related by a constant and therefore have distributions that have the same underlying shape but possibly differ in the variances.

Since the only difference between the distributions of E_s/N_0 and SNR_P (or $SNR_{P/N=1}$) is the variance, there exist a value \mathbf{s} such that the distribution of SNR_P is equivalent to the desired distribution of E_s/N_0 . Assuming that the value of \mathbf{s} that makes both of these distributions equal is known, the probability of error for BPSK and QPSK can be rewritten as

$$P_{AWGN,BPSK}^e = Q(\sqrt{2x}), \quad P_{AWGN,QPSK}^e = 2Q(\sqrt{x}) - [Q(\sqrt{x})]^2 \quad (7.6)$$

where $f_X(x)$ describes the probability density function of the variable x (or E_s/N_0) and is equal to the distribution of the SNR_P (with N set to 1) for a given value \mathbf{s} . If $f_X(x)$ describes the random variable E_s/N_0 , the average E_s/N_0 can be computed by evaluating

the first moment of the distribution. When all symbols are equally likely, $\overline{E_s/N_0}$ becomes

$$\frac{\overline{E_s}}{N_0} = \bar{x} = \int_0^{\infty} x f_X(x) dx \quad (7.7)$$

The above is a general result that applies for both QPSK and BPSK. The distribution of the envelope of both diversity branches is assumed to be Rayleigh distributed. This means that the $SNR_{V,2}$ for a noise power of unity is described by the probability density function given in (4.43). For the Rayleigh channel, $f_X(x)$ is the distribution of the SNR_P with a noise power set to unity which can be found to be

$$f_X(x) = \frac{1}{2\mathbf{s}^2} e^{-\frac{x}{2\mathbf{s}^2}} \quad (7.8)$$

from Chapters 5 and 6. As stated earlier, because of the proportionality that exists between E_s/N_0 and SNR_P , there exists a value \mathbf{s} that will make both of these distributions equal. The average E_s/N_0 at each Rayleigh branch using (7.7) for the $f_X(x)$ given in (7.8) evaluates to

$$\left(\frac{\overline{E_s}}{N_0} \right)_{Branch1,2} = 2\mathbf{s}_{1,2}^2 \quad (7.9)$$

The average probability of symbol error for the fading channel, P^e , can be computed by averaging P_{AWGN}^e over all possible values the probability density of x (or E_s/N_0) can take. This average probability of error can be written as the integral

$$P^e = \int_0^{\infty} P_{AWGN}^e(x) f_X(x) dx \quad (7.10)$$

where P_{AWGN}^e is the probability of symbol error in additive white Gaussian noise given in (7.3) for BPSK and (7.5) for QPSK. When (7.3) and $f_X(x)$ in (7.8) are substituted into equation (7.10), the result is the average symbol error probability of coherent BPSK in a Rayleigh fading channel (which has also been derived in [1]) can be integrated from

$$P_{Rayleigh,BPSK}^e = \int_0^{\infty} P_{AWGN,BPSK}^e(x) f_X(x) dx = \int_0^{\infty} Q(\sqrt{2x}) \frac{1}{2\mathbf{s}^2} e^{-\frac{x}{2\mathbf{s}^2}} dx \quad (7.11)$$

Noting that the Q function can be written in terms of the error function as follows

$$Q(\sqrt{2x}) = \frac{1}{2} - \frac{1}{2} \operatorname{erf}(\sqrt{x}) \quad (7.12)$$

and from [2], the integration of an exponential and the error function (erf) over the limits from 0 to ∞ is given by

$$\int_0^{\infty} e^{-pl} \operatorname{erf}(\sqrt{al}) dl = \frac{1}{p} \sqrt{\frac{a}{a+p}}, \operatorname{Re} p, \operatorname{Re}(p+a^2) > 0 \quad (7.13)$$

The results given in (7.12) and (7.13) can be used to integrate (7.11) producing the average symbol error of coherent BPSK in a Rayleigh channel which is given by

$$P_{Rayleigh,BPSK}^e = \frac{1}{2} - \frac{1}{2} \sqrt{\frac{2\mathbf{s}^2}{1+2\mathbf{s}^2}} \quad (7.14)$$

Equivalently, the average symbol error of QPSK in the Rayleigh fading channel can also be computed from (7.10). The distribution of $f_X(x)$ for the Rayleigh channel is given in (7.8) and the probability of symbol error of QPSK is AWGN is given in (7.5). The error

probability P^e in an AWGN channel can be averaged over the possible values E_s/N_0 using (7.10) as was done for BPSK. The solution of the integral

$$P_{Rayleigh,QPSK}^e = \int_0^{\infty} P_{AWGN,QPSK}^e(x) f_X(x) dx = \int_0^{\infty} \left[2Q(\sqrt{x}) - Q(\sqrt{x})^2 \right] \frac{1}{2\mathbf{s}^2} e^{-\frac{x}{2\mathbf{s}^2}} dx \quad (7.15)$$

will therefore result in the average symbol error of coherent QPSK in the Rayleigh channel. From the relationship between the erf and the Q function given in (7.12) and the integral found in [2] as

$$\int_0^{\infty} e^{-pl} \operatorname{erf}^2(a\sqrt{l}) dl = \frac{4a}{\mathbf{p}} \left(\frac{1}{p\sqrt{p+a^2}} \arctan \frac{a}{\sqrt{p+a^2}} \right) \quad (7.16)$$

the solution of the integral given in (7.15) can be achieved. This process produces the following expression for the average probability of symbol error of coherent QPSK for a Rayleigh channel

$$P_{Rayleigh,QPSK}^e = \frac{3}{4} - \sqrt{\frac{\mathbf{s}^2}{(1+\mathbf{s}^2)}} \left[\frac{1}{2} + \frac{1}{\mathbf{p}} \arctan \sqrt{\frac{\mathbf{s}^2}{(1+\mathbf{s}^2)}} \right] \quad (7.17)$$

The average E_s/N_0 of QPSK is equal to that of BPSK and is given (7.9) because in both cases the same probability density function $f_X(x)$ was used. In the following section, the average symbol error rate of coherent QPSK and BPSK after two-branch maximal ratio combining will be computed.

7.4 Performance of Coherent QPSK and BPSK after Maximal Ratio Combining for the Rayleigh Channel

7.4.1 Average E_s/N_0 After Two-Branch Maximal Ratio Combining

The probability density function of the output SNR_P for a two branch maximal ratio combining system is given in (6.31), (6.32), and (6.33). These equations were derived for the Rayleigh channel taking into account the possibility that both branches might be correlated or have different average powers. As was noted in the previous section, the SNR_P and the E_s/N_0 are proportional to each other and therefore have probability density functions that have the same shape. As was also mentioned, there exists a value of \mathbf{s} that makes both distributions equal. The average E_s/N_0 after maximal ratio combining can be found by solving (7.7) using the three versions of the SNR_P that are valid over different intervals. Using the equation for perfectly correlated signals given in (6.33) first, produces the following average E_s/N_0

$$\left(\frac{\overline{E_s}}{N_0}\right)_{Max(r=1)} = \int_0^{\infty} \frac{y}{2(\mathbf{s}_1^2 + \mathbf{s}_2^2)} e^{-\frac{y}{2(\mathbf{s}_1^2 + \mathbf{s}_2^2)}} = 2(\mathbf{s}_1^2 + \mathbf{s}_2^2) \quad (7.18)$$

When the above procedure is repeated for the other two probability density functions, (6.31) and (6.32) using a table of integrals such as [3] yields the same result. The average E_s/N_0 after maximal ratio combining can be found to be independent of correlation and always

$$\left(\frac{\overline{E_s}}{N_0}\right)_{Max} = \left(\frac{\overline{E_s}}{N_0}\right)_{Branch1} + \left(\frac{\overline{E_s}}{N_0}\right)_{Branch2} = 2(\mathbf{s}_1^2 + \mathbf{s}_2^2) \quad (7.19)$$

The average E_s/N_0 of QPSK is equal to that of BPSK and both yield (7.19) because in both cases the same probability density function $f_X(x)$ is used to describe the distribution of E_s/N_0 . What is of interest is to find the improvement in average symbol error rate that occurs in a Rayleigh channel when coherent BPSK or QPSK is used in the presence of a maximal ratio combiner. With the assumptions of a flat and slow fading channel, the derivations for the symbol error rate for coherent BPSK and coherent QPSK can be made from the equations introduced in this and the previous chapters. These assumptions on the channel assure that the signal is not affected by inter-symbol-interference and that the modulation is preserved over the duration of the symbol. In diversity systems, the demodulator works on the combined signal of both branches and hence the probability density function over which the probability of error is averaged in (7.10) is the computed pdf of the SNR_P in section 6.3.

7.4.2 Average probability of Bit Error using Coherent BPSK

Considering first the case of perfectly correlated signals between both branches and BPSK modulation as described by the probability density function after maximal ratio combining given in (6.33). Replacing (7.6) for P^e of BPSK and (6.33) for $f_X(x)$ into (7.10) and solving

$$P^e_{Max,BPSK} = \int_0^{\infty} Q(\sqrt{2y}) \frac{1}{2(\mathbf{s}_1^2 + \mathbf{s}_2^2)} e^{-\frac{y}{2(\mathbf{s}_1^2 + \mathbf{s}_2^2)}} dy \quad (7.20)$$

results in the average symbol error probability of BPSK. The solution of the above integral can be found by noting that this integral is exactly the same as the integral in (7.11) except that \mathbf{s}^2 in (7.11) is replaced by $\mathbf{s}_2^2 + \mathbf{s}_1^2$. Hence the result of (7.20) can be directly inferred from (7.14) to yield

$$P^e_{Max,BPSK} = \frac{1}{2} - \frac{1}{2} \sqrt{\frac{2(\mathbf{s}_1^2 + \mathbf{s}_2^2)}{1 + 2(\mathbf{s}_1^2 + \mathbf{s}_2^2)}} \quad \text{valid for } \mathbf{r} = \mathbf{r}_P = 1 \quad (7.21)$$

when both branches are perfectly correlated. Sometimes both branches may be partially correlated, the probability density function that describes this event is given in (6.31).

The bit error rate for this case can be found by replacing $f_X(x)$ in (7.10) by the probability density function in (6.31). Using the relationship between Q and the error function given in (7.12), simplifies the integral to

$$P_{Max,BPSK}^e = \int_0^{\infty} \left[\frac{e^{-\frac{((s_1^2+s_2^2)-\sqrt{(s_2^2-s_1^2)+4s_1^2s_2^2r_p})x}{s_1^2s_2^2(1-r_p)}}}{s_1^2s_2^2(1-r_p)} - e^{-\frac{((s_1^2+s_2^2)+\sqrt{(s_2^2-s_1^2)+4s_1^2s_2^2r_p})x}{s_1^2s_2^2(1-r_p)}}}{s_1^2s_2^2(1-r_p)} \right] - \operatorname{erf}(\sqrt{x}) e^{-\frac{((s_1^2+s_2^2)-\sqrt{(s_2^2-s_1^2)+4s_1^2s_2^2r_p})x}{s_1^2s_2^2(1-r_p)}}}{s_1^2s_2^2(1-r_p)} + \operatorname{erf}(\sqrt{x}) e^{-\frac{((s_1^2+s_2^2)+\sqrt{(s_2^2-s_1^2)+4s_1^2s_2^2r_p})x}{s_1^2s_2^2(1-r_p)}}}{s_1^2s_2^2(1-r_p)} \right] dx \quad (7.22)$$

$$4\sqrt{(s_2^2-s_1^2)+4s_1^2s_2^2r_p}$$

which can be solved by integrating each of the terms individually with the aid of the integral given in (7.13). Finally, for partially correlated signals, the average bit error rate of coherent BPSK after maximal ratio combining reduces to

$$P_{Max,BPSK}^e = \frac{1}{2} \left[\frac{((s_1^2+s_2^2)+\sqrt{(s_2^2-s_1^2)^2+4s_1^2s_2^2r_p})}{4\sqrt{(s_2^2-s_1^2)^2+4s_1^2s_2^2r_p}} \sqrt{\frac{((s_1^2+s_2^2)+\sqrt{(s_2^2-s_1^2)^2+4s_1^2s_2^2r_p})}{1+((s_1^2+s_2^2)+\sqrt{(s_2^2-s_1^2)^2+4s_1^2s_2^2r_p})}} \right. \quad (7.23)$$

$$\left. + \frac{((s_1^2+s_2^2)-\sqrt{(s_2^2-s_1^2)^2+4s_1^2s_2^2r_p})}{4\sqrt{(s_2^2-s_1^2)^2+4s_1^2s_2^2r_p}} \sqrt{\frac{((s_1^2+s_2^2)-\sqrt{(s_2^2-s_1^2)^2+4s_1^2s_2^2r_p})}{1+((s_1^2+s_2^2)-\sqrt{(s_2^2-s_1^2)^2+4s_1^2s_2^2r_p})}} \right]$$

valid for $r, r_p < 1$,

for $s_2 \geq s_1$ except when both, $s_1=s_2$ and $a=b=0$ ($r_p=r=0$)

The above equation will only be valid for an arbitrary correlation when branch 2 is larger than branch 1 ($2s_2^2 > 2s_1^2$), or under the special case when the average powers are equal ($2s_2^2 = 2s_1^2$), the correlation between both branches has to be nonzero for (7.23) to apply.

The distribution of the signal-to-noise ratio when both branches are uncorrelated and have the same average received power is given in Chapter 6 (6.31). Repeating the

procedure described by (7.10) on the probability density function of the SNR_P given in (6.31), results in the average probability of bit error of BPSK valid for $r=0$ and $s_1=s_2=s$. The Q function when replaced by the equivalent error function relationship (7.12) and expanded produces the equation

$$P_{Max,BPSK}^e = \int_0^{\infty} \frac{x e^{-\frac{x}{2s^2}} - x \operatorname{erf}(\sqrt{x}) e^{-\frac{x}{2s^2}}}{8s^4} dx \quad (7.24)$$

whos solution is the average bit error of BPSK after two-branch maximal ratio combining for balanced and uncorrelated branches. The second term in the above integral can be solved my using a result found in the integral table [2]. The answer can be derived through differentiation and evaluates to

$$\int_0^{\infty} x \operatorname{erf}(\sqrt{ax}) e^{-px} dx = \sqrt{a} \left(\frac{3p+2a}{2p^2(p+a)^{3/2}} \right), \operatorname{Re} p, \operatorname{Re}(p+a^2) > 0 \quad (7.25)$$

Finally, by combining both (7.25) and (7.24) produces an equation for the average symbol error rate for BPSK after maximal ratio combining for uncorrelated and balanced branches.

$$P_{Max,BPSK}^e = \frac{1}{2} - \frac{\sqrt{2}}{4} \left[\frac{(3s + 4s^3)}{(1 + 2s^2)^{3/2}} \right] \quad (7.26)$$

valid for $s_2 = s_1 = s$ and $a = b = 0$ ($r = r_p = 0$)

In the following section, expressions for the average symbol error of QPSK will be developed after two-branch maximal ratio combining for the Rayleigh channel.

7.4.3 Average probability of Symbol Error using Coherent QPSK

The average probability of symbol error for QPSK can be evaluated in a similar fashion as was described in the previous section for BPSK. The three expression of symbol error rate that will be developed are valid for different combinations of correlation and average power of the branches. As mentioned before, (7.10) applies for QPSK as it did for BPSK. The probability of symbol error for coherent QPSK in an additive white Gaussian noise channel is given by (7.5). Hence, the average probability of symbol error after maximal ratio combining can be found by integrating

$$P_{Max,QPSK}^e = \int_0^{\infty} P_{AWGN,QPSK}^e(y) f_Y(y) dy \quad (7.27)$$

where $f_Y(y)$ is the probability density function described by (6.31), (6.32) and (6.33). The pdf $f_Y(y)$ describes the distribution of E_s/N_0 . For perfectly correlated branches, the distribution of the signal-to-noise ratio is given in (6.33). When (6.33) is substituted into (7.27) an integral is produced with the same characteristics as was already examined in (7.15). The average probability of symbol error of QPSK for $r=1$ can be found by noting that the integral of interest is the integral in (7.15) with s^2 replaced by $s_2^2 + s_1^2$. Hence the average symbol error of QPSK after two-branch maximal ratio combining can be directly inferred to give

$$P_{Max,QPSK}^e = \frac{3}{4} - \sqrt{\frac{s_1^2 + s_2^2}{(1 + s_1^2 + s_2^2)}} \left[\frac{1}{2} + \frac{1}{p} \arctan \sqrt{\frac{s_1^2 + s_2^2}{(1 + s_1^2 + s_2^2)}} \right] \quad (7.28)$$

valid for $r = r_p = 1$

When both branches are partially correlated and unbalanced, the probability density function in (6.31) describes the signal-to-noise ratio distribution at the output of the maximal ratio combiner. As before, the symbol error rate for this event can be found by

replacing $f_Y(y)$ in (7.27) by the probability density function given in (6.31). As an intermediate result in the process of finding the average probability of symbol error, the integral can be simplified to

$$P_{Max,QPSK}^e = \int_0^{\infty} \frac{\left[\frac{3}{4} - \frac{1}{2} \operatorname{erf} \left(\sqrt{\frac{x}{2}} \right) - \frac{1}{4} \operatorname{erf}^2 \left(\sqrt{\frac{x}{2}} \right) \right] e^{\frac{\left((\mathbf{s}_2^2 + \mathbf{s}_1^2) - \sqrt{(\mathbf{s}_2^2 - \mathbf{s}_1^2)^2 + 4\mathbf{s}_1^2 \mathbf{s}_2^2} \right) x}{4\mathbf{s}_1^2 \mathbf{s}_2^2 (1-r_p)}} - e^{\frac{\left((\mathbf{s}_2^2 + \mathbf{s}_1^2) + \sqrt{(\mathbf{s}_2^2 - \mathbf{s}_1^2)^2 + 4\mathbf{s}_1^2 \mathbf{s}_2^2} \right) x}{4\mathbf{s}_1^2 \mathbf{s}_2^2 (1-r_p)}}}{2\sqrt{(\mathbf{s}_2^2 - \mathbf{s}_1^2)^2 + 4\mathbf{s}_1^2 \mathbf{s}_2^2} r_p} dx \quad (7.29)$$

which can be constructed by using the equation that relates the erf and the Q function in (7.12). The solution of the individual terms of the above integral have already been stated in (7.13) and (7.16). Using (7.13) and (7.16) to solve the equation in (7.29) yields the average symbol error rate of QPSK after maximal ratio combining

$$P_{Max,QPSK}^e = \frac{3}{4} - \frac{1}{4\sqrt{(\mathbf{s}_2^2 - \mathbf{s}_1^2)^2 + 4\mathbf{s}_1^2 \mathbf{s}_2^2} r_p} \left[\frac{\left((\mathbf{s}_1^2 + \mathbf{s}_2^2) + \sqrt{(\mathbf{s}_2^2 - \mathbf{s}_1^2)^2 + 4\mathbf{s}_1^2 \mathbf{s}_2^2} \right)^{\frac{3}{2}}}{\sqrt{2 + (\mathbf{s}_1^2 + \mathbf{s}_2^2) + \sqrt{(\mathbf{s}_2^2 - \mathbf{s}_1^2)^2 + 4\mathbf{s}_1^2 \mathbf{s}_2^2} r_p}} \left(1 + \frac{2}{P} \arctan \sqrt{\frac{(\mathbf{s}_1^2 + \mathbf{s}_2^2) + \sqrt{(\mathbf{s}_2^2 - \mathbf{s}_1^2)^2 + 4\mathbf{s}_1^2 \mathbf{s}_2^2} r_p}{2 + (\mathbf{s}_1^2 + \mathbf{s}_2^2) + \sqrt{(\mathbf{s}_2^2 - \mathbf{s}_1^2)^2 + 4\mathbf{s}_1^2 \mathbf{s}_2^2} r_p}} \right) \right. \\ \left. - \frac{\left((\mathbf{s}_1^2 + \mathbf{s}_2^2) - \sqrt{(\mathbf{s}_2^2 - \mathbf{s}_1^2)^2 + 4\mathbf{s}_1^2 \mathbf{s}_2^2} \right)^{\frac{3}{2}}}{\sqrt{2 + (\mathbf{s}_1^2 + \mathbf{s}_2^2) - \sqrt{(\mathbf{s}_2^2 - \mathbf{s}_1^2)^2 + 4\mathbf{s}_1^2 \mathbf{s}_2^2} r_p}} \left(1 + \frac{2}{P} \arctan \sqrt{\frac{(\mathbf{s}_1^2 + \mathbf{s}_2^2) - \sqrt{(\mathbf{s}_2^2 - \mathbf{s}_1^2)^2 + 4\mathbf{s}_1^2 \mathbf{s}_2^2} r_p}{2 + (\mathbf{s}_1^2 + \mathbf{s}_2^2) - \sqrt{(\mathbf{s}_2^2 - \mathbf{s}_1^2)^2 + 4\mathbf{s}_1^2 \mathbf{s}_2^2} r_p}} \right) \right] \quad (7.30)$$

valid for $r, r_p < 1$

for $\mathbf{s}_2 \geq \mathbf{s}_1$ except when both, $\mathbf{s}_2 = \mathbf{s}_1$ and $\mathbf{a} = \mathbf{b} = 0$ ($r = r_p = 0$)

for partially correlated Rayleigh diversity branches. Repeating the procedure described by (7.27) on the probability density function of the SNR_p given in (6.32), results in the average probability of symbol error of QPSK for uncorrelated and balanced branches. The Q function when replaced by the equivalent error function relationship (7.12) reduces the integral to

$$P_{Max,QPSK}^e = \int_0^{\infty} \frac{x e^{-\frac{x}{2\mathbf{s}^2}} \left(\frac{3}{4} - \frac{1}{2} \operatorname{erf} \left(\sqrt{\frac{x}{2}} \right) - \frac{1}{4} \operatorname{erf}^2 \left(\sqrt{\frac{x}{2}} \right) \right)}{4\mathbf{s}^4} dx \quad (7.31)$$

The first term can be integrated by parts while the second term of the above equation can be solved from the result given in (7.25). The remaining third term can be solved from equations given in [2]. The third integral in (7.31) can be solved by using the following relationship

$$\int_0^{\infty} x e^{-px} \operatorname{erf}^2(\sqrt{ax}) dx = \frac{2\sqrt{a}}{pp} \left[\frac{3p+2a}{p(p+a)^{3/2}} \arctan \sqrt{\frac{a}{p+a}} + \frac{\sqrt{a}}{(p+2a)(p+a)} \right] \quad (7.32)$$

$\operatorname{Re} p, \operatorname{Re}(p+2a^2) > 0$

Applying the results from (7.25) and (7.32) to the integral (7.31) gives the solution for the symbol error rate of QPSK after maximal ratio combining for uncorrelated and equal branch powers. The final result after the appropriate substitutions produces a symbol error rate of

$$P_{Max,QPSK}^e = \frac{3}{4} - \frac{3\mathbf{s} + 2\mathbf{s}^3}{4(1+\mathbf{s}^2)^{3/2}} \left[1 + \frac{2}{p} \arctan \sqrt{\frac{\mathbf{s}^2}{1+\mathbf{s}^2}} \right] - \frac{\mathbf{s}^2}{2p(1+2\mathbf{s}^2)(1+\mathbf{s}^2)} \quad (7.33)$$

valid for $\mathbf{s}_2 = \mathbf{s}_1 = \mathbf{s}$ and $\mathbf{a} = \mathbf{b} = 0$ ($\mathbf{r} = \mathbf{r}_p = 0$)

In Sections 7.4.2 and 7.4.3, the average probability of symbol error after two-branch maximal ratio combining using QPSK or BPSK were developed. The equations (7.21), (7.23), and (7.26) represent the bit error rate of BPSK after diversity combining for a Rayleigh channel. The average probability of symbol error for QPSK for the same system and channel are given in the equations (7.28), (7.30), and (7.33). To get an idea how symbol error rate for these two modulations perform as a function of average E_s/N_0 of the branches and correlation, the following section examines some numerical results. The results after diversity combining are also compared to the performance of a single antenna receiver in a Rayleigh fading channel.

7.5 Example of the Performance of QPSK and BPSK after Two-Branch Maximal Ratio Combining

Figures 7.2 and 7.3 show plots of the equations of the average probability of symbol error for coherent BPSK for envelope correlations $r = 0$ and $r = 1$, respectively. The two abscissa axes are the average E_b/N_0 of the individual Rayleigh fading signals. The meshed surface is the probability of bit error after maximal ratio combining as described by the equations (7.21), (7.23), and (7.26). The solid lines bound the surface describing the performance of a single Rayleigh fading branch as described by (7.14), i.e. before combining.

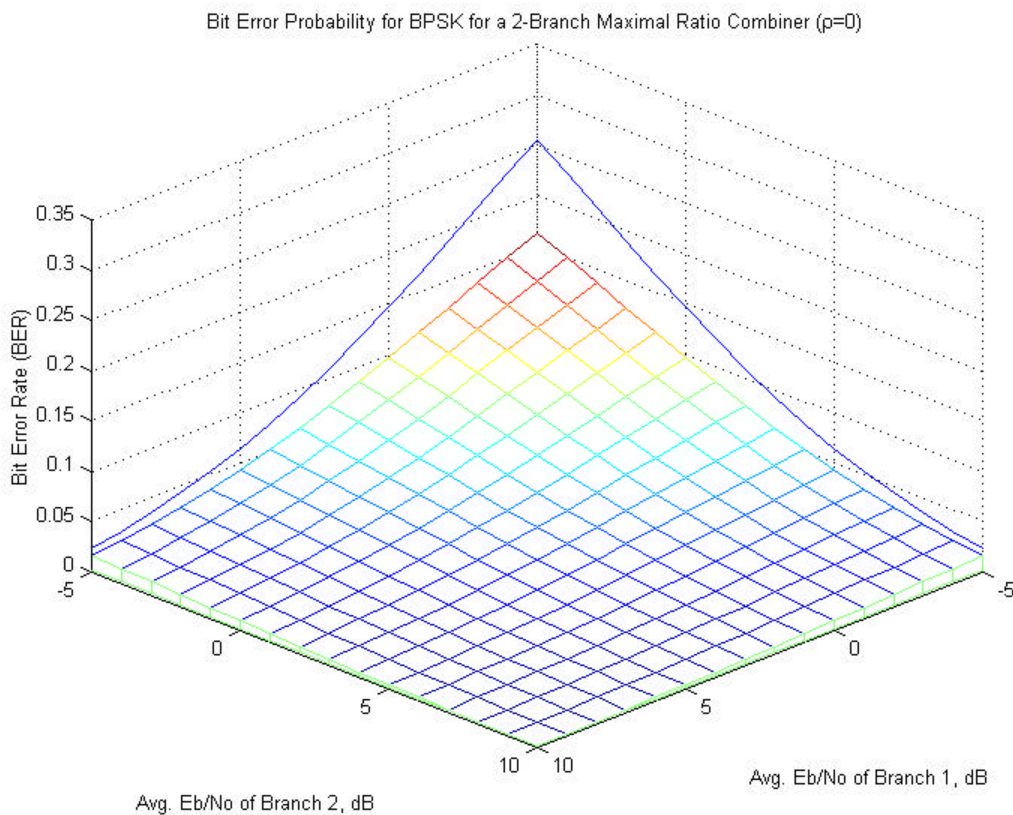


Figure 7.2 Average probability of bit error of a BPSK signal after (lower surface) and before (upper solid lines) two-branch maximal ratio combining for uncorrelated branches, as a function of average E_b/N_0 values in both branches.

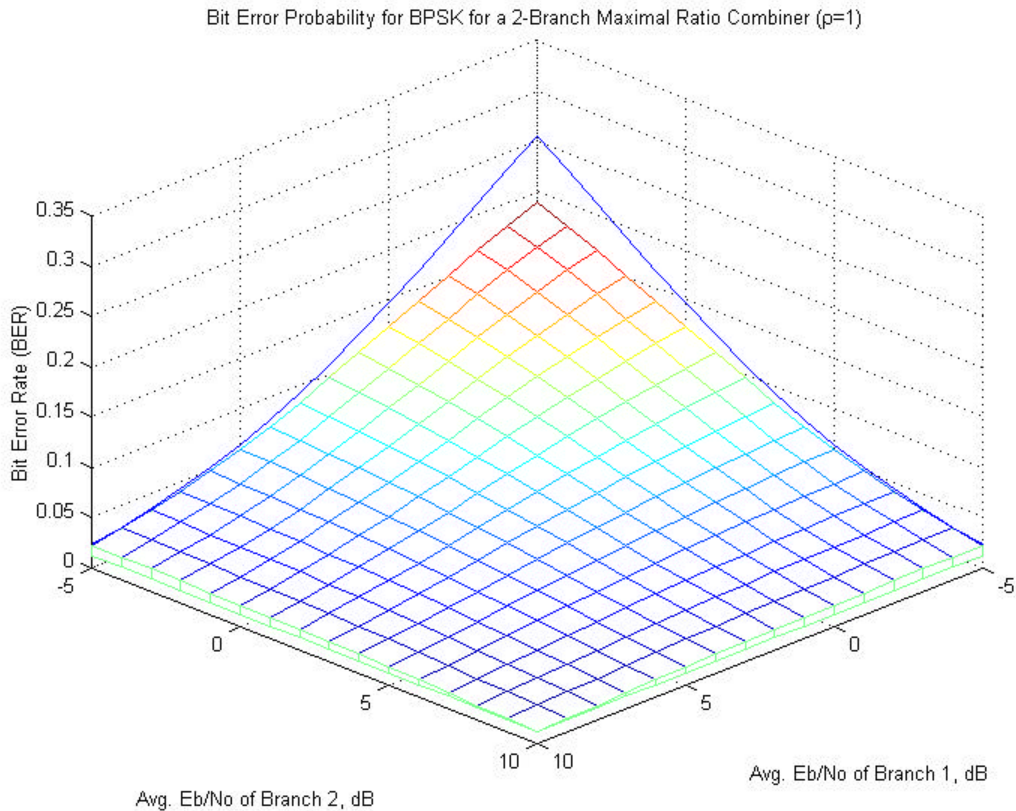


Figure 7.3 Average probability of bit error of a BPSK signal after (lower surface) and before (upper solid lines) two-branch maximal ratio combining for perfectly correlated branches, as a function of average E_b/N_0 in both branches.

The average symbol error probabilities for all other correlations fall between the results shown in Figure 7.2 and Figure 7.3. For comparison purposes, when $\overline{E_b/N_0} = -5$ dB in both branches, the average probability of error for $r = 1$ is BER=0.1888 while for $r = 0$ the bit error rate is BER=0.1618. These two values are a significant improvement over a single Rayleigh fading branch that produces an average bit error rate of BER=0.2549 for an average E_b/N_0 of -5 dB. The average E_b/N_0 at the output of the maximal ratio is simply the sum of the separate branches as seen from (7.19). As expected, when the branch correlation goes up the bit error rate increases. As the power in both branches

approaches zero, the bit error rate approaches $\frac{1}{2}$ which is expected for antipodal modulation scheme.

Figures 7.4 and 7.5 show the symbol error rate for coherent QPSK for the envelope correlations $\mathbf{r} = 0$ and $\mathbf{r} = 1$. The two abscissa axes are the average E_s/N_0 of each branch. The mesh describes the average probability of symbol error of coherent QPSK after two-branch maximal ratio combining given in (7.28), (7.30), and (7.33). The two solid lines on the faces of the graph show the performance of QPSK in the presence of only a single Rayleigh fading branch (7.17).

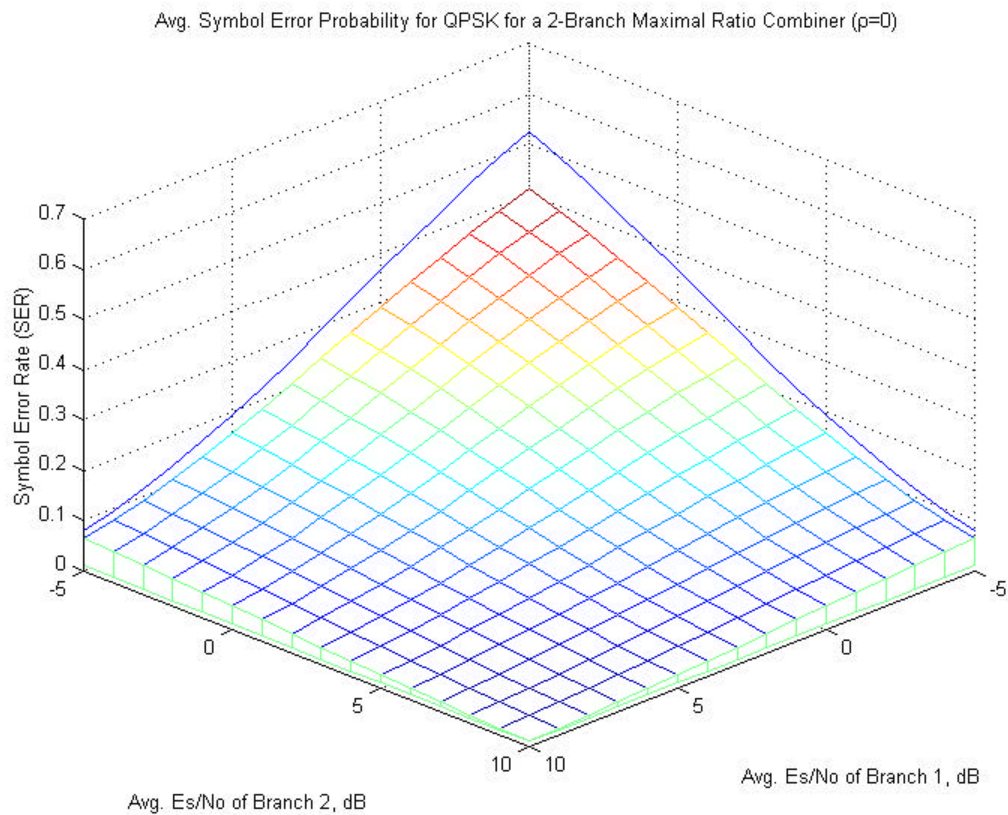


Figure 7.4 Average probability of symbol error of a QPSK signal after (lower surface) and before (upper solid lines) two-branch maximal ratio combining for uncorrelated branches, as a function of average E_s/N_0 values in both branches.

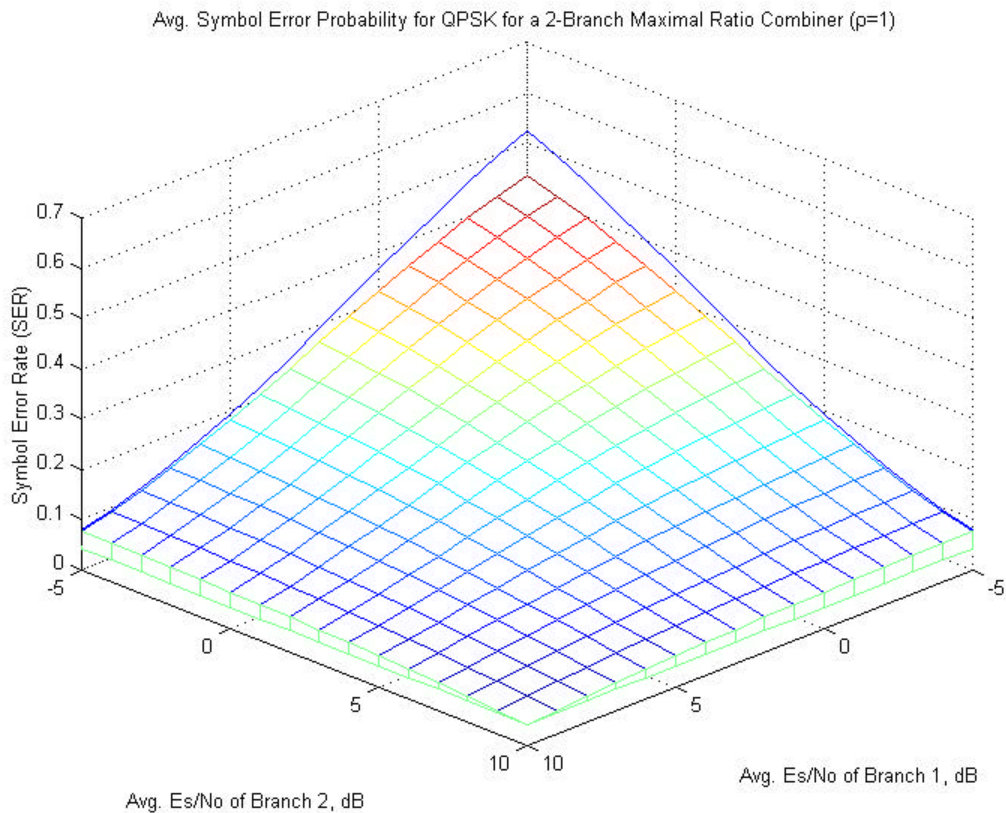


Figure 7.5 Average probability of symbol error of a QPSK signal after (lower surface) and before (upper solid lines) two-branch maximal ratio combining for perfectly correlated branches, as a function of average E_s/N_0 values in both branches.

An average value of E_s/N_0 equal to -5 dB in both branches yields an average symbol error of $SER=0.4094$ for $r = 0$ and $SER=0.4338$ for $r = 1$. The performances for other envelope correlations under the same conditions lie between the results presented in Figures 7.4 and 7.5. A single Rayleigh branch naturally performs worse than the maximal ratio combiner and yields a symbol error rate of $SER=0.5236$ when using coherent QPSK with an $\overline{E_s/N_0} = -5dB$. The average E_s/N_0 at the output of the maximal

ratio combiner is also the sum of the average E_s/N_0 of both branches as given by (7.19). As the power in both branches approaches zero, the average symbol error rate of QPSK approaches $3/4$ which is a result that is expected for a 4 symbol equal power modulation scheme. The translation from symbol error rate to bit error rate depends on how the bits are assigned to each symbol and cannot be derived without this knowledge.

In the following chapter, statistics from measurements taken with a two-branch diversity system in a Rayleigh channel will be compared to the cumulative distribution functions of the SNR_P at the output of a selection and maximal ratio diversity system.

References:

- [1] John G. Proakis, *Digital Communications*, McGraw-Hill, New York, NY, 1995.
- [2] A. P. Prudnikov, Yu. A. Brychokov, *Integrals and Series Volume 4 Direct Laplace Transforms*, Gordon and Breach, Philadelphia, PA, 1992.
- [3] I. S. Gradshteyn and I. M. Ryzhik, *Table of Integrals, Series, and Products*, Academic Press Inc., San Diego, CA, 1994.

Chapter 8

Comparison of Theory to Measurements

To this point, this report has developed a theoretical framework for modeling the statistics of antenna diversity in a Rayleigh channel. The results can be used directly for modeling and simulation. However, validation is a necessary next step. In this chapter, the theory is validated through experimentation. This chapter uses experimental data from a measurement campaign that investigates antenna diversity in handheld devices to verify that the theory properly predicts measurements.

In this chapter, the theoretical probability density function after selection and maximal ratio combining, derived in Chapters 5 and 6, will be compared to measured data of a two-branch diversity system in a Rayleigh fading channel. The diversity combining algorithm, as would be normally done in practice, is applied to the time domain waveforms of both branch signals. The distribution of the time combined signal will be compared to the expected theoretical probability density function.

8.1 Experiment Setup

The measurements presented in this report are from a much larger measurement campaign given in [1]. Measurements were taken in an indoor non line of sight environment with a four channel receiver. The receiver consisted of four vertically polarized dipole antennas separated by spacings of 0.2λ at a frequency of 2.05 GHz. Figure 8.1 shows the receiver system with the four receive antennas and the vertically transmitting dipole antenna that was broadcasting a constant tone. Measurements were recorded continuously over a distance of approximately 60 m at walking speeds.

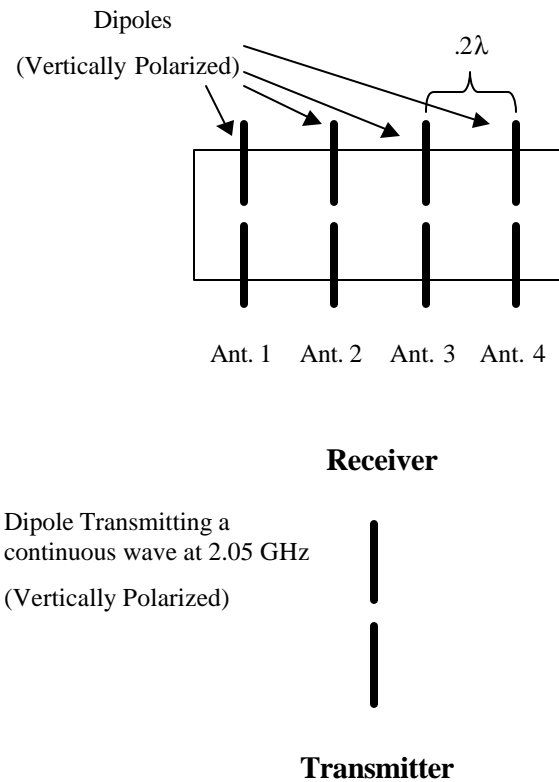


Figure 8.1 Diagram of the transmitter and the four channel receiver system

The measurements were performed along a hallway on the 6th floor in Whittemore Hall at Virginia Tech. Figure 8.2 depicts the route that was taken in the environment under test. The transmitter was located in a room behind a closed door (labeled Tx in the Figure 8.2). The plane of the antennas was aligned perpendicular to the line of motion and always remained vertical as the receiver was carried along a path described by the dashed arrow. The envelope of the signal was extracted during post processing on the computer for all four branches. The long term variation of the average received signal levels was also removed during post processing. This ensures that only the statistics of the small scale fading is left to ensure accurate statistic comparison with theory.

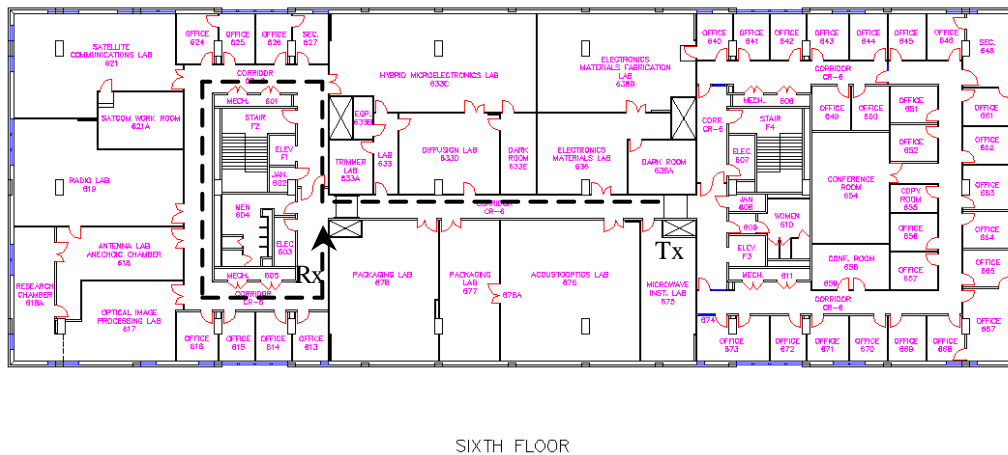


Figure 8.2 Floor plan of the 6th floor in Whittemore Hall where the measurements were performed.

The performance of a diversity system depends on the difference in average branch power, so the received signals during post processing are normalized to the mean of the largest branch. The envelopes were found to be very much Rayleigh distributed as can be seen from Figures 8.4 and 8.5.

The assumption that is being made on the measured envelope data is that the effects of noise are negligible compared to received envelope. This is valid since in post

processing most of the noise has been removed through filtering such that the recovered envelope is an exact representation. This, of course, is a good assumption for large levels of r but for low levels, when the signal is in a fade for example, these assumptions might not be valid. Hence by using this method, the CDF distributions values for low signal levels are less accurate. But this is a common method reported in literature and, as will be seen, matches very well to theoretical expectations at the 10% level.

8.2 Comparisons of Experiments to Theory

The time average power of the individual branches after normalization was computed from the sampled envelope data of all four antennas. The second moment (or average power) can be computed by performing the following operation on the sampled envelope data

$$\overline{r^2(t)} = \frac{\sum_{i=1}^N r_i^2(t)}{N} \quad (8.1)$$

The correlation between two time sampled signals can be computed by using the formula

$$\mathbf{r} = \frac{\sum_{i=1}^N [r_{i1}(t) - \overline{r_1(t)}][r_{i2}(t) - \overline{r_2(t)}]}{\sqrt{\sum_{i=1}^N [r_{i1}(t) - \overline{r_1(t)}]^2} \sqrt{\sum_{i=1}^N [r_{i2}(t) - \overline{r_2(t)}]^2}} \quad (8.2)$$

Both (8.1) and (8.2) have similarities between their ensemble counterparts given in (4.44,4.45) and (4.46) respectively. If the statistics gathered from a time signal are equal to the ensemble statistics, the signal is said to be ergodic. The assumptions of ergodicity will be applied to the measured data. This means that the ensemble statistics given in (4.44,4.45) and (4.46) can be evaluated from the time varying behavior of the signals. If

this postulation is correct, the theoretical statistics after combining, developed in Chapters 5 and 6, should match the statistics of the time combined signals.

The time average power of the individual branches after normalization was computed and this value was used as the average power of the Rayleigh distributed signal for that branch in (4.44, and 4.45). The time average power of the envelopes at antenna 1, 2, 3, and 4 are (using (8.1))

$$\begin{aligned}
 \overline{r_1^2} &= 1.08 = E[r_1^2] = 2\mathbf{s}_1^2 \\
 \overline{r_2^2} &= 0.53 = E[r_2^2] = 2\mathbf{s}_2^2 \\
 \overline{r_3^2} &= 0.78 = E[r_3^2] = 2\mathbf{s}_3^2 \\
 \overline{r_4^2} &= 1.12 = E[r_4^2] = 2\mathbf{s}_4^2
 \end{aligned} \tag{8.3}$$

and these values were used for the second moment of the Rayleigh probability density functions. The average power between the branches varies between 0.53 and 1.12 (8.3) even though all channels have identical antennas and are in the same scenario. The lower average power measured by the two center elements compared to the outer elements is probably due to antenna coupling. The center elements are both surrounded by antennas on both sides as opposed to just one for the outer elements. Closely spaced antennas can have significant coupling, distorting the patterns and altering impedance of the individual elements. More information on antenna patterns affected by mutual coupling can be found in [1].

Additionally, the performance of the combining algorithm depends on the correlation between the envelopes in the branches. The envelope correlations between two branches were computed using (8.2) to be

$$\begin{aligned}
\mathbf{r}_{12} &= \mathbf{r}_{21} = 0.271 \\
\mathbf{r}_{13} &= \mathbf{r}_{31} = 0.059 \\
\mathbf{r}_{14} &= \mathbf{r}_{41} = 0.071 \\
\mathbf{r}_{23} &= \mathbf{r}_{32} = 0.051 \\
\mathbf{r}_{24} &= \mathbf{r}_{42} = 0.057 \\
\mathbf{r}_{34} &= \mathbf{r}_{43} = 0.311
\end{aligned} \tag{8.4}$$

for all branch combinations. The computed time envelope correlation between signals r_1 and r_2 was used as the probabilistic envelope correlation \mathbf{r} defined in (4.46). At first, selection combining was applied to the envelopes of the received signals in the time domain. Two branches at a time were monitored and the largest envelope at a given instant was selected during post processing as described by the equation

$$s(t) = \max(r_1(t), r_2(t)) \tag{8.5}$$

The above process is modeled by the equation that corresponds to the SNR_V (for a noise power of unity) of a selection combining system given in (5.2). The distribution of the signal $s(t)$ in (8.5) achieved after time combining can be compared with an equivalent random process which uses the correlation and average powers computed in (8.3) and (8.4). If the random process is ergodic, both the distributions found through probabilistic combining found in Chapter 5 and time combining should match. Figure 8.3, shows a snapshot of the received envelope at antenna 1 and antenna 4 as a function of time. The dashed line on the figure corresponds to the signal that would result after selection combining is applied to both envelopes.

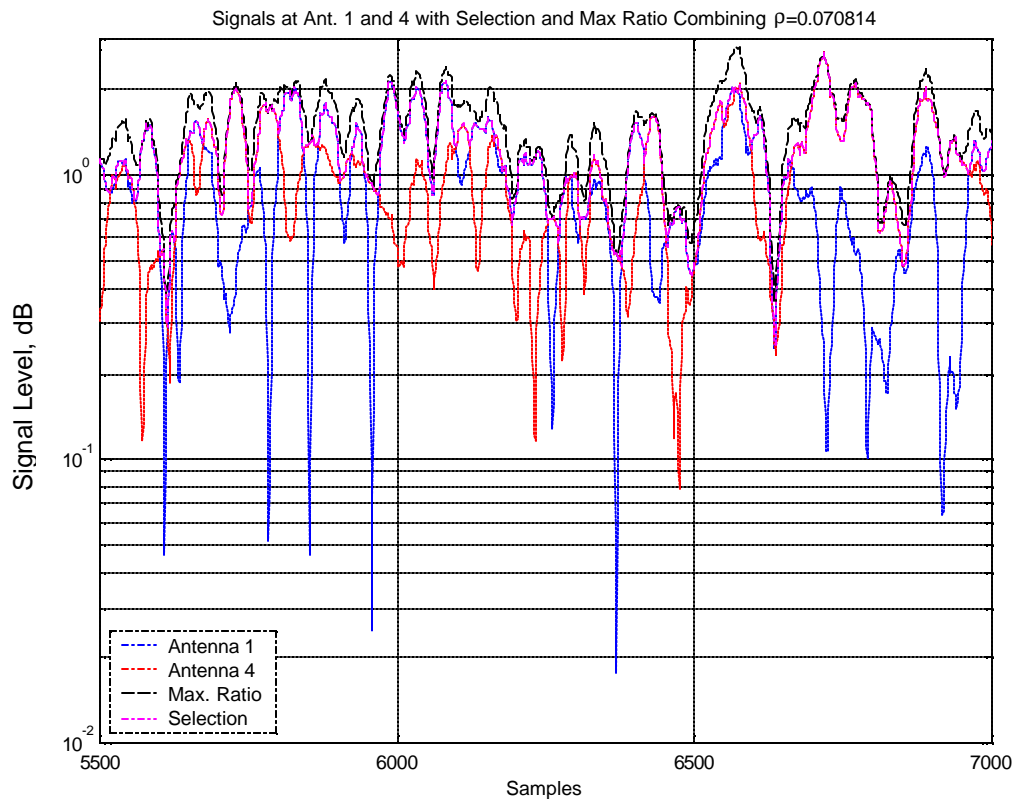


Figure 8.3 Snapshot of measured signal envelopes received at antenna 1 and 4 and the resulting signal after selection and maximal ratio combining for the receiver configuration in Figure 8.1 along the path described by Fig. 8.2 at 2.05 GHz.

Figure 8.3 shows a snapshot of the received envelopes at antenna 1 and 4. For this case, the average branch power at antenna 1 and antenna 4 is 1.08 and 1.12 respectively. The correlation between both branches was computed in (8.4) to be 0.071. With this information the theoretical probability density function can be constructed using (5.11) that describes the distribution of the SNR_V at the output of the selection combiner. The data collected at antenna 1 and 4 can be used to construct the cumulative distribution function of the collected data in both branches. The improvement of the combining system can be appreciated by analyzing the cumulative distribution function of the time combined signal developed from (8.5). Figure 8.4 shows both the measured and the

theoretical cumulative distribution functions constructed by extracting \mathbf{r} , \mathbf{S}_1 , and \mathbf{S}_2 from the time data.

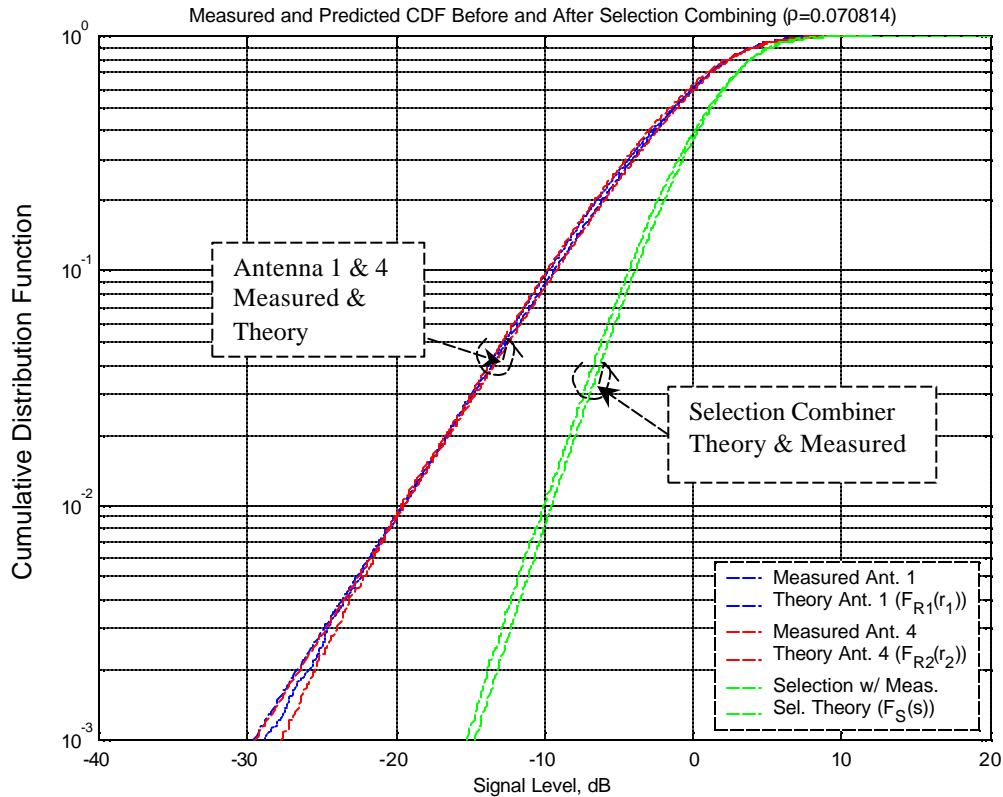


Figure 8.4 Measured (based on data in Fig. 8.3) and theoretical cumulative distribution function for antenna 1 and 4 as seen in Figure 8.1 for selection combining.

It is clear from Figure 8.4 that signals are Rayleigh distributed because the theoretical Rayleigh cumulative distributions match the statistical behavior of both branches very closely. The expected cumulative distribution function of the combined signal computed from (5.11), which uses the measured envelope correlation and average power of the branches, is consistently within 1 dB of the distribution computed through time combining. This means that the statistics of a selection combiner in the Rayleigh channel can be predicted very well from the time envelope correlation and the individual average branch powers using probability theory.

As a second example, the process of two-branch selection combining can be repeated for signals received at antennas 1 and 2. Using the correlations and average powers in (8.3) and (8.4) for branch 1 and 2, a prediction can be made of the output cumulative distribution function using (6.25). Figure 8.5 shows the statistical distributions of envelopes received at port 1, port 2 and of the time combined signal.

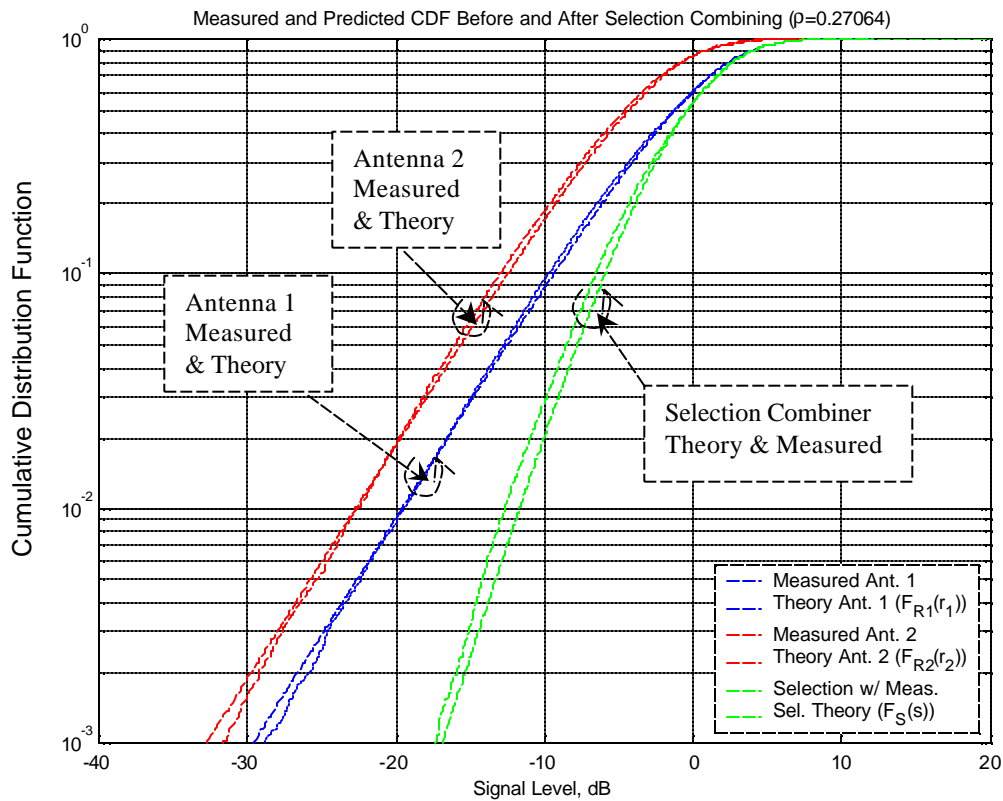


Figure 8.5 Measured and theoretical cumulative distribution function of the envelopes of the signals received at antenna 1 and 2 as seen in Figure 8.1 for selection combining.

The theoretical Rayleigh curves have been chosen to have the same average power as the measured envelope data and their CDF curve for $r=0.271$ fits the measured envelope distributions very well. As before, both theoretical and time combined cumulative distribution functions are within 1 dB of each other.

The cumulative distribution function of the SNR_V (for a noise power of unity) at the output of a maximal ratio combining for correlated and unbalanced Rayleigh channels is given in (6.25), (6.26), and (6.27). In the time domain the combining algorithm is applied to the received envelopes in the following manner

$$m(t) = \sqrt{r_1^2(t) + r_2^2(t)} \quad (8.6)$$

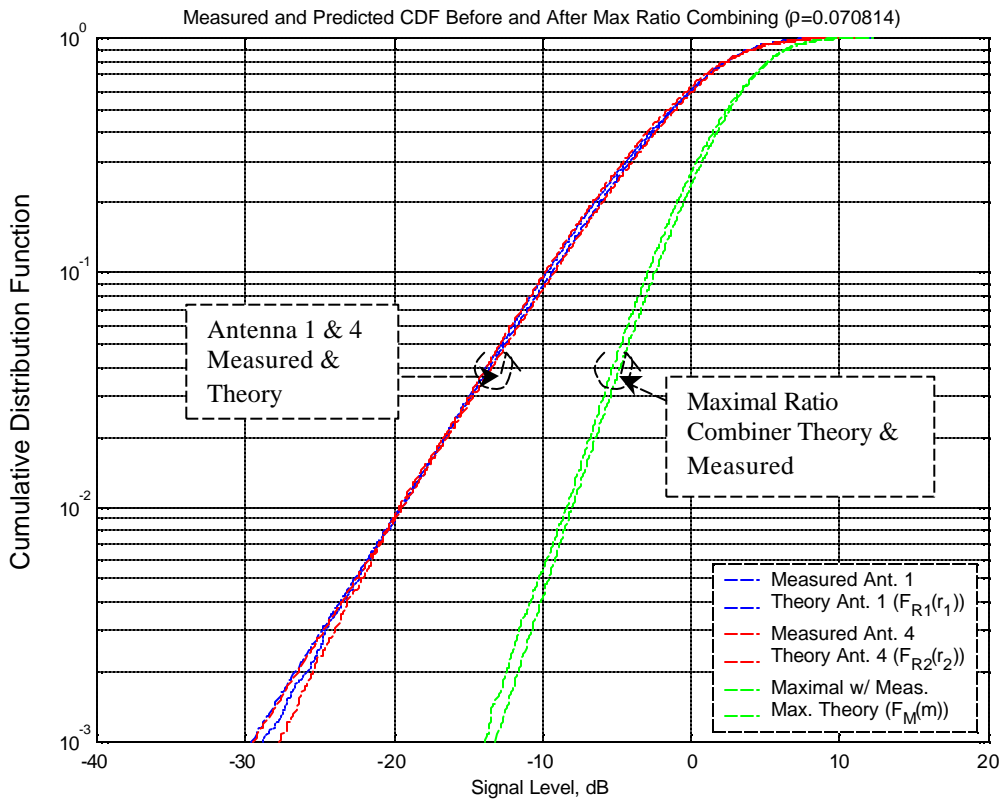


Figure 8.6 Measured (based on data in Fig. 8.3) and theoretical cumulative distribution function for antenna 1 and 4 (as seen in Figure 8.1) for maximal ratio combining.

As with selection diversity, the distribution after time combining can be compared with the equivalent probabilistic approach using the correlation and average branch powers computed in (8.3) and (8.4). If ergodicity applies, both the distributions found through probabilistic combining and time combining should match. Figure 8.6 shows the comparisons achieved by using maximal ratio combining on the envelopes measured on

antennas 1 and 4. As before both distributions achieved theoretically and experimentally matched very well.

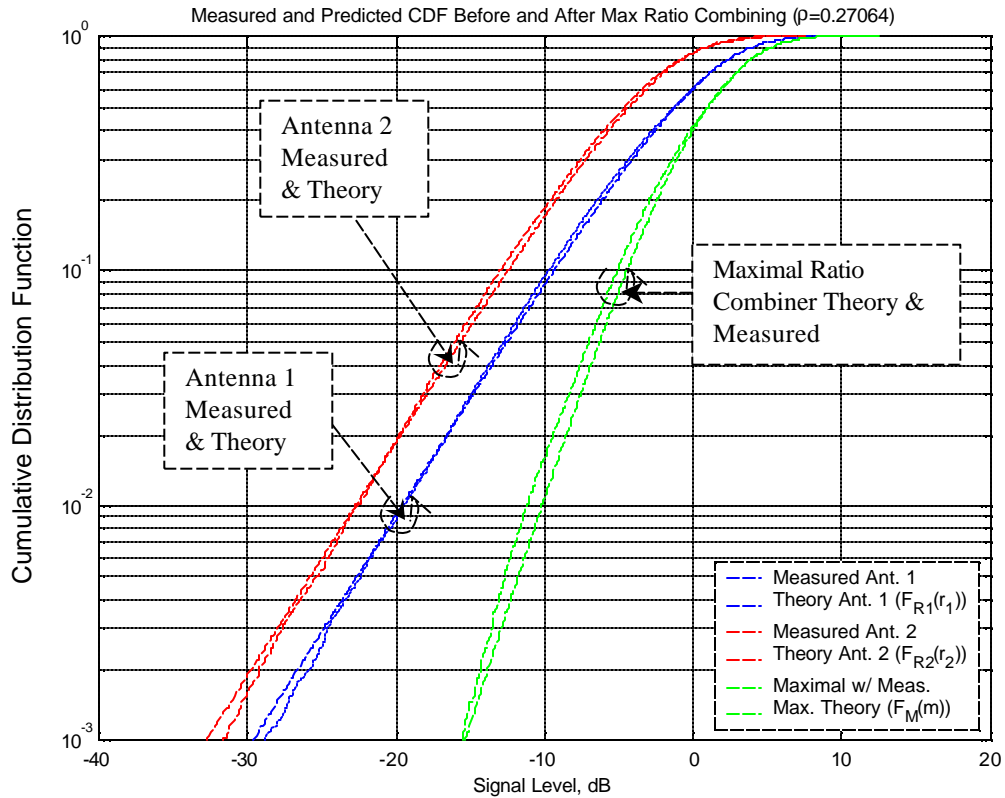


Figure 8.7 Measured and theoretical cumulative distribution function of the envelopes of the signals received at antenna 1 and 2 as seen in Figure 8.1 for maximal ratio combining.

As a second example, the two-branch maximal ratio combining is repeated for the envelopes received at antennas 1 and 2. Using the correlations and average powers in (8.3) and (8.4), a theoretical cumulative distribution function can be developed for the maximal ratio combiner using (6.25). Figure 8.7 shows the statistical distributions of the envelopes received at branches 1 and 4 and the resulting CDF of the time combined signal using the algorithm in (8.6). The theoretical maximal ratio curves fit the

distribution of measured distributions well. As before, the predicted cumulative distribution function derived theoretically is within 1 dB of the distribution that was achieved from time combining.

The effect of the noise power N , as was stated in previous chapters, does not affect the gain of the diversity system. Introducing the effect of noise power will cause all three curves to shift left or right by the same amount depending on the value of N but the relative difference between the three curves would remain the same. The improvement (in dB) between the distributions of the combined signal and the individual branches therefore remains the same. The following section will define diversity gain in detail and examine diversity gains extracted from extensive measurements found in literature.

8.3 Comparison of Theory to Measured Data Found in Literature

Diversity gain was introduced in Chapter 2 and will be examined in more detail in this section. Diversity gain is a parameter used to quantify the performance of a diversity system and is defined as the difference between the distribution of the output signal after diversity combining and the strongest branch for a given cumulative distribution function. The equation for diversity gain can be written as

$$G_D(p) = \frac{(\mathbf{g}_c)^2}{\max[(\mathbf{g}_1)^2, (\mathbf{g}_2)^2]} \quad (8.7)$$

$$F_c(\mathbf{g}_c) = p$$

$$F_{R_1}(\mathbf{g}_1) = p$$

$$F_{R_2}(\mathbf{g}_2) = p$$

where $F_C(c)$, $F_{R_1}(r_1)$, and $F_{R_2}(r_2)$ are the SNR_V cumulative distribution functions (CDF) of the combined signal, of branch 1, and of branch 2 respectively. p is the fractional percentage of occurrence at which the diversity gain is desired. $\mathbf{g}_1, \mathbf{g}_2, \mathbf{g}_c$ are the signal

levels of the SNR_V CDF's of the variables r_1 , r_2 , and the combined signal, respectively, that result in a given fractional occurrence p . To illustrate diversity gain using Figure 5.2, the cumulative distribution function of the selection combined signal at $p=0.01$ (the 1% level or 99% reliability) is 5 dB ($G_D(.01)$) higher than that of the largest branch at the same p level for an envelope correlation of 0.8. When branches are uncorrelated, Figure 5.2 shows a diversity gain of 8.6 dB at the 1% CDF level. On the CDF plots, diversity gain is the horizontal distance between the CDF curve after combining and that of the strongest branch at a given reliability.

Diversity gain is a function of correlation and power imbalance in the branches.

Figure 8.8 shows a three-dimensional plot relating diversity gain (G_D) to the envelope correlation (\mathbf{r}) and signal imbalance (D_M) between the branches of two Rayleigh fading signals after selection combining. Signal imbalance (D_M) is defined as

$$D_M = \frac{\max(E[r_1^2], E[r_2^2])}{\min(E[r_1^2], E[r_2^2])} = \frac{\max(\mathbf{s}_1^2, \mathbf{s}_2^2)}{\min(\mathbf{s}_1^2, \mathbf{s}_2^2)} \quad (8.8)$$

which is the ratio of the largest average branch power to the weakest average branch power. The diversity gain plot in Figure 8.8 shows the results at the 10% cumulative distribution level or 90% reliability. The diversity gain was evaluated using the probability density function given in (5.11) and (5.12) and from the definition of diversity gain, G_D , given in (8.7). From Figure 8.8, when both branches are uncorrelated and have equal powers, a diversity gain of 5.57 dB can be achieved at the 10% level using selection combining. Figure 8.8, also gives an indication on how G_D varies with branch power imbalance, D_M . Even when both signals r_1 and r_2 are completely uncorrelated, a negligible gain is achieved from selection diversity if a second branch is added with a mean power that is 15 dB lower than that of the first branch.

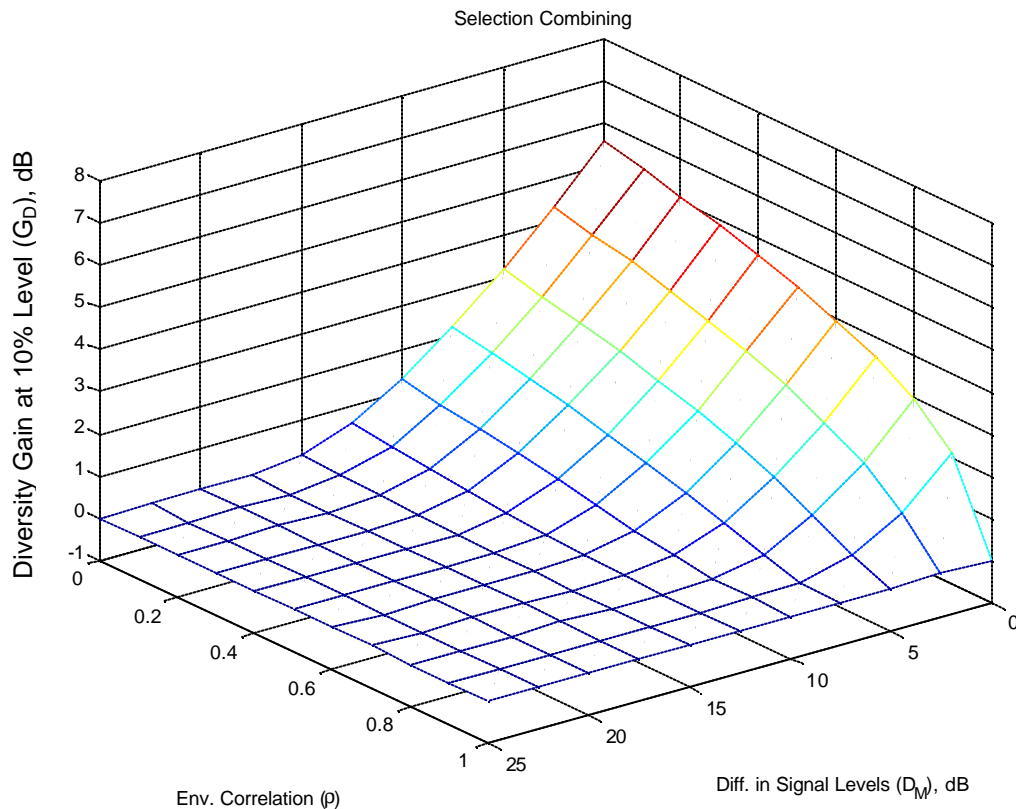


Figure 8.8 Diversity gain of a two-branch selection diversity system in a Rayleigh channel as a function of envelope correlation and power imbalance at the 10% level computed using the probability density functions for selection combining in Chapter 5.

In a paper written by Turkmani et al. [2], a large number of measurements of a two-branch diversity system that uses selection, equal gain, and maximal ratio combining were made at a frequency of 1800 MHz. Data from over 900 measurements in urban, suburban, rural, and motorways were used to arrive at an equation for diversity gain. Turkmani et al. [2] produced an equation that best described the diversity gain at the 10% level as a function of branch power imbalance and envelope correlation. The diversity gain for the 10% level after two-branch selection diversity is given in [2] and repeated here

$$G_D(10\%) = 5.71e^{-0.87r-0.16D_M(dB)} \quad (8.9)$$

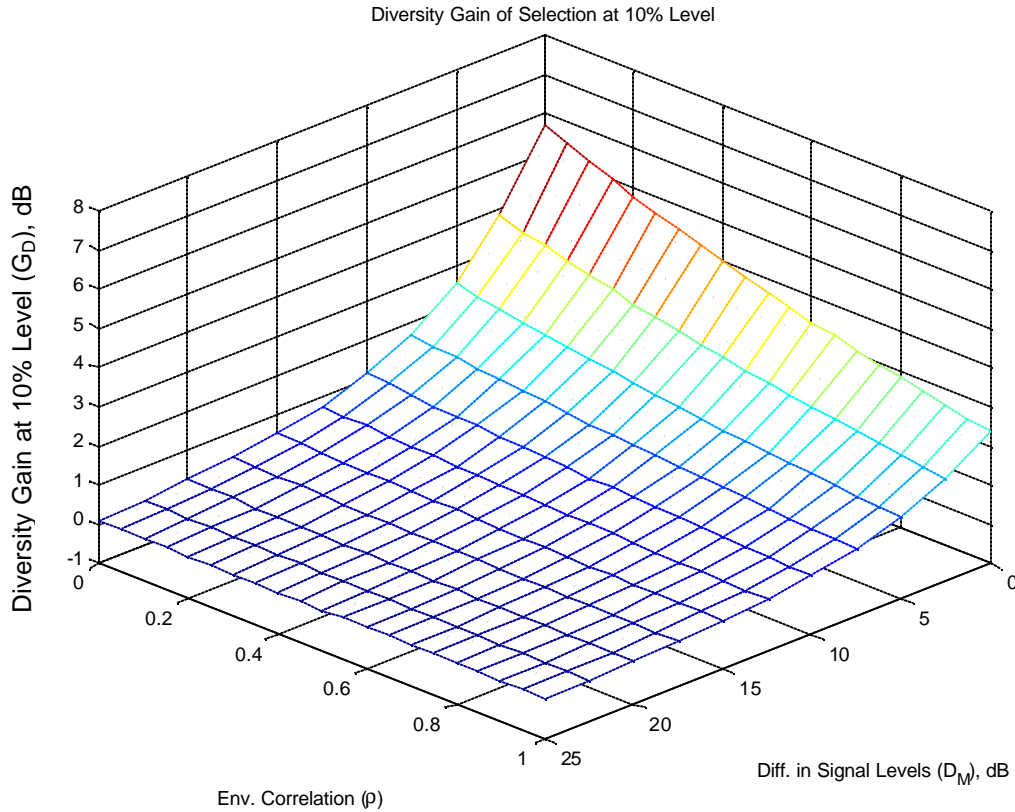


Figure 8.9 Diversity gain of a two-branch selection diversity system as a function of envelope correlation and power imbalance at the 10% level as given in [2] and (8.9).

Figure 8.9 shows a three-dimensional plot of the relationship between diversity gain, correlation, and difference in average branch power as described by (8.9). Even though the measurements in [2] were performed in channels that were not necessarily constrained to Rayleigh, Figure 8.8 and Figure 8.9 show very good agreement. Using the equations of selection diversity for the Rayleigh channel results in a diversity gain that describes the average physical channels very well. A similar result was observed when the diversity gain of maximal ratio was computed for the 90% reliability level.

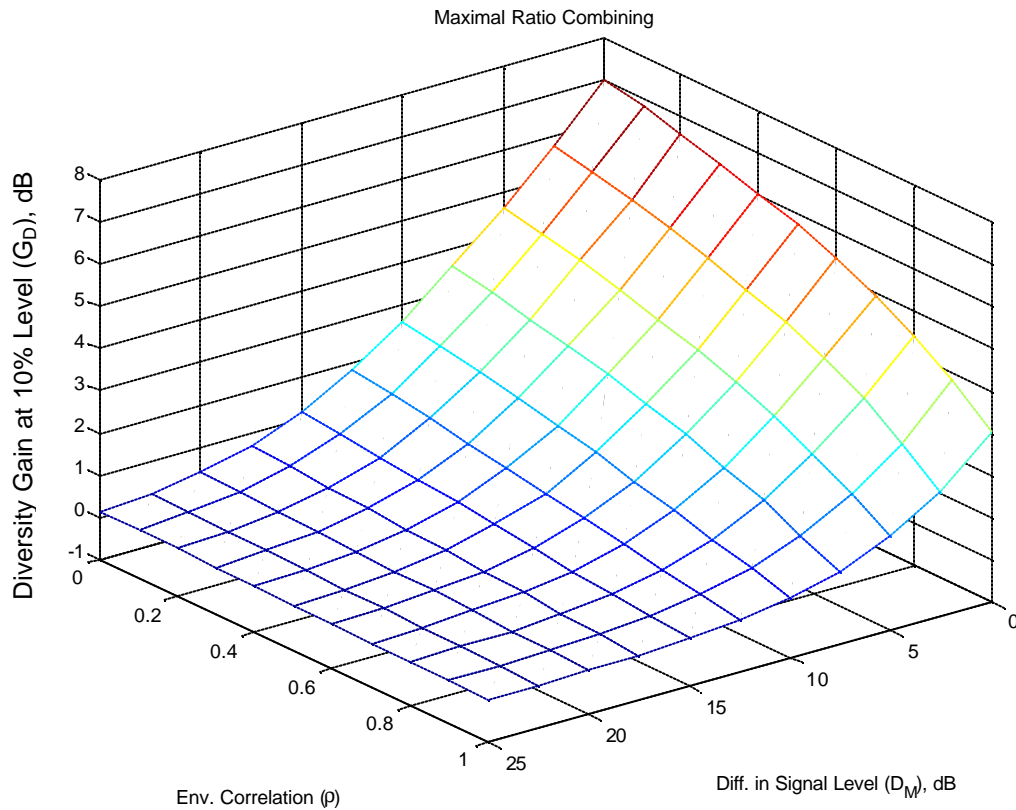


Figure 8.10 Diversity gain of a two-branch maximal ratio diversity system in a Rayleigh channel as a function of envelope correlation and power imbalance at the 10% level computed using the cumulative distribution function given in Chapter 6.

Figure 8.10 shows the attainable diversity gain (G_D), at the 10% level, as a function of envelope correlation and signal imbalance (D_M) between the branches after maximal ratio combining for the Rayleigh channel. The cumulative distributions of the signal to noise ratio after maximal ratio combining given in (6.25), (6.26) and (6.27) were used to produce Figure 8.10. When Rayleigh signals r_1 and r_2 are uncorrelated ($\mathbf{r} = 0$) and are of equal branch powers, a diversity gain of 7.03 dB can be achieved at the 10% level through maximal ratio combining. As opposed to selection combining, diversity gain can be achieved using maximal ratio combining even with r_1 and r_2 perfectly correlated ($\mathbf{r} = 1$). For example, Figure 8.10 shows that for balanced branches a diversity gain of 3

dB is attainable for perfectly correlated signals. Turkamani et al. also presented in [2] an equation that best describes the diversity gain at the 10% level as a function of branch power imbalance and envelope correlation for a maximal ratio combiner. Measurements in many different environments showed that

$$G_D(10\%) = 7.14e^{-0.59r-0.11D_M(dB)} \quad (8.10)$$

best fits the diversity gain for two-branch maximal ratio combiner [2]. Figure 8.11 shows a three dimensional plot that relates diversity gain to envelope correlation and power imbalance. Figures 8.10 and 8.11 both show comparable gains from what was predicted for the maximal ratio combiner in a Rayleigh channel to measured data.

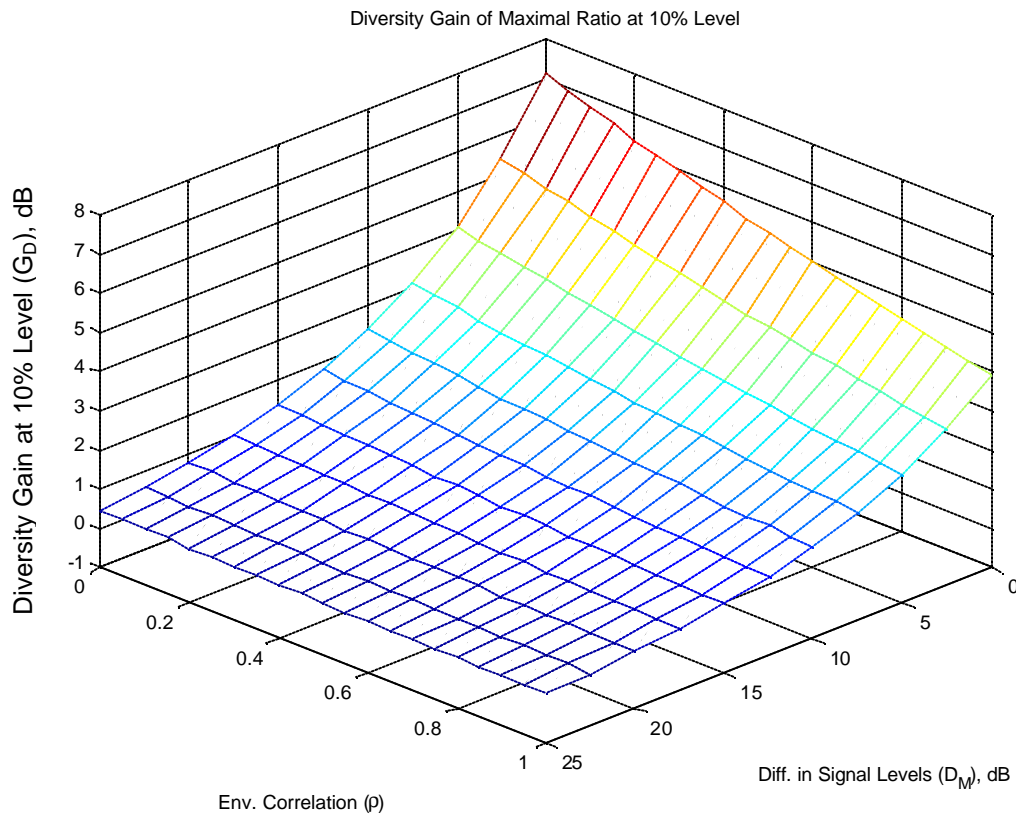


Figure 8.11 Diversity gain of a two-branch maximal ratio diversity system as a function of envelope correlation and power imbalance at the 10% level as given in [2] and (8.10).

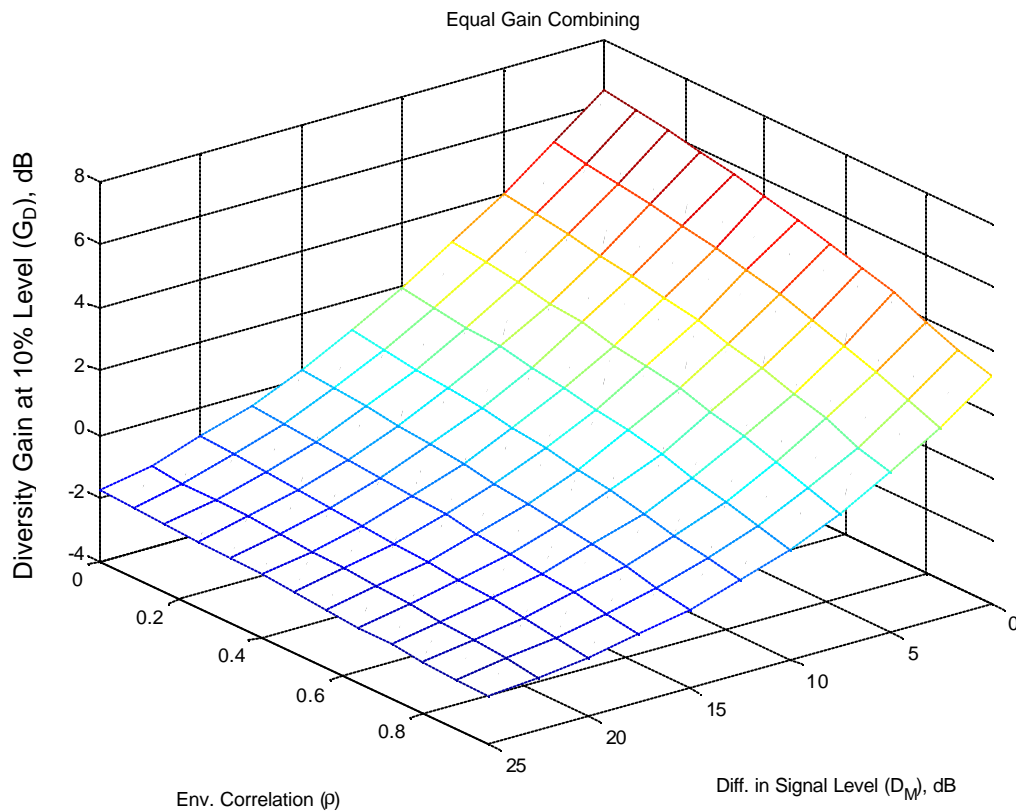


Figure 8.12 Diversity gain of a two-branch equal gain diversity system in a Rayleigh channel as a function of envelope correlation and power imbalance at the 10% level computed numerically.

Even though the equal gain combining equations have not been presented in this thesis, the diversity gain at the 10% level can be evaluated numerically. The results are presented here for completeness. The 10% diversity gain plot for equal gain combining in a two-branch Rayleigh fading channel is shown in Figure 8.12. The power imbalances were evaluated from 0 to 25 dB in steps of 2.5 dB, and the envelope correlations were evaluated for 0, 0.08, 0.16, 0.24, 0.32, 0.4, 0.48, 0.56, 0.64, 0.72, 0.8, 0.88, and 0.96. The diversity gain using equal gain combining and uncorrelated signals drops from 6.44 dB with balanced branches to -1.79 dB when the differences in signal power is 25 dB. From Figure 8.12, it can be seen that using equal gain combining can actually be worse than

choosing the branch with the largest signal-to-noise ratio for large differences in signal level (D_M). This can also be observed at the instantaneous level when one branch has a large signal while the other branch is faded as was discussed in Chapter 3. This could lead to a lower signal to noise ratio of the combined signal than at the largest branch. Equal gain might not be a desirable combining technique for diversity branches that experience large variations of power between branches.

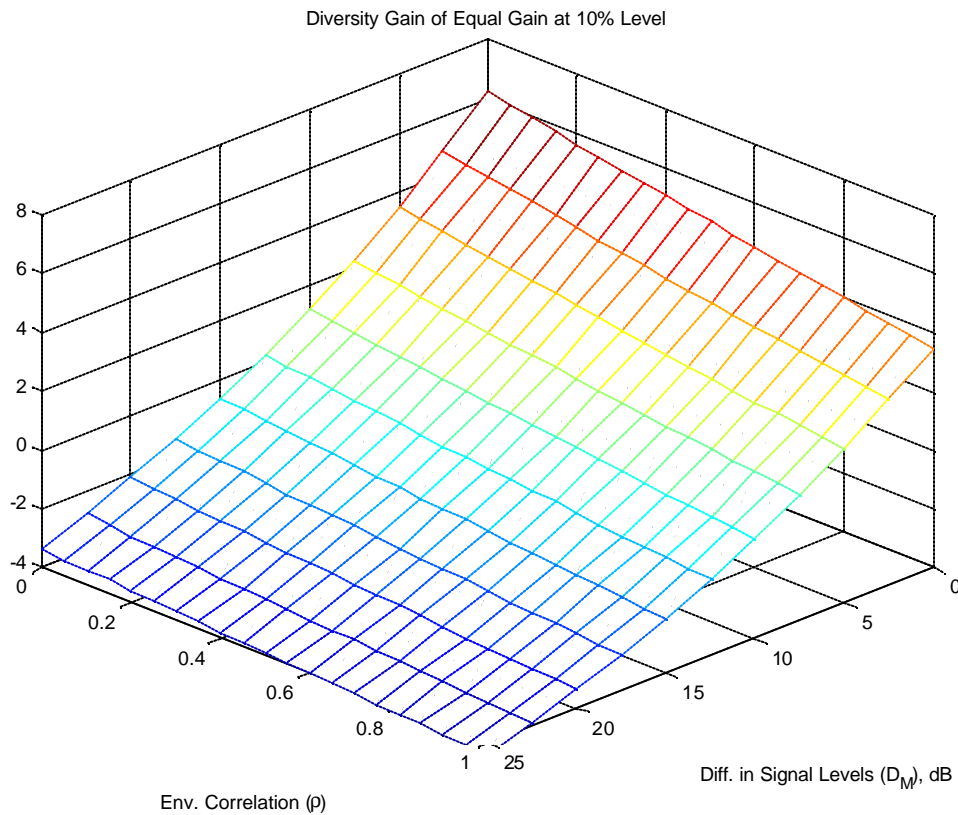


Figure 8.13 Diversity gain of a two-branch equal gain diversity system as a function of envelope correlation and power imbalance at the 10% level as given in [2] and (8.11).

Turkamani et al. also presented in [2] an equation for the diversity gain at the 10% level as a function of branch power imbalance and envelope correlation for two-branch equal gain combiner. This result was computed by fitting diversity gains extracted from measured data which resulted in the equation

$$G_D(10\%) = -8.98 + 15.22e^{-0.20r - 0.04D_M(dB)} \quad (8.11)$$

Figure 8.13 shows a plot of the function given in (8.11). The diversity gain plots at the 10% level for equal gain combining computed for the Rayleigh channel follows the same pattern and closely match the results achieved from measurements by Turkmani et al. [2]. The measurements in [2] were probably not all Rayleigh fading which probably accounts for the small discrepancies. The performance degradation that is characteristic of equal gain combining when both branches greatly vary in average power is also evident in the measured data.

The diversity gain plots (Figures 8.8-8.13) show that there is very little gain achieved through diversity when average power level in both branches are very far apart. As mentioned in Chapter 2, it is not unlikely for the average power between two polarization diversity branches to differ greatly. From the diversity gain plots, it would seem that such a diversity system would not bring considerable improvement in signal quality. This conclusion is however often incorrect as illustrated by the following example. First, it must be remembered that diversity gain is defined as the gain achieved over the strongest branch. A polarization diversity system using horizontal and vertically polarized receive antennas will most likely receive a significantly stronger signal on the horizontal branch when the transmitting antenna is horizontally polarized and the medium introduces little depolarization. The large difference in power would result in a system with a very small diversity gain. If on the other hand, two vertically polarized receive antennas are used at the receiving end, both branches would probably receive low but balanced signal-to-noise ratios at both branches due to the polarization mismatch with the transmitting antenna. In this second case, the balanced SNRs guarantee a higher diversity gain. Concluding that the vertical pair of antennas would outperform the polarization diversity configuration on the basis of just diversity gain would be erroneous in this example. The signal-to-noise ratio after combining on both the spatial and polarization pair of antenna will most likely show a higher SNR at the output of the polarization diversity configuration. This is because the horizontal antenna of the polarization diversity example is receiving a

considerably higher signal level than the vertical branch so much of the SNR after combining is due to the horizontal branch. Since diversity gain quantifies the improvement of adding the vertical branch compared to having just the horizontal branch, the gain is small.

The use of just diversity gain to quantify the performance of a diversity system or configuration is an inadequate performance measure as was seen by the previous example. Diversity gain, however, is a good indicator for comparing different combining algorithms.

References:

- [1] C. B. Dietrich, Jr., K. Dietze, J. R. Nealy, and W. L. Stutzman, "Spatial, Polarization, and Pattern Diversity for Wireless Handheld Terminals," *IEEE Antennas and Propagation*, to appear Sept. 2001.
- [2] A.M.D. Turkmani, A.A. Arowogolu, P.A. Jefford, and C.J. Kellent, "An Experimental Evaluation of Performance of Two-Branch Space and Polarization Diversity Schemes at 1800 MHz," *IEEE Trans. Veh. Tech.*, vol. 44, no.2, pp. 318-326, May 1995.

Chapter 9

Conclusions

This report presents a theoretical approach for analyzing a two-branch diversity system in a Rayleigh channel. In a Rayleigh fading channel, a single antenna can experience large fluctuations in received signal levels over small distances (when compared to λ).

Diversity is a very tractable solution to increase the reliability of the received information without increasing the transmit power. The motivation was to analyze the performance of a two antenna handheld unit. Due to physical size constraints of the unit, antennas are in close proximity of each other. This close proximity or the use of different antennas could cause both received signals to be correlated and/or have branches with different average powers. As was shown in this thesis, these two factors affect the performance of diversity system. The effectiveness of the diversity also depends on the combining method that is being used.

From the three combining methods presented in this report, maximal ratio combining performs the best. Selecting the better performer between selection and equal gain is not as straightforward. When both antennas have matched average powers, equal gain

combining on the average is more effective. But as the difference between average powers becomes larger, there is a point when selection diversity outperforms equal gain combining on the average as well as the instantaneous level. This effect can be observed when examining Figures 8.8 and 8.12 as well as following the discussions in Chapter 3.

This report presents an exact expression for the probability density function of the signal-to-noise ratio at the output of a two-branch selection and maximal ratio combining system for a Rayleigh fading environment. Both Rayleigh branches can potentially be correlated and have unequal average branch powers. Selection combining is examined in Chapter 5 and maximal ratio is discussed in Chapter 6. Section 1.4 summarizes some of the previous work in the areas of selection combining and maximal ratio combining for Rayleigh channels. Most of the work has only treated uncorrelated branch signals.

Measurements were performed in Rayleigh channels to verify the applicability of the theoretical results. One of the assumptions made in this paper is that the ensemble operations over probability distributions agree with time averages applied to measured signals. The measurements shown in Chapter 8 show that there is a very good agreement between what is predicted using probability distributions and distributions achieved from measured data through time combining. The measurements show an agreement within 1 dB between the cumulative distribution function predicted by theory and the distributions achieved from measured data; see Figures 8.4-8.7.

The diversity gain achieved by using selection, equal gain, and maximal ratio combining was examined as a function of envelope correlation and power imbalance between the branches. As can be seen from diversity gain plots at the 10 % level (Figures 8.8-8.13) the performance of such a system depends greatly on the correlation and average power difference between the branches. The computed diversity gains for the two-branch Rayleigh system match very closely what Turkmani et al. [1] have found by performing extensive measurements for a wide range of channels. The diversity gains for the Rayleigh channel describe the average physical channels very well.

Diversity combining can also significantly increase the performance of a digital communication system in a flat and slow Rayleigh fading channel. The exact bit error rate of coherent BPSK after two-branch maximal ratio combining has been derived and is given in Chapter 7 with (7.21), (7.23), and (7.26). These equations are given as a function of correlation and average power in the branches. Additionally, the symbol error rate of coherent QPSK for a two-branch maximal ratio combining in the Rayleigh channel is given in (7.28), (7.30), and (7.33). For these results, as well, correlation and unbalanced branch power have been considered. Figures 7.2, 7.3, 7.4, and 7.5 are plots of the symbol error rates for coherent BPSK and QPSK after maximal ratio combining for perfectly correlated and uncorrelated branches using the equations presented in this paper. As stated in Section 1.4, significant amounts of papers in literature have computed the average bit error rates for non-coherent modulation schemes but coherent modulation schemes are rarely addressed. In [3] an expression for the average probability of bit error is presented for coherent BPSK after maximal ratio combining but requires to be numerically integrated. To the authors best knowledge, there has been no closed form expression for the average symbol error rate of coherent QPSK reported in literature for correlated Rayleigh signals.

Transmit diversity has become increasingly important as an alternative or in addition to receive diversity systems for present commercial systems. Assuming that perfect channel estimates are available, the same gains can be achieved through transmit diversity as with a receive diversity system. Instead of having multiple antennas on a small handset receiver, the complexity is moved to the base station which can more readily handle the additional hardware. In a transmit maximal ratio combining diversity system, the base station adjusts the phase and amplitude of the signals being transmitted on both antenna elements in such a way that the single antenna handheld receiver receives the signal with optimal signal-to-noise ratio. This process, however, requires that channel information be fed back from the receiver to the transmitter. Selection transmit diversity also requires feedback, the receiver informs the transmitter to switch to a particular antenna based on the received signal-to-noise ratio. In a receive diversity system, on the other hand, channel information is readily available to the receiver. Because of duality, the

distributions of the signal-to-noise ratio presented in this report can also be used for two-branch transmit diversity since propagation channels are reciprocal. The probability of average symbol error of coherent BPSK and QPSK also hold for two branch transmit diversity as long as the transmitter has perfect channel estimates.

In a parallel effort, an extensive measurement campaign was performed in various types of channels for a two and four branch diversity system. Factors such as antenna configuration and antenna spacing have been addressed and how it affects diversity gain and correlation in [2]. The goal of diversity is to improve the received signal to noise ratio for all time. Even though this report considers only two-branch diversity systems, there is a higher achievable gain by using more branches. As more and more branches are added to a diversity system, eventually flat fading can be completely mitigated.

References:

- [1] A.M.D. Turkmani, A.A. Arowogolu, P.A. Jefford, and C.J. Kellent, "An Experimental Evaluation of Performance of Two-Branch Space and Polarization Diversity Schemes at 1800 MHz," *IEEE Trans. Veh. Tech.*, vol. 44, no.2, pp. 318-326, May 1995.
- [2] C. B. Dietrich, Jr., K. Dietze, J. R. Nealy, and W. L. Stutzman, "Spatial, Polarization, and Pattern Diversity for Wireless Handheld Terminals," *IEEE Trans. on Antennas and Propagation*, to appear Sept. 2001.
- [3] Pierfrancesco Lombardo, Gennaro Fedele, and Murli Mohan Rao, "MRC Performance for Binary Signals in Nakagami Fading with General Branch Correlation," *IEEE Trans. Commun.*, vol. 47, no. 1, pp. 44-52, Jan. 1999.

Vita

Kai Dietze was born on February 16, 1974 in Frankfurt/Main, Germany. He received his Bachelors of Science in Electrical Engineering in May 1995 from Michigan Technological University, Houghton, Michigan. In May 2001, he obtained his Masters of Science in Electrical Engineering from Virginia Tech, Blacksburg, Virginia. He is currently enrolled in the Ph.D. program in the Bradley Department of Electrical Engineering at Virginia Tech.

Kai is a Research Assistant at the Virginia Tech Antenna Group (VTAG) where he has been involved in developing and testing smart multiple antenna receive and transmit diversity systems for wideband communications. His interests are in signal processing when applied to wireless communications systems. His current research focuses on the areas of adaptive antenna arrays and diversity systems.